



Residual Engineering Properties of Corroded Conventional Steel, High  
Chromium Steel and Stainless Steel Reinforcing bars in Concrete

by  
Shaima Mohammed Aziz

A Thesis submitted to the Department of Civil and Environmental Engineering,

Cullen College of Engineering

in partial fulfillment of the requirements for the degree of

Master of Science

in Civil Engineering

Chair of Committee: Abdeldjelil Belarbi

Committee Member: Ahmed Senouci

Committee Member: Mina Dawood

University of Houston

December 2019

Copyright 2019 Shaima Mohammed Aziz

## **DEDICATION**

This thesis is lovingly dedicated to my Mother. Her support, encouragement, and constant love have sustained me throughout my life. Also, it is dedicated to my precious kids Ryan, Lillian, and Ava Jaf, my supporter husband, and wonderful brothers and sisters.

## **ACKNOWLEDGEMENTS**

Thank GOD who lightened my way during the critical times. Sincere thanks go in particular to my supervisor Professor Abdeldjelil Belarbi for valuable, guidance, and constructive suggestions he provided in undertaking this research and in preparation of this thesis. I explicitly thank Associate Professor Mina Dawood for selecting this topic from the very beginning of my thesis journey as well as giving me guidance and instruction. Furthermore, special thanks to the distinguished faculty members who served on my committee: Professors: Ahmed Senouci and Mina Dawood. Thanks to all my committee members for their support, patience, encouragement, and useful suggestions and guidance.

The author would like to thank the Higher Committee for Education Development in Iraq for their support in the form of scholarship.

Sincere and warm thanks to my friends and colleagues in the civil and environmental engineering department who supported me during my research journey.

Finally, and above all, I owe much gratitude to my family for their encouragement and interest in seeing this thesis completed.

## **ABSTRACT**

Corrosion can be a major concern in term of durability and the safety of the reinforced concrete structures. However, there are no relations specified by codes and standards to evaluate the reduction in the engineering properties of corroded steel rebar. This work presents the findings of the experimental study of the effect of corrosion on the engineering properties of conventional and common resistant corrosion steel rebar that are commonly used in reinforced concrete structures. Sets of tensile strength tests are carried out to evaluate the residual engineering properties namely; yield strength, ultimate strength, and ductility of embedded steel reinforcement subjected to accelerated corrosion. The experimental work comprised of testing three types of steel rebar- mild steel (MS), high chromium (HC) and stainless steel (SS), with two rebar sizes (No. 3 and No. 4), and for 1%-17% mass loss range. Results from the tests indicate that the yield strength, ultimate strength and ductility of steel reinforcement decreases significantly with the increase of mass loss levels, however, rebar size has a slight effect on these reductions. In addition, mass loss level due to corrosion is utilized to predict the reduction of yield and ultimate strength, while both mass loss and pitting factor play a crucial role in the ductility of the corroded rebar. Furthermore, the test results were utilized to propose a set of simple empirical equations to predict the residual strengths and ductility of the corroded steel rebars subjected to accelerated corrosion, which could also be used to evaluate the residual responses of corroded reinforcement in reinforced concrete structures in practice.

# TABLE OF CONTENTS

Dedication .....	iii
Acknowledgements .....	iv
Abstract .....	v
Table of Contents .....	vi
List of Tables.....	ix
List of Figures.....	x
Chapter One .....	1
INTRODUCTION .....	1
1.1 General .....	1
1.2 Deterioration Levels in Reinforced Concrete Structures.....	3
1.3 Magnitude of Corrosion Problem in Structure.....	4
1.4 Objective and Scope of this Research .....	6
1.5 Research Methodology.....	7
1.6 Thesis Layout .....	8
Chapter Two.....	10
STATE OF THE ART REVIEW .....	10
2.1 General .....	10
2.2 Mechanism of the Corrosion in Steel Reinforcement Rebar.....	10
2.3 Enviromental Factors Influencing Corrosion Rate of Reinforcement Rebar in Structures .....	14
2.4 Corrosion Methodology.....	16
2.5 Current Code and Standard Provisions on Traditional and Corrosion Resistant Reinforcement Rebar.....	16
2.5.1 Carbon-steel reinforcement rebar .....	16

2.5.2 High chromium reinforcement rebar .....	18
2.5.3 Stainless steel reinforcement rebar .....	21
2.6 Previous Experimental Studies on Corrosion in Reinforcement Steel Rebar.....	23
2.6.1 General .....	23
2.6.2 Previous experimental studies.....	23
2.6.3 Knowledge gap .....	27
Chapter Three .....	29
CORROSION TEST EXPERIMENTS.....	29
3.1 General .....	29
3.2 Test Parameters.....	29
3.3 Experimental Details.....	30
3.3.1 Specimens Fabrication .....	30
3.3.2 Concrete Compositions .....	31
3.3.3 Chloride solution.....	31
3.3.3 Chloride Solution .....	31
3.3.4 Specimens Preparation Procedures .....	32
3.3.5 Accelerated Corrosion Test Setup .....	35
3.4 Experimental Measurements .....	37
3.4.1 Mass Loss (ML).....	38
3.4.2 Residual Cross Section of Corroded Rebar (Volume Measurement) .....	39
3.4.3 Pitting Factor (PF).....	41
3.5 Tensile Strength Test .....	42
3.6 Summary.....	43
Chapter Four .....	44
results and discussions.....	44
4.1 General .....	44
4.2 Experimental Results .....	44
4.3 Effect of Steel Type on Engineering Properties.....	45

4.3.1 Stress-strain response.....	45
4.3.2 Yield strength.....	51
4.3.3 Ultimate strength.....	54
4.3.4 Ductility (ultimate strain).....	55
4.4 Effect of Rebar Size on the Engineering Properties .....	59
4.5 Proposed Equations for Corroded Steel Rebars .....	65
4.5.1 Mild steel rebar .....	65
4.5.1.1 Yield strength reduction factor.....	65
4.5.1.2 Ultimate strength reduction factor.....	65
4.5.1.3 Ductility reduction factor .....	65
4.5.2 High chromium steel rebar.....	67
4.5.2.1 Yield strength reduction factor.....	67
4.5.2.2 Ultimate strength reduction factor.....	67
4.5.2.3 Ductility reduction factor .....	68
4.5.3 Stainless steel rebar.....	70
4.5.3.1 Yield strength reduction factor.....	70
4.5.3.2 Ultimate strength reduction factor.....	70
4.5.3.3 Ductility reduction factor .....	70
4.6 Summary.....	74
Chapter Five .....	75
conclusionS and recommendations .....	75
5.1 General .....	75
5.2 Conclusions.....	75
5.3 Recommendations for Future Work.....	76
References.....	78
Appendix .....	83

## LIST OF TABLES

Table 2-1: Mechanical properties requirement of carbon-steel reinforcement rebar....	17
Table 2-2: Maximum chloride ion content for corrosion protection of.....	18
Table 2-3: Chemical compositions of high chromium steel reinforcement rebar types	20
Table 2-4: Mechanical properties requirement in high chromium reinforcement rebar	20
Table 2-5: Chemical compositions of stainless steel reinforcement rebar types. ....	22
Table 2-6: Mechanical properties requirement in stainless steel reinforcement rebar types.....	22
Table 2-7: Summary of previous experimental work of corroded steel reinforcement	28
Table 3-1: Concrete compositions design for the specimens.....	31
Table 3-2: Summary of chloride solution preparation.....	32
Table 3-3: Summary of test matrix of rebar specimens.....	38
Table 4-1: Summary of accelerated corrosion test on mild steel rebar.....	49
Table 4-2: Summary of accelerated corrosion test on high chromium steel rebar.....	50
Table 4-3: Summary of accelerated corrosion test on stainless steel rebar.....	51
Table 4-4: Summary of the statistical analysis of the yield and ultimate strength of ...	73
Table 4.5: Summary of the statistical analysis of ultimate strain of mild steel(MS),highchromium steel(HC), and stainless steel (SS) .....	74

## LIST OF FIGURES

Fig. 1-1: Schematic illustration of the deterioration levels in steel (continued) .....	4
Fig. 1-2: Corrosion induced deterioration in reinforced concrete structures .....	5
Fig. 1-3: Economic impact of corrosion in the United States (continued),.....	6
Fig. 1-4: Research flowchart.....	8
Fig. 2-1: Reinforcing steel corrosion in concrete.....	14
Fig. 2-2: Mild steel, high chromium steel and stainless steel reinforcing rebar .....	19
Fig. 3-1: Layout of test specimen .....	30
Fig. 3-2: The specimens after casting the concrete.....	33
Fig. 3-3: Specimens fabrication .....	33
Fig. 3-4: Details of specimens' preparation for accelerated corrosion test.....	34
Fig. 3-5: Details of specimen ends protection from corrosion .....	34
Fig. 3-6: Stainless steel cathodes rebar .....	36
Fig. 3-7: Accelerated corrosion test setup.....	37
Fig. 3-8: Volume measurements of corroded steel rebar specimens .....	40
Fig. 3-9: The residual cross sectional of corroded specimen (continued).....	39
Fig. 3-10: Schematic illustration of pitting factor.....	42
Fig. 3-11: Test setup for tensile strength tests of corroded steel rebars.....	43
Fig. 4-1: Stress-strain curves of Mild steel (MS) at various mass loss levels.....	46
Fig. 4-2: Stress-strain curves of High Chromium steel (HC) (continued).....	47
Fig. 4-3: Stress-strain curves of Stainless steel (SS) at various mass loss levels .....	48
Fig. 4-4: Effect of steel type on the yielding strength of corroded rebars .....	53

Fig. 4-5: Effect of steel type on the ultimate strength of corroded rebars .....	55
Fig. 4-6: Effect of steel type on the ultimate strength of corroded rebars .....	57
Fig. 4-7: Effect of pitting attack on failure mode of Mild steel rebars .....	57
Fig. 4-8: Failure modes of corroded Mild steel rebar .....	58
Fig. 4-9: Failure modes of corroded High Chromium steel rebar.....	58
Fig. 4-10: Failure modes of corroded Stainless steel rebar.....	59
Fig. 4-11: Effect of rebar size on the yielding strength of Mild, High (continued).....	61
Fig. 4-12: Effect of rebar size on the ultimate strength of Mild, High (continued).....	63
Fig. 4-13: Effect of rebar size on the ductility of Mild, High Chromium(continued)..	64
Fig. 4-14: Linear regression of yield strength of Mild steel (MS).....	66
Fig. 4-15: Linear regression of ultimate strength of Mild steel (MS).....	66
Fig. 4-16: Multi-regression of ductility of Mild steel (MS).....	67
Fig. 4-17: Linear regression of yield strength of High Chromium steel (HC) .....	68
Fig. 4-18: Linear regression of ultimate strength of High Chromium steel (HC) .....	69
Fig. 4-19: Multi-regression of ductility of High Chromium steel (HC) .....	69
Fig. 4-20: Linear regression of yielding strength of Stainless steel (SS) .....	71
Fig. 4-21: Linear regression of ultimate strength of Stainless steel (SS) .....	71
Fig. 4-22: Multi-regression of ductility of Stainless steel (SS) .....	72

## **Chapter One**

### **INTRODUCTION**

#### **1.1 General**

Reinforced concrete is a predominant construction material that generally performs well throughout the service life. However, the corrosion of the reinforcement component is a major concern on the durability and the safety of the reinforced concrete structures. Corrosion is well known as the primary and most expensive deterioration phenomenon in reinforced concrete structures. It is predicted that the corrosion deteriorates steel at a rate of 5 tons per second in the world which is equivalent to 1/4 of the world's annual steel production (Landolt, 2007).

Corrosion is induced by carbonation or/and chloride attack. Carbonation induced corrosion occurs when the relative humidity maintained in range between 50%-75% in the environment surrounded by the structure member and it is insignificant when it is below 25% (PCA, 2002). Therefore the deterioration due to carbonation takes place over a long period of time. On the other hand, corrosion induced by chloride attack is the primary cause of premature deterioration in the reinforced concrete structure. This type of premature deterioration is linked to the use of the dicing salts and continuous exposure to seawater. The degradation due to chloride attack may take place over a short period of time depending on the aggressiveness of the corrosive environment exposure. Therefore many structure's elements are subjected to this type of deterioration, such as bridge decks and reinforced concrete pile in marine structure, and have led to public concern for the integrity of the structural system.

Deterioration due to corrosion leads to many changes in the structure such as reduction of the load-carrying capacity of the structural members due to the cracking and spalling of the concrete cover caused by corrosion. Also, reinforcement corrosion reduces the cross section area of the reinforcing bars, and deteriorates the bond between the concrete and the reinforcement rebar. Furthermore, the steel reinforcement mechanical properties such as yield, tensile strength, and ductility are affected by corrosion. Therefore, the corroded concrete structures need to be evaluated carefully. In the evaluation, the residual engineering properties of the corroded reinforcement are critical inputs.

The influence of the corrosion in the service life has been significantly high since early 1900. According to the data that was collected by the American Iron and Steel Institute, the average useful life of steel in 1920 and 1940 was 23 and 35 years respectively (Speller, 1951). Since then, there is a high demand to build long lasting structures by using material with greater durability and low life cycle cost.

In the last decades, extensive experimental work has been carried out on the effect of corrosion on the engineering properties of steel reinforcements. These studies focused on the residual mechanical properties of conventional steel reinforcement. However, there is a lack of experimental data on other types of steel rebars used in concrete structures such as high chromium and stainless Steel rebars. These types of steel reinforcement have significant corrosion resistance. Recently, the uses of these types of corrosion resistant reinforcements have increased in the reinforced concrete structures subjected to an aggressive corrosion environment. Therefore, this research project

presents an experimentally study of the effect of accelerated corrosion on the engineering properties of mild, high chromium, and stainless steel rebars.

## **1.2 Deterioration Levels in Reinforced Concrete Structures**

The use of steel reinforcement in concrete is based on the perfect alkaline environment of the concrete which protects the reinforcement by forming a passive layer of iron oxide. This layer protects the steel reinforcement from further corrosion. But, when the reinforced concrete is exposed to extensive and continues corrosive environmental conditions due to structure exposure to dicing salts or marine water, this layer start to destructed and the steel reinforcement start deteriorate with time due to the propagation of the corrosion.

Deterioration due to corrosion can be divided into two primary time periods, the initiation period and the propagation period. During total corrosion periods, the reinforced concrete structure experience four significant deterioration levels

The first deterioration level happens in the initiation period and it is known as reinforcement depassivation. In this stage, the reinforcement changes from uncorroding condition (passive) to corroding condition. This happens when the reinforced concrete is contaminated by carbonation or/and chloride attack which destroys the protecting passive layer on the surface of the steel reinforcement rebar. The deterioration in the initiation period is on the reinforcement level, unlike the other deterioration levels in the propagation period which are on the structure level. As the propagation period starts, a series of chemical reactions occur which result in inducing corrosion products (rust), then corrosion develops causing the formation of cracks which considered the second level of the deterioration. The crack formation is caused by the expansion of the corrosion

products which have a volume higher than the original steel material several times. The expansion induces internal stress in the concrete leading to crack formation. After the cracking, the third deterioration level starts when the cracks increase leading to spalling of concrete cover. The fourth deterioration level starts when the structure is exposed more to the corrosive environment. In this level, the steel reinforcement corrodes more causing a reduction in the cross section or debonding which leads to the collapse of the structure (Cairns et al., 2011). A schematic of the deterioration levels due to corrosion is illustrated in Fig. 1-1.

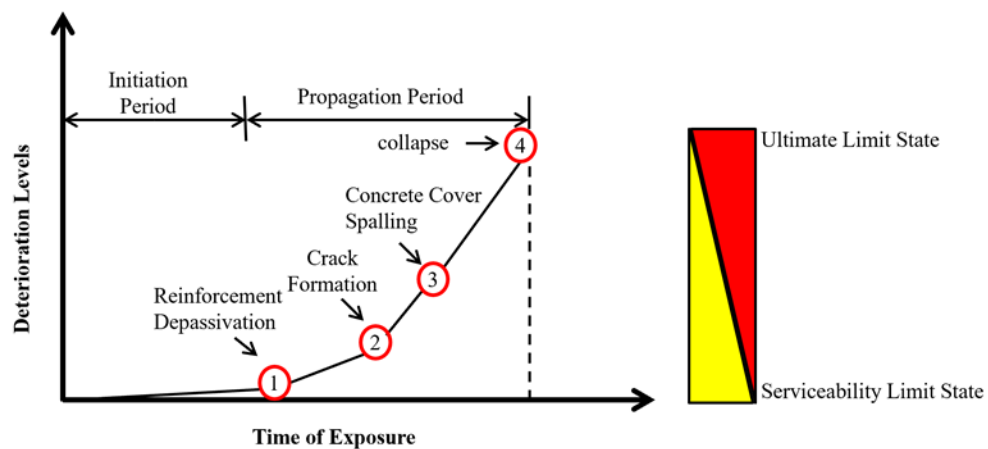


Fig. 1-1: Schematic illustration of the deterioration levels in steel reinforced concrete structure due to corrosion (Cairns et al., 2011).

### 1.3 Magnitude of Corrosion Problem in Structure

Corrosion induced deterioration has been a major concern not only in the steel structures but also in the reinforced concrete structures. It is directly influencing the durability, aesthetics, and safety of the structure. This form of deterioration attacks the main elements in the structural members in the infrastructure such as bridge, concrete

piles in highway, and many other important components of structures that are either exposed to deicing products in the northern or in seawater in the southern of the United States. Examples of corrosion induced deterioration on structural members are shown in Fig. 1-2.



(a) Concrete cracking and spalling in bridge (TxDOT)



(b) Prestressed concrete piles in Hamilton, 2007 (Moser, et. al. 2011)

Fig. 1-2: Corrosion induced deterioration in reinforced concrete structures

An economic survey in 2002 reported that the economic influence of the corrosion in metal in the United States predicted as 3.1% of gross domestic product (GDP) (Koch et al. 2002). According to Federal Highway Administration (FHWA) in 2006's report to Congress, shown that 13% of the total 595,000 bridges in the United States were listed as structurally deficient significantly due to corrosion in steel reinforcement. The retrofitting of these bridges has been estimated by 8.3 Billion Dollars annually and the rehabilitation was predicted by 150 billion dollars (Moser et al. 2011). Furthermore, 50 to 200 billion dollars have been estimated as indirect costs can be added

to the cost of the maintenance and rehabilitation of the corrosion induced deterioration such as bridge and parking decks closures, increased traffic congestion, and affected businesses (NACE, 2008). Finally, the most recent study about the corrosion problem cost in the United States showed that the economic cost of corrosion is significantly high compared with the cost of other major life issues as illustrated in Fig. 1-3 (Angst 2018). It can be seen in the Fig. 1-3 that the total economic impact of corrosion in the United States exceed 480 billion dollars for one year while 10% of it represents the economic impact of corrosion in reinforced concrete structures and bridges.

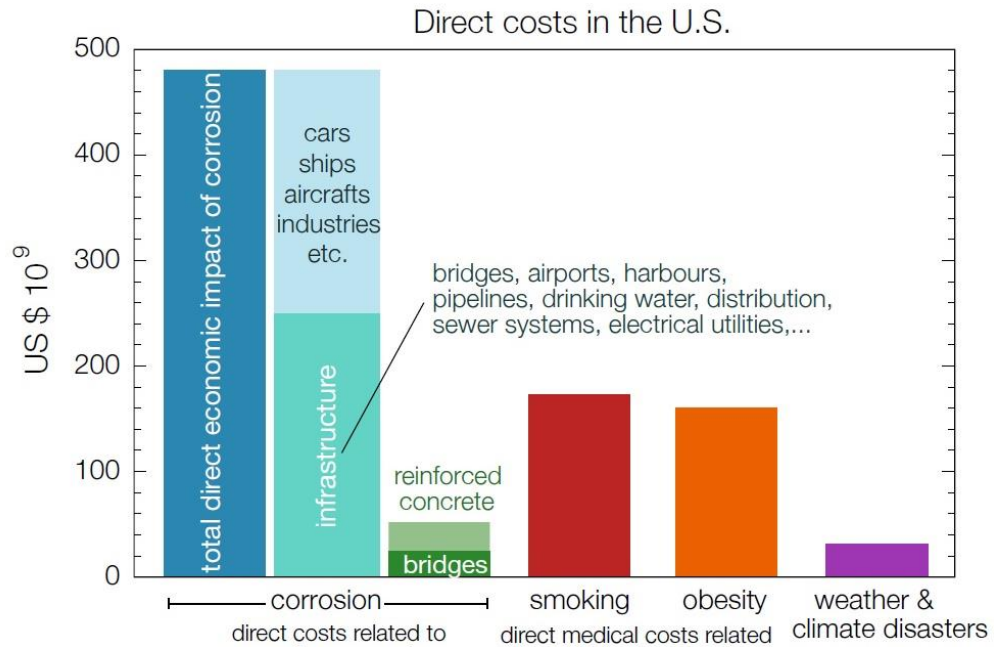


Fig. 1-3: Economic impact of corrosion in the United States for 2010-2011(Angst, 2018).

#### 1.4 Objective and Scope of this Research

This research project was carried out on different types of steel reinforcing rebar embedded in concrete and exposed to electrical accelerated corrosion process. The study included three types of steel rebars commonly used in reinforced concrete structures, namely, mild steel (MS), high chromium (HC) and stainless steel (SS), with two rebar

sizes (No.3 and No.4) and with 1-17% mass loss range. The following are the objectives of this thesis:

1. Determine the reduction factors of yield strength, tensile strength, and ductility of corroded reinforcement rebar subjected to accelerated corrosion.
2. Investigate the effect of the localized degradation (pitting factor) on the engineering properties of corroded reinforcement rebar
3. Propose simple empirical equations to predict the residual strengths and ductility of the corroded steel rebars subjected to accelerated corrosion.

### **1.5 Research Methodology**

To achieve the objectives of this research, an accelerated corrosion test was conducted on different types and sizes of common reinforcing rebars. Then a few experimental measurements performed to estimate the corrosion levels (mass loss), and the residual cross section of the corroded rebars. Following that strength tensile tests were carried out to determine the engineering properties of the corroded specimens rebars. Result data from the experimental measurements and experimental tests were utilized in statistical analysis to propose simple empirical equations to predict the residuals strengths and ductility of corroded steel rebars. A summary of research flowchart is illustrated in Fig. 1-4.

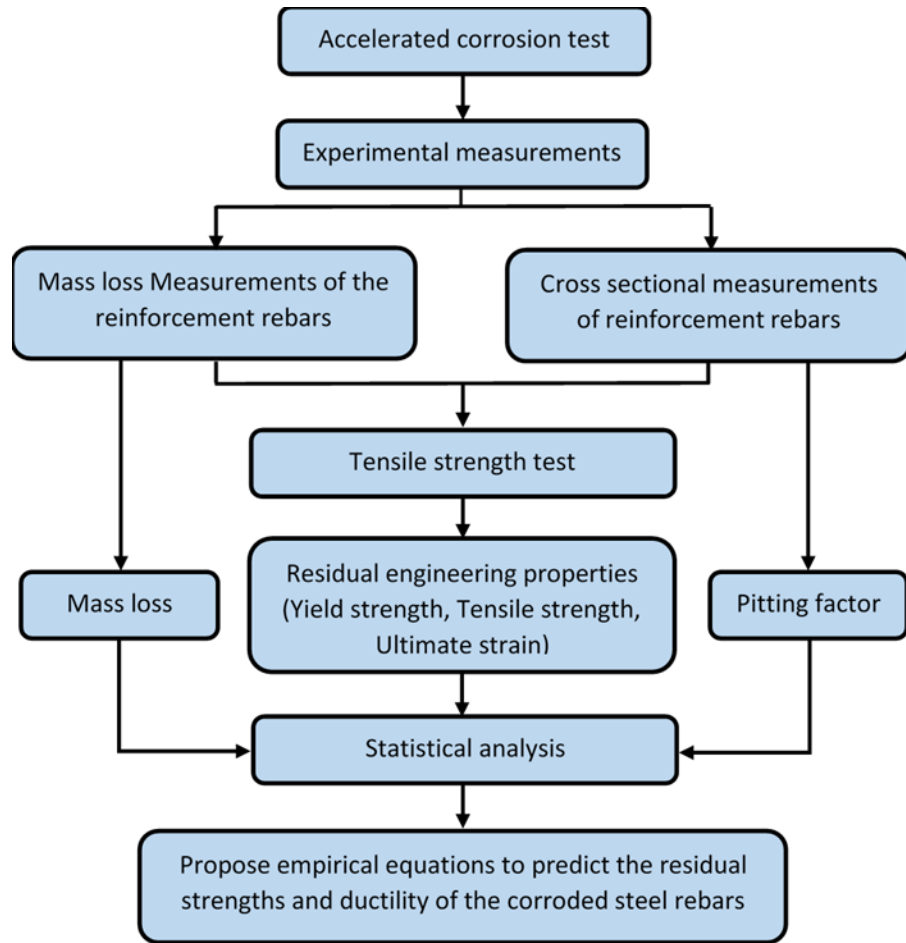


Fig. 1-4: Research flowchart

## 1.6 Thesis Layout

This thesis is organized into five chapters. The brief description of the content is presented in the following

Chapter 1: presents background information about the corrosion problem in reinforced concrete structures exposed to a continuous corrosive environment

Chapter 2: presents the state of the art on the performance of different reinforcement in reinforced concrete under corrosion, factors controlling the corrosion test, and finally, previous experimental studies on corrosion test and the influence of the corrosion on the mechanical properties of the reinforcement rebar

Chapter 3: presents the experimental details of the accelerated corrosion test conducted on reinforcement rebar specimens embedded in concrete including the material properties results.

Chapter 4: presents result data of the engineering properties of the corroded reinforcement rebar including the residual tensile strength, ductility, and the residual cross section of the corroded rebar as well as discussion of these data

Chapter 5: presents the summary of the main finding from the study and future research recommendation.

## **Chapter Two**

### **STATE OF THE ART REVIEW**

#### **2.1 General**

Engineering properties of corroded rebar is considered one of the important components needed in the evaluation of deteriorated reinforced concrete structure due to corrosion. In the last decades, extensive experimental work has been carried out on the effect of corrosion on the mechanical properties of steel reinforcements. These studies focused on the residual mechanical properties of conventional steel reinforcement, However, there is a lack of experimental data on other types of steel rebar used in concrete structures such as high chromium and stainless steel rebar. These types of steel reinforcement have excellent corrosion resistance. Recently, the uses of these types of corrosion-resistant reinforcements have increased in the reinforced concrete structures subjected to aggressive corrosion environments. This chapter provides background information about the mechanism of corrosion in reinforced concrete structures, environmental factors influencing the corrosion rate of the reinforcement rebar in structure, corrosion methodology, the current code and standard provisions of steel reinforcement rebar properties, and the state of the art review of previous experimental studies on corroded reinforcement rebars..

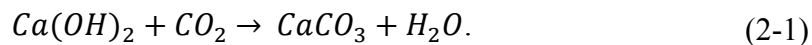
#### **2.2 Mechanism of the Corrosion in Steel Reinforcement Rebar**

Corrosion can be defined as irreversible reaction between the surfaces of the metal with the environment resulting in dissolving of the metal material or one of its compositions (Heusler et al., 1989). Iron is the main component in steel compositions

produced by the thermal treatment of iron oxide rocks which is found in nature in form of rocks and minerals mixed with other impurities. Therefore, when steel reinforcement is exposed to a corrosive environment, corrosion occurs and the iron in steel returns to its natural form which is Iron oxide (Wilson and Oates, 1968).

Steel reinforcement similar to other metallic material has many desirable properties such as ductility, high tensile strength (Landolt, 2007). In addition to these properties, steel reinforcement is considered as compatible material with concrete due to the high alkaline environment of the Cement Portland in concrete, which has a PH value of 12 to 13. This alkaline environment causes the steel reinforcement to form a passive layer known as gamma-  $Fe_2O_3$  that prevents further corrosion (Broomfield, 1995a). This passive layer doesn't completely prevent the corrosion. However, it lets the corrosion to occur at rate of  $0.1 \mu\text{m}/\text{year}$  which is 1000 times lower than the corrosion rate when this layer does not exist (ACI, 2001).

The corrosion process starts with the destruction of the passive layer on the steel surface due to carbonation and/or chloride attack. During the carbonation process, a chemical reaction occur when  $CO_2$  from the atmosphere reaches inside the concrete and combines with calcium hydroxide  $Ca(OH)_2$  in the concrete forming calcium carbonate  $CaCO_3$  as illustrated in Eq. 2-1



The above chemical reaction reduces the PH as low as 8.5 at which the passive layer on the steel surface becomes unstable. The carbonation degree is considered

insignificant when relative humidity is below 25% (PCA, 2002). On the other hand, chloride ions attack is the main cause of the passive layer depassivation. The chloride ion which exist in sea water and deicing products penetrate the concrete untill it reaches the steel reinforcement and causes the destruction of the passive layer. There is a certain limit of chloride ion concentration on the steel reinforcemnt surface that destroy the protective layer called “threshold value”(ACI, Building Code Requirements for Structural 2002).

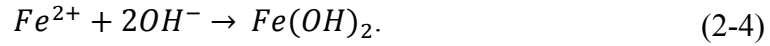
After the protective layer destruction, the presence of oxygen and water acts like a chemical driving force to cause a series of electrochemical reactions. These reactions starts with two main reactions called oxidation-reduction reactions. oxidation-reduction reactions happens simultaneously in two adjacent locations in the steel rebar surface microscopically distanced. and form this reactions, electrochemical cell forms with anode and cathode on the steel surface. In the first half of the chemical cells, the iron in the steel (Fe) loses electrons and changes to ion form ( $Fe^{2+}$ ). This location on the steel surface represent the anodic part of the chemical cells and this reaction called “oxidation reaction” as illustrated in Eq. 2-2



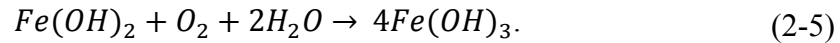
On the other hand, the oxygen with the presence of water receives the released electrons from the oxidation reaction in the adjacent location of the steel surface to induce another chemical reaction which produces hydroxyl ( $OH^{-}$ ). This location on the steel surface represent the cathodic part of the chemical cells and this reaction called “reduction reaction” as illustrated in Eq. 2-3



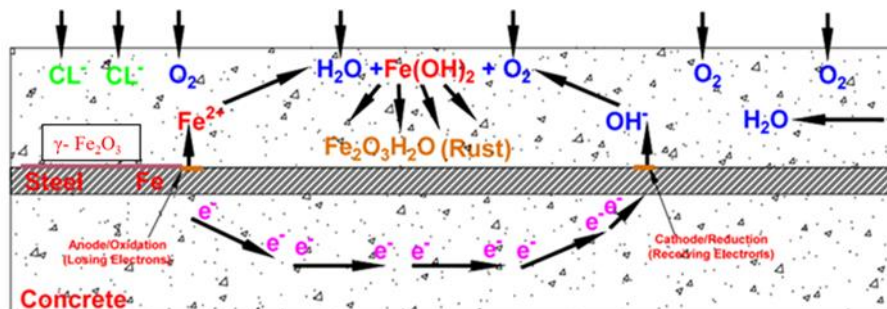
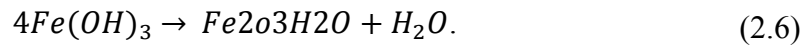
Next to the oxidation and reduction reaction, the resultants of both reactions react to form ferrous hydroxide  $Fe(OH)_2$  as given in Eq. 2-4



With the presence of more water and oxygen, which react with ferrous hydroxide to form ferric hydroxide as illustrated in Eq. 2-5

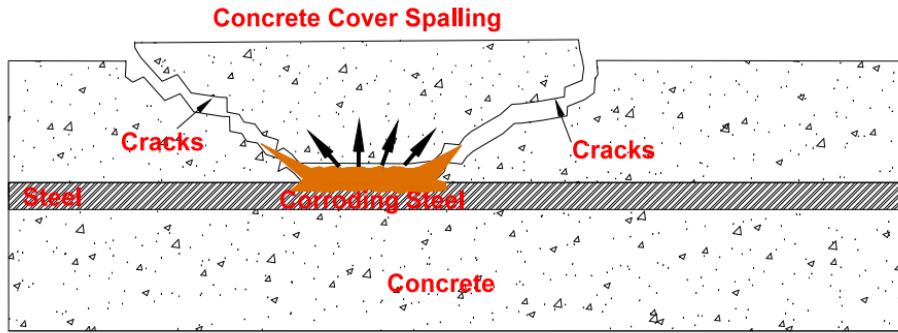


The last product undergoes a dehydration process to produce ferric oxide  $Fe_2O_3 \cdot H_2O$  which is known the final layer of corrosion (rust). This process is illustrated in Eq. 2-6 while the schematic of the steel corrosion processes is illustrated in Fig 2-1.



(a) A schematic illustration of steel corrosion process

Fig. 2-1 (continued on the next page)



(b) Corrosion effects on reinforced concrete

Fig. 2-1: Reinforcing steel corrosion in concrete

As the corrosion proceeds along the surface of the rebar, the rust products increase and cause concentrated stresses on the concrete that led to forming cracks in the concrete in addition to the reduction of the cross section of the reinforcement rebar as shown in Fig 2-1(b). The deterioration of the steel reinforcement rebar depends on the rate of the corrosion which is influenced by the several environmental factors

### **2.3 Enviromental Factors Influencing Corrosion Rate of Reinforcement Rebar in Structures**

The environmental factors which influence the corrosion rate are directly related to one another. The following is a summary of factors influencing the corrosion rate:

1. Dissolved Oxygen: the corrosion rate is directly dependent on the presence of the dissolved oxygen in the cathodic region of the steel reinforcement. Some experimental studies reported that the corrosion in natural water is proportional to the dissolved oxygen content (Walker et al., 1907) and (Speller, 1922). The rate of oxygen supply is interdependent with porosity of the concrete, the relative humidity, concrete cover thickness, and the temperature. According to (Broomfield, 2003), the moisture content in the concrete pores has the greater influence on the dissolved

oxygen supply. The dissolved oxygen from the air into the water solution agitates the surface of water leading to increase in the rate at which oxygen dissolves (Speller, 1951).

2. **Relative humidity:**The corrosion only happens when there is water which is the main reactant consumed in the electrochemical corrosion. The water is reached to the concrete pore from direct exposure to water or from the moisture level in the air (relative humidity). It is worth mentioning that the rate of moisture content causes more damage due to corrosion in the northern side of the United States than the southern side because of the low evaporation rate of the moisture in northern side compared to southern side (Speller, 1951).
3. **Temperature:** such as other chemical reactions, temperature plays significant role in increasing the corrosion rate up to a certain limit. A 10 °C increase in temperature, doubles the chemical reaction rate. However, at a high temperature above 40 °C , the solubility of oxygen is decreased which lead to decrease the corrosion rate (Markeset and Mvrddal, 2008).
4. **Chloride Concentration:** the destruction of the protected layer of reinforcing rebar starts when the chloride penetrates to the surface of the rebar. With increasing the amount of the chloride, the corrosion rate also increases (Markeset and Mvrddal, 2008). The minimum concentration of chloride that will activate the corrosion process is called chloride threshold value. The reported threshold values is highly scattered and the factors that affect this value for specific structure of member are not clear. There are not specific value limits to chloride threshold for a given concrete structure or a member of structure (Angst et al., 2009).

5. In addition the mentioned factor, there are other factors affecting the corrosion rate such as alkalinity and resistivity of the concrete, galvanic interaction between different parts of steel rebar and the effect of the rust formation.

## **2.4 Corrosion Methodology**

There are two techniques to induce corrosion in steel reinforcement namely; natural corrosion and accelerated corrosion. The natural corrosion technique occurs to reinforcement in existing structure subjected to aggressive and corrosive environmental condition or by exposing the specimens to marine water. The effect of natural corrosion due to carbonation or chloride attack on the reinforcement rebar was adopted by (Zhang et al., 1995) and (Morinaga et al., 1996) respectively. However, this type of corrosion may take many years so that the corrosion affect the mechanical properties of the reinforcement rebar significantly. Therefore the electrical accelerated corrosion test is adopted by the researchers to address the effect of corrosion on mechanical properties of the steel reinforcement. This type of corrosion is accelerated to obtain a significant amount of corrosion in a short time period through impressing electrical current to the bare reinforcement (not embedded in concrete) or reinforcement specimens embedded in concrete to accelerate the corrosion process. More details about this type of corrosion are presented in Chapter 3.

## **2.5 Current Code and Standard Provisions on Traditional and Corrosion Resistant Reinforcement Rebar**

### **2.5.1 Carbon-steel reinforcement rebar**

Carbon-steel reinforcement has been considered the most widely used rebar due to the low cost compared with other type of reinforcement rebar. In the United States,

carbon-steel reinforcement rebar used in the civil engineering application must meet the requirements of ASTM A615 (ASTM A615, 2018). This type of steel rebar comes with four grades, grade 40, grade 60, grade 80, and grade 100. The mechanical properties of this type of reinforcement rebar are tabulated in Table 2-1.

Table 2.1: Mechanical properties requirement of carbon-steel reinforcement rebar

Minimum Strength	Grade 40 [280]	Grade 60 [420]	Grade 80 [550]	Grade 100 [690]
Tensile strength KSI [MPa]	60 [420]	90 [620]	105 [725]	115 [790]
Yielding strength KSI [MPa]	40 [280]	60 [420]	80 [550]	100 [690]
Minimum Elongation % in 8 inch [200 mm]				
Rebar designation No.	Grade 40	Grade 60	Grade 80	Grade 100
10	11	9	7	7
12,16	12	9	7	7
20	-	9	7	7
25	-	8	7	7
28,32,36	-	7	6	6
40,50,60	-	7	6	6

Carbon-steel rebar is corrosion resistant because of the alkaline environment of the concrete. However, the passivation of the reinforcement will be compromised when chloride ions reaches the surface of the steel reinforcement. Therefore, this type of reinforcement should be used to in application with low to moderate exposure of deicing products and salt water. Furthermore using the steel reinforcement in structure should meet the requirement ACI318-02 regarding the corrosion protection of steel

reinforcement such as minimum concrete cover, maximum water cementitious, and the soluble chloride ion limit. Table 2-2 illustrates the limit of soluble chloride ion in reinforced concrete for different types of structural members.

Table 2.2: Maximum chloride ion content for corrosion protection of reinforcement.

Type of the member	Maximum water soluble chloride ion (Cl <sup>-</sup> ) in concrete. (% weight of cement)
Prestressed concrete	0.06
Reinforced concrete exposed to chloride in service	0.15
Reinforced concrete that will be dry or protected from moisture in service	1
Other reinforced concrete construction	0.3

The service life of structure with carbon–steel reinforcement can be ranged from 20-100 years depending on the concrete cove and the exposure of corrosive environment. In application, where the structure is exposed to extensive and continues corrosive environment, the use of more corrosion resistant reinforcement such as high chromium and stainless steel reinforcement rebar is necessary to advantage the maximize the service life of the structure.

### 2.5.2 High chromium reinforcement rebar

High chromium steel reinforcement or as known commercially by MMFX, is a special steel reinforcement which has different microstructure from the traditional carbon-steel reinforcement rebar. The design of the microstructure of this steel is

intended to improve the physical and the mechanical properties and as well the corrosion resistance. This steel originally was produced in 2001 at a higher cost than mild steel reinforcement rebar by 0.3 dollar per pound (Barr and Wixom, 2009). MMFX has dark gray-black color as compared to traditional and stainless steel reinforcement in (see Fig. 2-2).

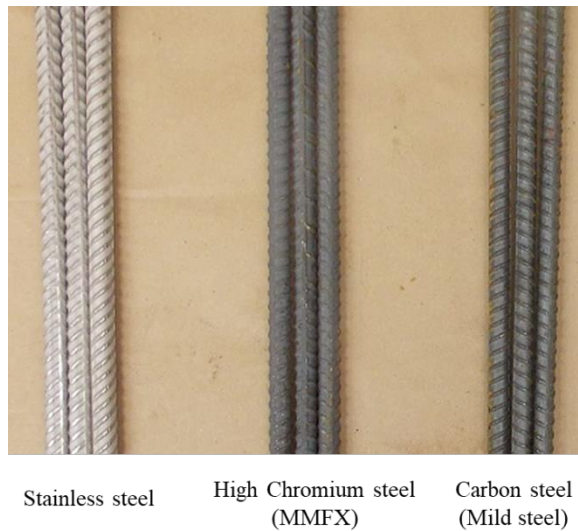


Fig. 2-2: Mild steel, high chromium steel and stainless steel reinforcing rebar

High chromium steel reinforcement rebar used in the civil engineering applications should meet ASTM A1035 (ASTM A1035, 2016). This type of steel rebar comes with three types named as 1035 CL, 1035 CM, and 1035CS depending on the chromium content and each type has two grades, grade 100, and grade120. The chemical composition and mechanical properties of high chromium reinforcement rebar are tabulated in Table 2-3 and Table 2-4.

Table 2.3: Chemical compositions of high chromium steel reinforcement rebar types

Maximum Chemical Composition (weight %)							
Alloy Type	Carbon	Chromium	Manganese	Nitrogen	Phosphorus	Sulfur	Silicon
A1035CL	0.3	2.0-3.9	1.5	0.05	0.035	0.045	0.5
A1035CM	0.2	4.0-7.9	1.5	0.05	0.035	0.045	0.5
A1035CS	0.15	8.0-10.9	1.5	0.05	0.035	0.045	0.5

Table 2.4: Mechanical properties requirement in high chromium reinforcement rebar

Type	A1035CL		A1035CM		A1035CS	
Minimum Strength	Grade 100	Grade 120	Grade 100	Grade 120	Grade 100	Grade 120
	[690]	[830]	[690]	[830]	[690]	[830]
Tensile strength KSI [MPa]	130 [900]	150 [1030]	130 [900]	150 [1030]	130 [900]	150 [1030]
Yielding strength (0.2%) offset KSI [MPa]	100 [690]	120 [830]	100 [690]	120 [830]	100 [690]	120 [830]
Minimum Elongation % in 8 inch [200 mm]						
Rebar designation No	Grade 100	Grade 120	Grade 100	Grade 120	Grade 100	Grade 120
	[690]	[830]	[690]	[830]	[690]	[830]
3 through 11 [10 through 36]	7	7	7	7	7	7
14,18 [43,57]	6	6	6	6	6	6

The corrosion resistance of high chromium reinforcement rebar (MMFX) in the long term tests is limited. However, some researchers reported that the MMFX steel

reinforcement corrodes slower than mild steel and has a chloride threshold limit higher than steel reinforcement by four times (Barr and Wixom, 2009).

### **2.5.3 Stainless steel reinforcement rebar**

Stainless steel reinforcement rebar is well documented in the literature as the most corrosion resistant reinforcement. The anti-corrosion resistance in stainless steel is related to high Chromium and Nickel content in addition to Molybdenum in some types of stainless steel reinforcement. These chemical compositions are critical for the reinforcements resistant to corrosion. Stainless steel reinforcement has high initial cost compared with other reinforcement rebar. Therefore, it has been used in very limited applications. Because of the high corrosion resistant property of stainless steel, the structures reinforced with this type of reinforcement rebar have the potential to extend the service life of structure and lower the cost of maintenance. A study was carried out for FHWA in 1998 reported that stainless steel type 316 can achieve a service life of 75-100 years in bridges. The same study indicated that stainless steel has a corrosion rate 800 times lower than traditional carbon steel rebar therefore it is recommended for use in bridge, tunnel, and marine substructure that are exposed to aggressive and continuous corrosive environment (McDonald, Pefifer and Sherman, 1998).

Stainless steel reinforcement rebar used for the industrial purposes should meet the requirement and guidelines of ASTM A1035. This type of steel rebar is available under three grades: grade 60, grade 75, and grade 80. Each grade has several types due to the variation of its chemical composition. The chemical composition and mechanical properties of stainless steel reinforcement rebar are tabulated in Table 2-5 and Table 2-6 respectively (ASTM A955, 2018).

Table 2.5: Chemical compositions of stainless steel reinforcement rebar types.

Designation	S24000	S24100	S30400	S31603	S31653	S31803
Alloy type	XM-29	XM-28	304	316L	316LN	-
Carbon	0.08	0.15	0.08	0.03	0.03	0.03
Manganese	11.5-14.5	11-14	2	2	2	2
Phosphorus	0.06	0.06	0.045	0.045	0.045	0.03
Sulfur	0.03	0.03	0.03	0.03	0.03	0.02
Silicon	1	1	1	1	1	1
Chromium	17-19	16.5-19	18-20	16-18	16-18	21-23
Nickle	2.25-3.75	0.5-2.5	8-10.5	10-14	10-14	4.5-6.5
Molybdenum	-	-	-	2-3	2-3	2.5-3.5
Nitrogen	0.20-0.40	0.2-0.45	0.1	0.1	0.10-0.16	0.08-0.20

Table 2.6: Mechanical properties requirement in stainless steel reinforcement rebar types.

Minimum Strength	Grade 60 [420]	Grade 75 [520]	Grade 80 [550]
Tensile strength, KSI [MPa]	90 [620]	100 [690]	100 [690]
Yielding strength KSI [MPa]	60 [420]	75 [520]	80 [550]
Minimum Elongation % in 8 inch [200 mm]			
Rebar designation No.	Grade 60 [420]	Grade 75 [520]	Grade 80 [550]
3,4,5 [10,13,16]	20	20	16
6 [19]	20	20	16
7, 8, 9, 10, 11, 14, 18 [22, 25, 29, 32, 36, 43, 57]	20	20	16

As it can be seen in Table 2-5, that the chromium content in stainless steel is range between 16% - 23% which higher than the chromium content in high chromium steel reinforcement which ranges between 2.0% - 10.9% in Table 2-3. The high content of chromium is what gives the stainless steel the characteristic of the highly resistant to corrosion compared to high chromium.

## **2.6 Previous Experimental Studies on Corrosion in Reinforcement Steel Rebar**

### **2.6.1 General**

In the last decades, extensive experimental studies have been carried out on corrosion of steel reinforcement rebar. In these experiments, attempts have been made to evaluate the effect of corrosion on the mechanical properties of corroded rebar namely yielding, ultimate strength, and ductility. Summary of the reported work is illustrated in Table 2-7.

### **2.6.2 Previous experimental studies**

Almusallam (2001) conducted an accelerated corrosion test on 6mm and 12mm ribbed reinforcement steel embedded in concrete with corrosion level ranged between 0%-75%. The study reported that the tensile strength of the steel rebar is not affected by the corrosion levels of the reinforcement when the stress is calculated on the actual corroded cross section. However, when nominal cross section of rebar is utilized in calculating the tensile strength, the specimens strength decreased and did not meet the strength requirement by ASTM A615 when the corrosion level exceed 11% and 24% for 6mm and 12mm reinforcement diameter receptively.

Another experimental study was carried out by (Du et al., 2005) addressed the corrosion of bare and embedded reinforcement steel rebar corroded in range of 0%-25% by accelerated corrosion test indicated that the stress-strain curves of the corroded specimens rebar were similar to uncorroded specimens up to 16% corrosion. The study also reported that reduction of residual yield and ultimate strength of smaller and plain corroded rebar reduce more than larger and ribbed ones. The authors stated that such differences in reduction are not significant. It is important to mention that this study calculated the strength based on the average corroded cross section rebar.

Similar to previous study, (Cairns et al., 2005) conducted an experimental study to two three group of specimens. These groups addressed the influence of stimulated corrosion, chloride accelerated, and electrical accelerated corrosion process respectively on the engineering properties of plain and ribbed steel reinforcement. The specimens in group stimulated corrosion were damaged by removing a part of the cross section to get corrosion cross section loss levels between 5%-50% for ribbed rebar with diameter between 12-24mm. The specimens in chloride accelerated group were plain rebar with a diameter of 16mm embedded in concrete. These specimens were subjected to cyclic wetting/drying for 1 day by 3% salt solution followed by 6 days at 70% relative humidity condition. During the not spray period, the specimens were accelerated by impressing electric from DC supply. Finally the third groups consisted of ribbed steel specimens with 20mm diameter. This group was exposed to electrical accelerated corrosion. The authors represent the corrosion level as maximum cross section loss expressed as percentage of the nominal cross section.

The results from the first group (stimulated corrosion damage) showed that the ultimate and yield force decreased proportionally with decreasing section loss. However ductility reduced significantly, for example 12mm diameter rebar with section loss of 5% and 50% led to reduction in ductility by 30% to 40% and by 80% respectively. On the other hand, the results from the second group (accelerated chloride corrosion) showed that when the stress is calculated on the residual cross section of corroded rebar, there will be no reduction in yield strength and ultimate strength will increase with increasing the cross section loss, for example 7% cross section loss caused increased the ultimate strength by 5.7%. While ductility decreased significantly with increasing the cross section loss. Finally in the last group, electrical accelerated corrosion, the outcome results of the specimens in this group revealed that when the nominal cross section is utilized for stress calculation, all the engineering properties decreased with reduction of maximum section loss.

Another experimental study carried out by (Lee and Cho, 2009) addressed the effect of corrosion for both accelerated corrosion test and accelerated chloride corrosion and carbonation on the mechanical properties of steel reinforcement. The study revealed that specimens corroded by constant electric current tend to have uniform corrosion and accelerated chloride corrosion and carbonation which are done by cyclic chloride wetting and drying under high humidity and high temperature tend to induce pitting corrosion. The outcome of this study showed that the yield and tensile strength which are calculated based on nominal cross section decreased with increase the mass loss. However, the ductility reduces significantly with increase of the mass loss.

Chen Ou et al., (2015) conducted study to recognize the difference between the effect of natural chloride corrosion and electrical accelerated corrosion on the mechanical properties of reinforcement rebar. The authors extracted rebar from a 45year old building on the coastline which is subjected to sea wind to represent the natural chloride corrosion. In addition, they conducted electrical acceleration test on other specimens for mass loss between 0%-31%. This study reported that strength factor of yield and ultimate tensile strength was similar for natural and electrical accelerated corrosion test. However, reduction factor in ductility of electrical accelerated corrosion was much smaller than the reduction factor for ductility in natural corrosion.in addition the study reported also that the rebar sizes effect were not significant. It is worth mentioning that the authors used the nominal cross section of the calculation of stress.

In addition to experimental studies on rebar embedded in concrete, other researchers conducted experiment studies on electrical accelerated corrosion on bare rebar (not embedded in concrete) such as Imperatore et al., (2017) which carried out electrical accelerated test on ribbed specimens rebar for diameters ranged from 8mm to 20mm and to achieve corrosion levels between 0%-53%, the study revealed yield and tensile strength decreased with increase the corrosion levels and as well the ductility, but also stated that the effect of corrosion on ductility of small rebar diameter was significant compared to larger diameter rebar. The authors used nominal cross section area to calculate the stress. Finally the study proposed equations consists of the reduction factor for all the engineering properties of the corroded specimens.

Finally, recent experimental study was conducted by Sun et al., (2018) on electrical accelerated corrosion test on steel rebar for corrosion between 0%-15%. This

study employed 3D-scan of all the corroded specimens to address the effect of pitting on the specimens. The study linked increasing the corrosion rate in the corrosion test with increasing the number and the depth of pitting on corroded specimens. The authors have used the nominal cross section area to calculate the stress. The study also states that with increasing the corrosion the capacity of corroded specimens decreased as well nevertheless the non uniform corrosion has significant influence of the ductility of the corroded specimens

### **2.6.3 Knowledge gap**

The state-of- art review indicated that there are extensive experimental studies on the effect of corrosion on the mechanical properties of the carbon-steel reinforcement rebar type. However, there is lack of experimental data on other types of steel rebar used in concrete structures such as High Chromium and Stainless steels rebar. Also, most of the reported experimental investigations didn't address the effect of pitting attack on the mechanical properties of steel reinforcement or account for it in their proposed equations. This paper present an experimental study on the effect of accelerated corrosion on the engineering properties,namely yield and tensile strength and ductility of steel rebar of mild, high chromium, and stainless steels.

Table 2.7: Summary of previous experimental work of corroded steel reinforcement

Authors	Rebar type	Specimen condition	Rebar diameter (mm)	Corrosion condition	Mass loss range	Yield strength reduction	Ultimate strength reduction
Zhang et al.	Plain	Embedded in concrete	(8-14)	Natural (carbonation)	0-30%	0.0004	0.0005
	Ribbed		(10-25)				
Morinaga et al.	NA	Embedded in concrete	(9 and 13)	Natural (chloride)	0-25%	0.0160	0.0263
Almusallam	Ribbed	Embedded in concrete	(6 and 12)	Electrical accelerated	0-75%	NA	0.0139
Du et al.	Plain	Embedded in concrete/bare	(8 and 16)	Electrical accelerated	0-25%	0.0049	0.0065
	Ribbed	Embedded in concrete/bare	(8, 16, and 32)			0.012	0.015
Cairns et al.	Plain	Embedded in concrete	(16 and 20)	Accelerated (chloride)	0-4%	0.012	0.011
	Ribbed		(20)	Electrical accelerated			
Imperatore and Runaldi	Ribbed	Embedded in concrete/bare	(8 and 15)	Electrical accelerated	0-30%	0.0127	0.0119
Lee and Cho	SD295 A	Embedded in concrete	(13)	Electrical accelerated	0-35%	0.0124	0.0107
	SD345 D		(10 and 13)	Accelerated (chloride)		0.0198	0.0157
Ou et al.	Ribbed	Embedded in concrete	(13, 16, and 19)	Natural (chloride)	6-82%	0.0123	0.0115
			(13 and 29)	Electrical accelerated	0-31%	0.0127	0.0116
Imperatore et al.	Ribbed	bare	(8, 12, 16, and 20)	Electrical accelerated	0-53%	0.0150	0.0138
Sun et al.	Ribbed	bare	14 and 16	Electrical accelerated	0-15%	0.0100	0.0130

## **Chapter Three**

### **CORROSION TEST EXPERIMENTS**

#### **3.1 General**

The literature review presented in chapter 2 reveals adequate studies on the effect of the corrosion on the mechanical properties of the conventional carbon steel rebar at different levels of corrosion up to 80% mass loss. However, there is a lack of experimental data on other types of steel rebar used in concrete structures such as high chromium and stainless steel rebar. These types of steel reinforcement have excellent corrosion resistance. Recently, the uses of these types of corrosion-resistant reinforcements have increased in the reinforced concrete structures subjected to aggressive corrosion environments. To understand the effect of the corrosion on the engineering properties of resistant reinforcement rebar types, an experimental study was carried out to study the effect of accelerated corrosion on the engineering properties of mild, high chromium, and stainless steel reinforcement rebar embedded in concrete. The experimental program consisted of testing 78 different reinforcement rebar specimens with corrosion level range between 1%-17%. The main variable of the experimental work included rebar type, rebar size, and corrosion levels. Full details of specimens, test procedures, and instrumentation are presented in this chapter.

#### **3.2 Test Parameters**

In the experimental work, the test parameters consisted of mass loss range between 0%-15%, steel rebar type (mild steel rebar designated as (MS), high chromium steel rebar designated as (HC), and stainless steel rebar designated as SS), and rebar size (

No.3 and No. 4) with nominal diameter 3/8 inch (9.53) mm and 4/8 inch (1.27)mm respectively. For each test variable, three identical specimens were fabricated.

### 3.3 Experimental Details

#### 3.3.1 Specimens Fabrication

A total of 78 rebar specimens with a length of 16 inches (400mm) were fabricated. These specimens consisted of 18 rebar not embedded in concrete considered as non-corroded control specimens, and 60 rebar specimens embedded in concrete considered as corroded rebar specimens. The embedded specimens were divided into groups based on targeted mass loss. The geometry of the specimens embedded in concrete is shown in Fig 3-1.

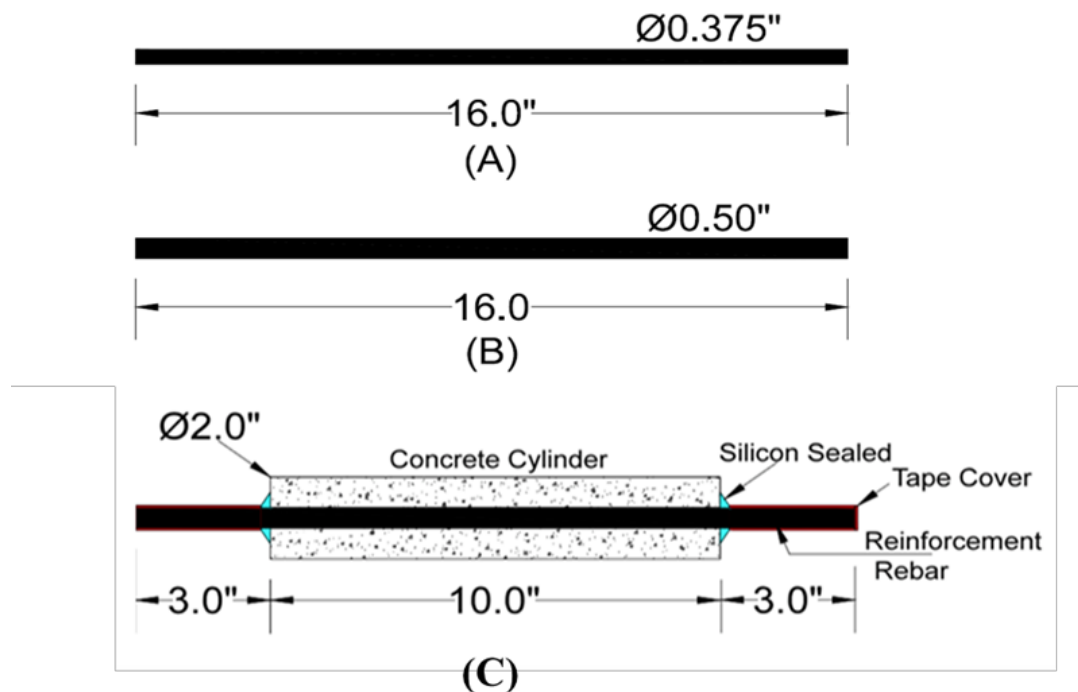


Fig. 3-1: Layout of the test specimen

### 3.3.2 Concrete Compositions

In the experimental work, ordinary Portland cement (OPC) type I was used. This type of cement meets the requirement of ASTM C-150 with a high water-cement ratio (w/c) of 0.5. The aggregate used was according to the requirement of ASTM C-33, with maximum gravel size not exceeding 3/8" due to the size of the specimens. In addition to the concrete compositions, 4% calcium chloride ( $\text{CaCl}_2$ ) by the mass of the cement with the purity of 86% was added to the composition. Summary of the concrete composition's design for one cubic yard is presented in Table 3-1.

Table 3-1: Concrete compositions design for the specimens

Concrete Compositions	Ratio	Weight (lb)
Cement Type I	1	653
Coarse Aggregate	2.04	1332
Fine Aggregate	2.49	1626
Water	0.495	323
Calcium Chloride ( $\text{CaCl}_2$ )	0.04	26.1

### 3.3.3 Chloride Solution

A calcium chloride solution was selected for the accelerated corrosion tests. A product named dowflake calcium chloride with 85% purity was used to prepare the solution. The solution contains 5% chloride ions by the weight of the water. Summary of the one cubic foot solution's preparation is presented in Table 3-2.

Table 3-2: Summary of chloride solution preparation

Solution components	Weight (lb)
Water	62.4
Chloride (cl)	3.1
Calcium Chloride (cacl <sub>2</sub> )	4.9
Dowflake Calcium Chloride 85% Purity	5.7

### 3.3.4 Specimens Preparation Procedures

After the rebar were prepared and designated, cardboard were prepared to be used as concrete molds. The cardboard had an inner diameter of 2.0 inches and length of 10.0 inches. Then a wood framework was prepared to support the cardboards and the rebar. The rebar were placed on the center of cardboard mold and the wood frame was prepared to have 3.0 inches of the rebar from both ends outside the concrete mold. Furthermore, plastic cups were holed in the center for both rebar sizes and placed on both ends of the molds to keep the rebar on the center of the concrete molds. After the wood frame fabrication, the rebar were weighed using a weigh scale with a precision of (0.1g) and placed in the concrete mold. The designation of the test specimens is as shown in Fig 3-2. Then, the test specimens were placed in the wood frame then the concrete was cast vertically as shown in Fig 3-3. After three days of the casting, the wood frame was disassembled, and the specimens were unmolded and they were left for 28 days of curing.



Fig. 3-2: Specimens fabrication



Fig. 3-3: The specimens after casting the concrete

Following the 28 days of curing, the test specimens were prepared for the accelerated corrosion process. In this process, the end parts of the reinforcement outside the concrete cylinder were brushed to remove the remaining concrete from casting. After that, copper cables (Gage14) with the length of 12.0 inches (304.8mm) were attached to both reinforcement ends as shown in Fig 3-4.

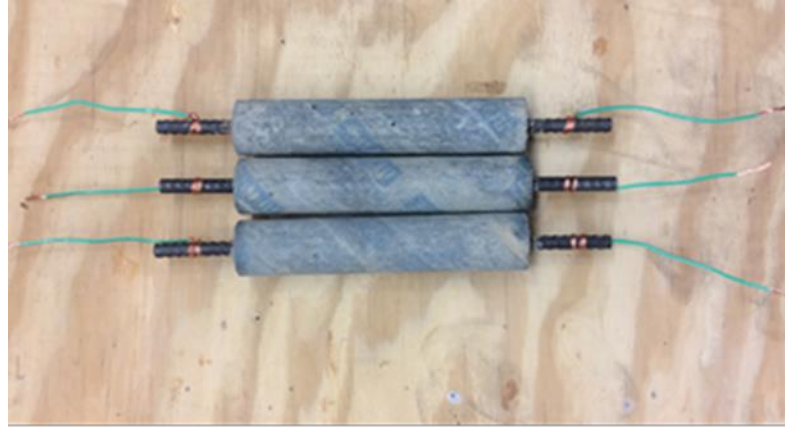


Fig. 3-4: Details of specimens' preparation for accelerated corrosion test

Then both ends of the rebar were wrapped with electric tape to protect them from corrosion. Furthermore, the end-surfaces of concrete cylinders were sealed with silicone glue. This was done to prevent the solution penetrating into the concrete through the end-surfaces of the concrete cylinder during the accelerated corrosion process as seen in Fig 3-5.



Fig. 3-5: Details of specimen ends protection from corrosion

### 3.3.5 Accelerated Corrosion Test Setup

Accelerated corrosion process is a technique used to induce corrosion on embedded steel rebar. This technique is used to achieve high levels of corrosion within a short period of time. This is unlike the natural process of corrosion in the field which takes many years in order to affect the mechanical properties of the reinforcement's rebar. Therefore, in the experimental work, this technique was used to produce corrosion in the test specimens to the targeted levels.

The accelerated corrosion test in this work was based on impressing a current using DC power supply from the anode (positive terminal) which was represented by the rebar specimen to the cathode (negative terminal) through calcium chloride solution (see Fig. 3-7(a)). The cathode was represented by metal with higher corrosion resistance than the test specimens. This was to ensure the occurrence of corrosion in the test specimen rather than the cathode (metal). Therefore, Stainless steel was used as a cathode for Mild steel and High Chromium rebar while, Titanium mesh was chosen as a cathode for Stainless steel rebar as shown in Fig. 3-6. Also, an air pump was used to provide the solution with oxygen that is required to accelerate the corrosion process. The accelerated corrosion test setup for this experiment is illustrated in Fig. 3-7. This process was carried out while the test specimen was immersed into Calcium chloride solution tank which consists of 5% chloride ions. For each specimen, the duration to achieve the targeted mass loss was obtained based on Faraday's law

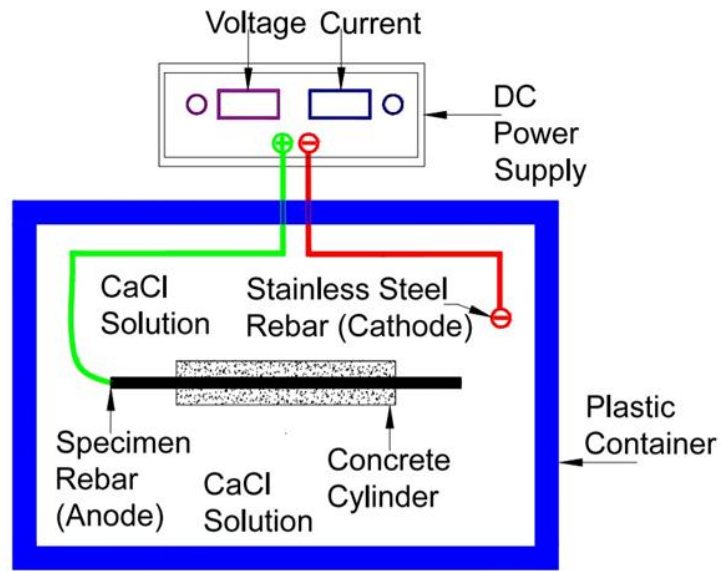
$$m = \frac{Mit}{nF}, \quad (3-1)$$

where (m) is the mass loss due to corrosion (gram), (M) is the atomic weight of steel (55.85gram/mole), (I) is current (Ampere), (n) valence of Fe= (2), (F) is Faraday's constant (96486 Columb/mole), and (t) is the time (second).

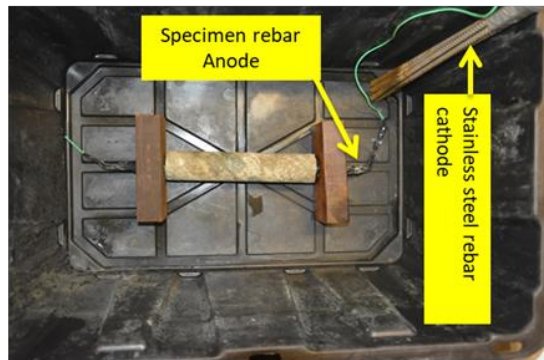
Due to the number of the specimens and the accelerated corrosion setup, high current density was utilized. The current density was varied in the range of  $2500\mu\text{A}/\text{cm}^2$  to  $20000\mu\text{A}/\text{cm}^2$  in the tests for all the types of rebar. In this current range, the prediction of the mass loss calculated from Farady's law was smaller than the experimental mass loss. From the results of experimental and predicted mass loss, an average reduction factor was obtained for each type of rebar. For current density range of  $2500\mu\text{A}/\text{cm}^2$  to  $20000\mu\text{A}/\text{cm}^2$ , reduction factors of 0.73, 0.64, and 0.5 are recommended for calculating the mass loss from Farady's law for mild steel(MS),high chromium(HC), and stainless steel(SS) recepectively.This means that for obtaining a targeted mass loss of 10%, the specimens of mild steel(MS),high chromium(HC), and stainless steel(SS) were subjected to time duration that is needed for getting a mass loss of 13.7%,15.6, and 20% calculated from farady's law.After the accelerated corrosion tests, the test specimens were taken out of the solution, the surrounding concrete was crushed, the steel rebars were cleaned with Clark's solution ASTM G1-03, and then the steel rebars were weighed.



Fig. 3-6: Stainless steel cathodes rebar



(a)



(b)

Fig. 3-7: Accelerated corrosion test setup

### 3.4 Experimental Measurements

The designation of the specimens and test matrix with the corresponding (measured) mass loss level as well as the pitting factor are illustrated in Table 3-3. The following sections explain how the mass loss and pitting factors are calculated.

Table 3-3: Summary of test matrix of rebar specimens

Designation	Mass Loss %	Pitting Factor (PF)	Designation	Mass Loss %	Pitting Factor (PF)	Designation	Mass Loss %	Pitting Factor (PF)
MS-#3-0% Ctrl	0.0	1.0	HC-#3-0% Ctrl	0.0	1.0	SS-#3-0% Ctrl	0.0	1.0
MS-#3-3.1%	3.1	2.9	HC-#3-3.1%	3.1	2.4	SS#3-4.9%	4.9	3.6
MS-#3-3.9%	3.9	1.5	HC-#3-5%	5.0	2.9	SS#3-5.5%	5.5	2.6
MS-#3-5.9%	5.9	3.8	HC-#3-5.9%	5.9	2.2	SS#3-6.3%	6.3	2.2
MS-#3-6.4%	6.4	2.7	HC-#3-7.5%	7.5	2.0	SS-#3-6.8%	6.8	1.8
MS-#3-6.8%	6.8	3.2	HC-#3-7.7%	7.7	2.8	SS-#3-7.3%	7.3	1.7
MS-#3-9.3%	9.3	2.4	HC-#3-8.9%	8.9	2.0	SS#3-9.0%	9.0	2.2
MS-#3-9.6%	9.6	2.2	HC-#3-9.2%	9.2	2.4	SS#3-10.7%	10.7	1.8
MS-#3-9.7%	9.7	2.4	HC-#3-15.4%	15.4	1.4	SS#3-11.9%	11.9	1.7
MS-#3-12.1%	12.1	2.8	HC-#3-16.7%	16.7	2.2	SS#3-15.6%	15.6	1.9
MS-#3-12.4%	12.4	1.6	HC-#4-0% Ctrl	0.0	1.0	SS#3-16%	16.0	1.6
MS-#3-16.4%	16.4	1.7	HC-#4-2.0%	2.0	2.2	SS#3-16.1%	16.1	2.3
MS-#4-0% Ctrl	0.0	1.0	HC-#4-2.9%	2.9	2.9	SS-#4-0% Ctrl	0.0	1.0
MS-#4-2.5%	2.5	2.5	HC-#4-3.1%	3.1	2.5	SS-#4-1.0%	1.0	1.7
MS-#4-3.0%	3.0	2.2	HC-#4-4.8%	4.8	2.4	SS-#4-3.2%	3.2	2.6
MS-#4-4.0%	4.0	2.9	HC-#4-6.1%	6.1	1.5	SS-#4-4.3%	4.3	1.4
MS-#4-4.4%	4.4	2.2	HC-#4-9.0%	9.0	1.6	SS-#4-7.6%	7.6	3.4
MS-#4-4.8%	4.8	1.6	HC-#4-9.4%	9.4	2.1	SS-#4-7.7%	7.7	3.6
MS-#4-7.1%	7.1	1.7	HC-#4-9.8%	9.8	3.5	SS-#4-9.2%	9.2	1.9
MS-#4-9.6%	9.6	2.3	HC-#4-10.5%	10.5	2.0	SS-#4-10.1%	10.1	2.4
MS-#4-10.3%	10.3	2.1	HC-#4-14.7%	14.7	2.6	SS-#4-11.3%	11.3	2.5
MS-#4-14.3%	14.3	2.2	HC-#3-0% Ctrl	0.0	1.0	SS-#4-13.8%	13.8	2.4
MS-#4-17.5%	17.5	1.6	HC-#3-3.1%	3.1	2.4	SS-#3-0% Ctrl	0.0	1.0

### 3.4.1 Mass Loss (ML)

The amount of the corrosion (mass loss %) was calculated based on the weight of the steel reinforcement rebar prior to the corrosion process and weight of the steel reinforcement rebar after it was corroded and cleaned in Clark's solution as described in ASTM G1-03 . The mass loss percentage was determined from the following relation

$$Mass\ loss\ (ML\%) = \frac{(W_i - W_f)}{W_i} 100\% , \quad (3-2)$$

where ML% is the percentage of the mass loss (corrosion) of the reinforcement,  $W_i$  is the weight of the steel reinforcement rebar before the corrosion process and  $W_f$  is the weight of the steel reinforcement rebar after it was corroded and cleaned in Clark solution.

### 3.4.2 Residual Cross Section of Corroded Rebar (Volume Measurement)

The cross section of the corroded rebar was calculated by volume measurement method. This method is based on the assumption that the volume of the corroded reinforcement rebar immersed in a tube of water is equal to the volume of the displaced water from the tube. The volume measurement setup is shown in Fig. 3-8. To apply this, the test rebar specimens were divided into many segments of 0.5inch (12.5mm) length. Each segment was immersed in a tube full of water and the displaced water was weighted. From the displaced water weight, the cross section diameter of the corroded rebar for each segment was calculated using the following equation (Du el al.,2005)

$$D_{corr.} = \sqrt{\frac{4(\Delta W_w)}{\pi \gamma_w (\Delta l)}} , \quad (3.3)$$

where  $D_{corr}$  is the average diameters of each segment of the corroded rebar from the volume measurement (in.) (mm),  $(\Delta l)$  is the length of each 0.5inch (12.5mm) segment of the corroded rebar immersed gradually into the water,  $\gamma_w$  is the density of tap water and it is equal to  $0.001\text{gram/mm}^3$ ,  $\Delta W_w$  is the weight of the displaced water in grams from the tube to the collective water container on the side of the tube.

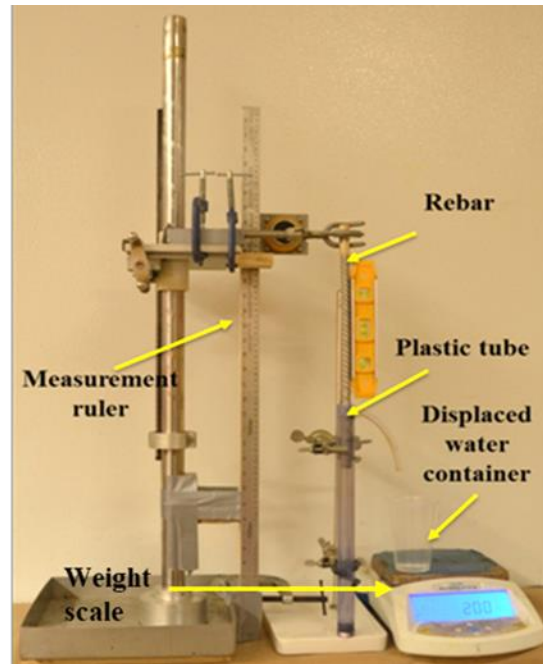


Fig. 3-8: Volume measurements of corroded steel rebar specimens

The residual cross sectional of the corroded specimen (MS-#3-16.4%) from the volume measurement method is shown in Fig. 3-9. In this figure, the varied line represents the corroded diameter calculated from the volume measurement for each 0.5 inch segment, while the average diameter dashed line represents the summation of the corroded diameter of all segments in single steel rebar divided by the number of the segments along the rebar length. In this profile, the average diameter was also calculated from mass loss (weight of steel rebar) which is represented by a dashed line. From the given profile, it can be seen that the average diameter calculated from both methods is in good agreement. Finally, the upper dashed line represents the nominal diameter of the uncorroded rebar. The residual cross sectional profile of other corroded test specimens are given in the Appendix.

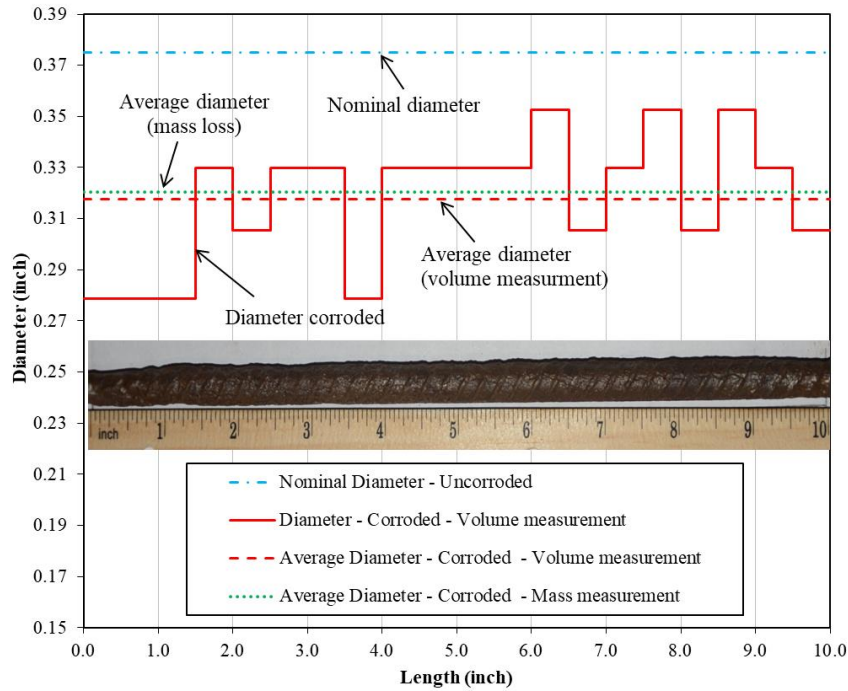


Fig. 3-9: The residual cross sectional of corroded specimen MS-#3-16.4% using volume measurement method

### 3.4.3 Pitting Factor (PF)

The extent of corrosion distribution along steel rebar can be measured by Pitting factor which is defined as the ratio of the maximum corrosion penetration to the average corrosion along the steel rebar length as illustrated in Fig. 3-10. The pitting factor for corroded steel rebar can be calculated from

$$Pitting\ factor\ (PF) = \frac{(D_{nominal} - D_{min.\ corr.})}{(D_{nominal} - D_{avg.\ corr.})}, \quad (3-4)$$

where  $D_{nominal}$  is the nominal diameter of the rebar,  $D_{(avg.\ corr.)}$  is equal to summation of  $D_{corr.}$  of all segments in a single steel rebar divided by the number of the segments along the rebar length, while  $D_{(min.corr.)}$  is equal to the minimum  $D_{corr.}$  measured among the segments.

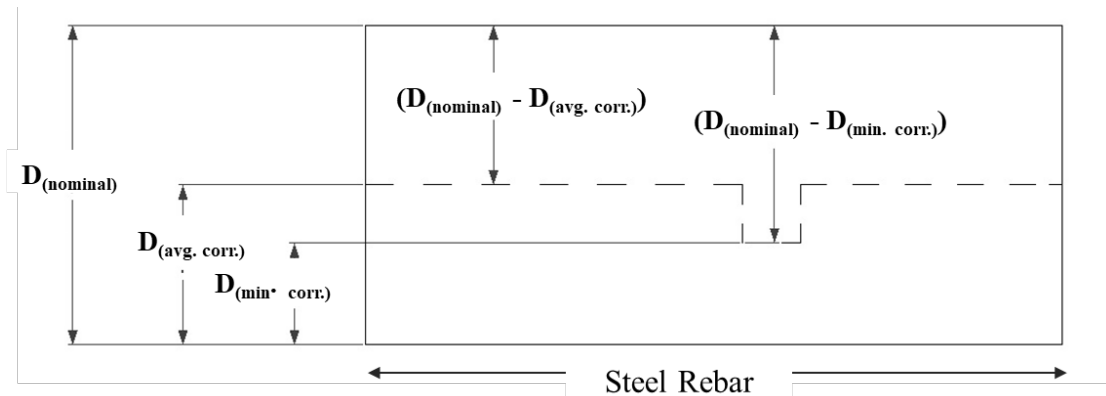


Fig. 3-10: Schematic illustration of pitting factor

### 3.5 Tensile Strength Test

Uniaxial tensile test of the reinforcement specimens was carried out according to ASTM E8/E8M-16. The test setup was comprised of the 110 kips (489.3 KN) MTS testing frame, the data acquisition system, and an electrical extensometer. The MTS was programmed to control the test under displacement and applying incremental displacement at a rate of 0.07 inch/min (1.78 mm/min). The data acquisition was programmed to record the applied loading and the corresponding elongation of the specimen from the extensometer. The extensometer with a gauge length of 8.0 inches (203 mm) was employed to record the elongation of the reinforcement till rupture. The tensile test setup of the reinforcement specimens is shown in Fig. 3-11.



Fig. 3-11: Test setup for tensile strength tests of corroded steel rebars

### **3.6 Summary**

Accelerated corrosion tests are carried out to study the effect of corrosion on the engineering properties of steel reinforcement rebars in order to evaluate the reduction in the engineering properties including; yielding and ultimate strength and ductility due to corrosion. As part of the experimental work, three sets of concrete embedded specimens of mild, high chromium, and stainless steels are fabricated from two rebar sizes No. 3 and No. 4 for mass loss level of 1%-17%. Then test specimens are subjected to accelerated corrosion and the mass loss and pitting factor is calculated by weight and volume measurement methods. Following the accelerated corrosion process, the corroded steel reinforcement specimens are tested for tensile strength.

## **Chapter Four**

### **RESULTS AND DISCUSSIONS**

#### **4.1 General**

As it was illustrated in the review of the literature in Chapter two, corrosion can affect the engineering properties of steel reinforcement rebar. Most of the previous studies have been done on carbon steel reinforcement rebar and there is lack of experimental data on the other types of reinforcements that are commonly used in concrete steel structures.

To fill the knowledge gap, a comprehensive experimental study was carried out to address the effect of the corrosion on engineering properties of high chromium and stainless reinforcement in addition to the mild steel reinforcement rebar. The experimental program performed accelerated corrosion test on embedded reinforcement rebars. Details of the tensile tests were undertaken on the specimens and presented in this chapter. The experimental investigation includes; stress- strain response, yielding and tensile strength, and ultimate strain of the specimens. Results from the tests are employed to propose relations between the mass loss percentage and engineering properties of the tested specimens.

#### **4.2 Experimental Results**

In the experimental work, sets of tensile strength tests are carried out using mild, (MS), high chromium (HC), and stainless steels (SS) rebars of diameter sizes of No. 3 and No. 4 for mass loss level of 1%-17%.

### **4.3 Effect of Steel Type on Engineering Properties**

#### **4.3.1 Stress-strain response**

The stress-strain response of all three types of corroded reinforcement at various mass loss levels were evaluated using data from tensile tests. The displacements recorded at different load levels from tensile tests were utilized to plot stress-strain curves for mild steel, high chromium, and stainless steel (MS, HC, and SS). The stress-strain curves for these types of steel at different mass loss levels are plotted in Figs. 4-1, 4-2, and 4-3, in which the stresses are calculated based on nominal steel cross sectional area un corroded reinforcement. From these figures, it can be seen that the general trend of stress-strain response is linear elastic up to yielding. The stress at which yielding occurs is varying with mass loss levels. Past the yielding stress, steel undergoes plastic deformation with increasing stress up to ultimate stress point. Following that the plastic deformation continues up to rupture. Well-defined yield plateau is recorded for MS steel except for mass loss level above 14%, this is unlike HC and SS steels that showed no clear yield plateau for all mass loss levels. The absence of distinct yield plateau of high chromium and stainless steel rebars is linked to the characteristic of the high strength of these reinforcement types.

From the stress-strain curves, the yield stress is evaluated based on strain level of 0.2%, while the ultimate stress is defined as the maximum stress reached during the tensile strength tests. The significant points on stress-strain curves namely yield strength, tensile strength, and ductility (ultimate strain) from the tensile strength test of corroded MS, HC, and SS steel rebars are summarized in Tables 4-1, 4-2, and 4-3. The yield and ultimate strength reduction factors given in the tables are the ratios of yield and ultimate strengths of corroded rebars to that of non-corroded ones. The ductility of reinforcement

was evaluated using the percentage of elongation at rupture. These values at various mass loss levels are also tabulated in Tables 4-1, 4-2, and 4-3.

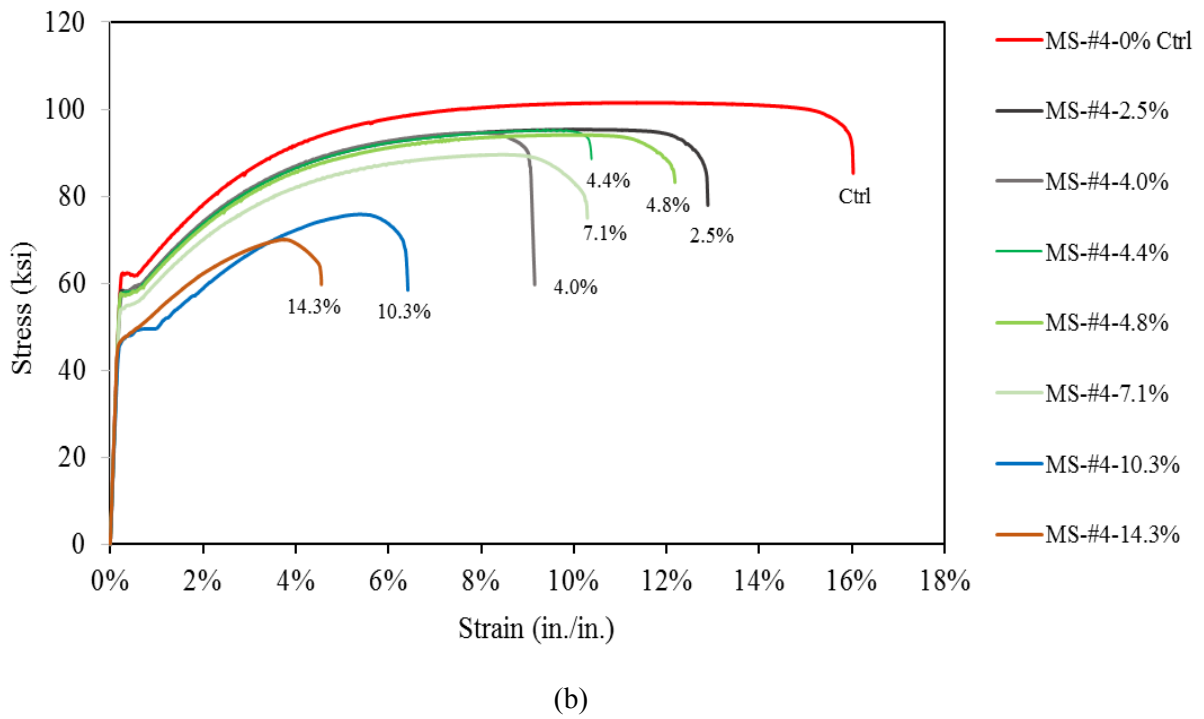
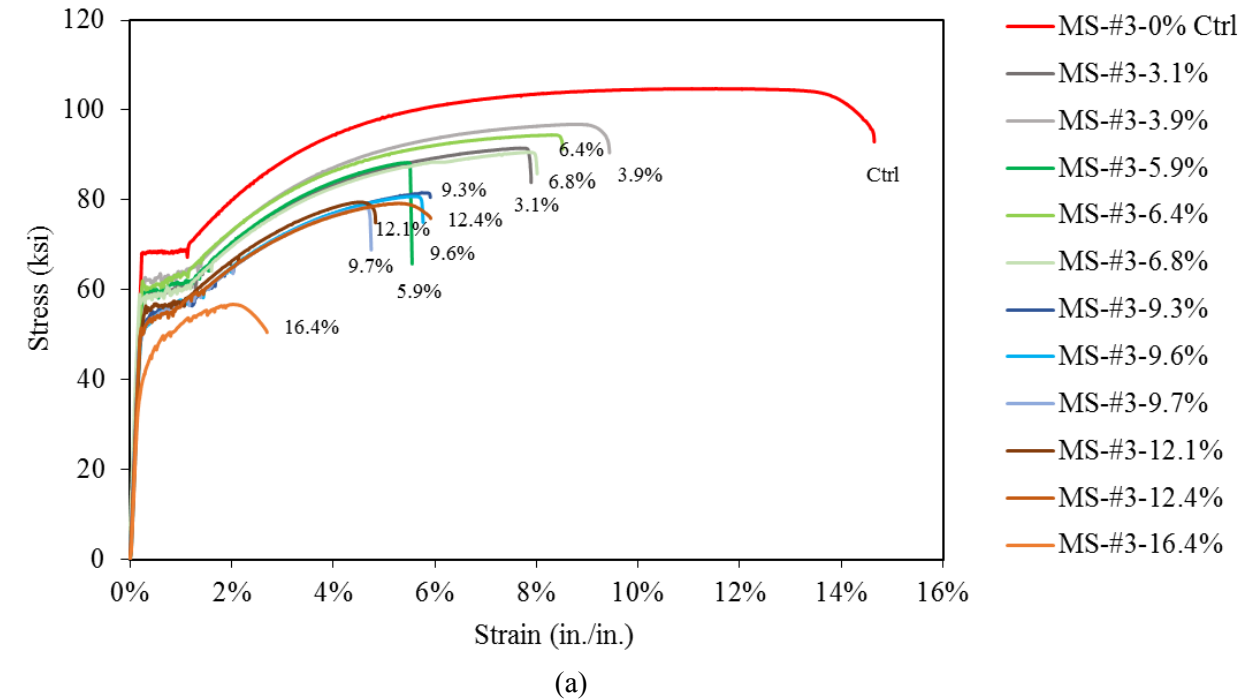
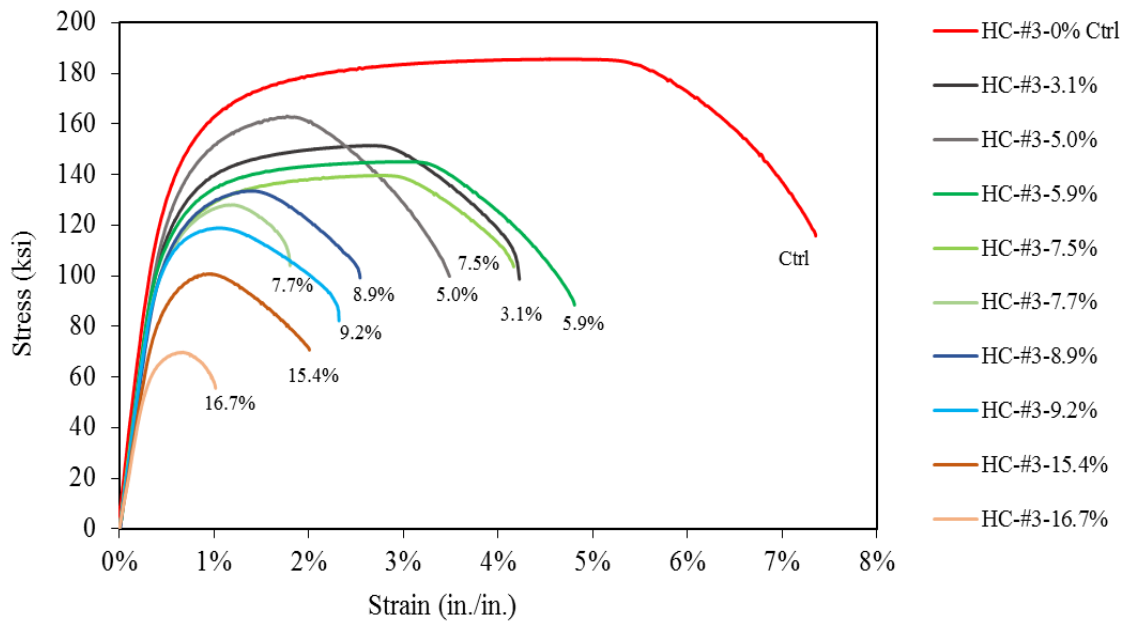
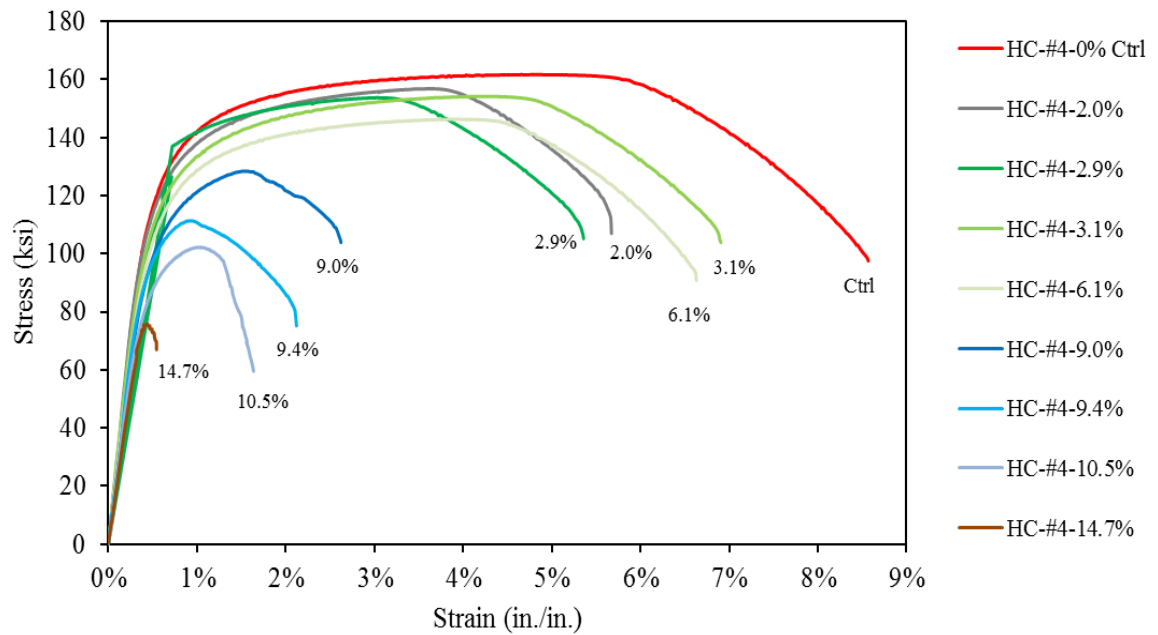


Fig. 4-1: Stress-strain curves of mild steel (MS) at various mass loss levels

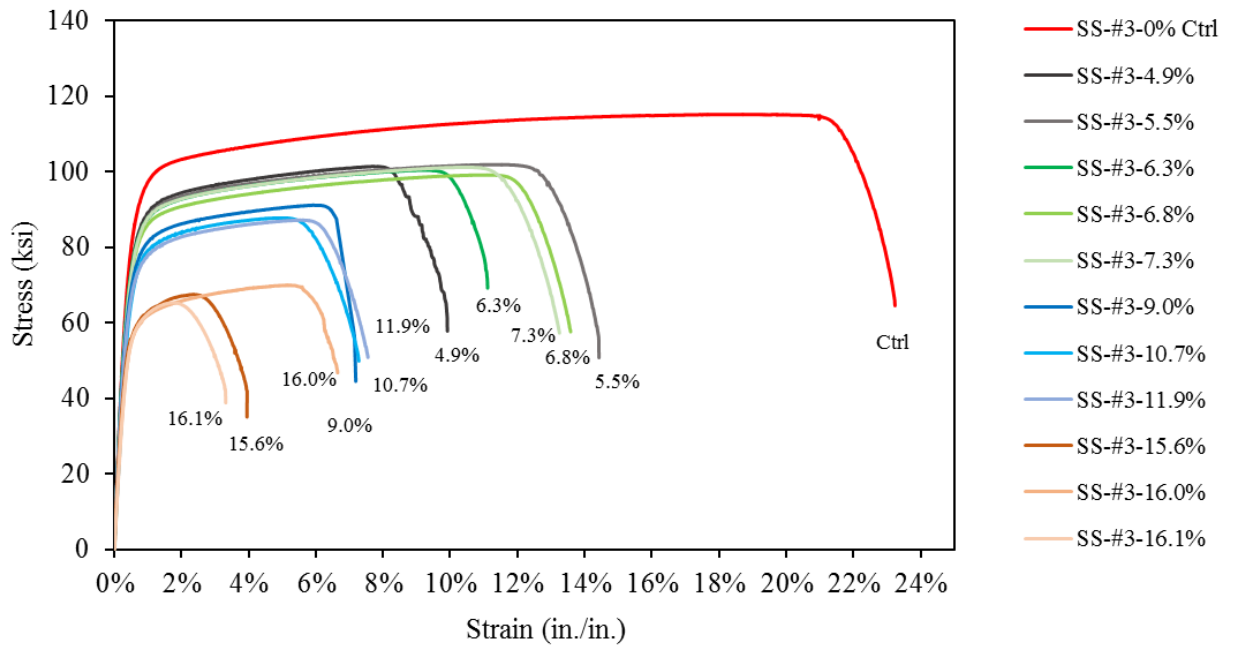


(a)

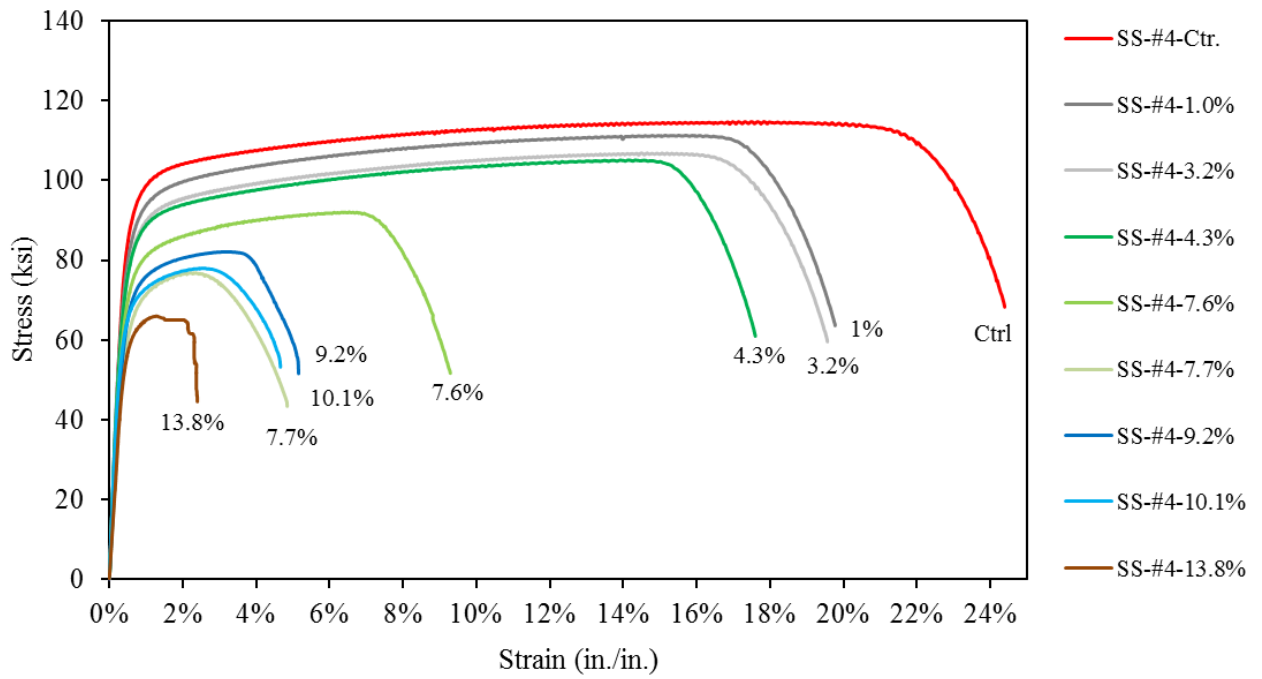


(b)

Fig. 4-2: Stress-strain curves of high chromium steel (HC) at various mass loss levels



(a)



(b)

Fig. 4-3: Stress-strain curves of stainless steel (SS) at various mass loss levels

Table 4-1: Summary of accelerated corrosion test on mild steel rebar

Designation	Mass Loss %	Pitting Factor (PF)	Yield Strength ( $f_y$ ) ksi	Ultimate Strength ( $f_u$ ) ksi	Strain at Rupture ( $\epsilon_u$ ) in./in.	( $f_{y,Corr.}/f_{y,Ctr.}$ )	( $f_{u,Corr.}/f_{u,Ctr.}$ )	( $\epsilon_{u,Corr.}/\epsilon_{u,Ctr.}$ )
MS-#3-0% Ctrl	0.0	1.0	67.4	104.1	0.151	1.00	1.00	1.00
MS-#3-3.1%	3.1	2.9	59.2	91.5	0.079	0.88	0.88	0.52
MS-#3-3.9%	3.9	1.5	61.8	96.8	0.094	0.92	0.93	0.62
MS-#3-5.9%	5.9	3.8	59.5	88.3	0.056	0.88	0.85	0.37
MS-#3-6.4%	6.4	2.7	61.3	94.4	0.085	0.91	0.91	0.56
MS-#3-6.8%	6.8	3.2	56.0	79.5	0.048	0.83	0.76	0.32
MS-#3-9.3%	9.3	2.4	54.8	81.6	0.059	0.81	0.78	0.39
MS-#3-9.6%	9.6	2.2	53.0	80.8	0.058	0.79	0.78	0.38
MS-#3-9.7%	9.7	2.4	53.0	78.3	0.047	0.79	0.75	0.31
MS-#3-12.1%	12.1	2.8	50.0	79.5	0.048	0.74	0.76	0.32
MS-#3-12.4%	12.4	1.6	50.7	79.2	0.059	0.75	0.76	0.39
MS-#3-16.4%	16.4	1.7	44.1	56.7	0.027	0.65	0.55	0.18
MS-#4-0% Ctrl	0.0	1.0	62.1	101.4	0.160	1.00	1.00	1.00
MS-#4-2.5%	2.5	2.5	58.3	95.4	0.129	0.94	0.94	0.80
MS-#4-3.0%	3.0	2.2	57.5	94.4	NA	0.93	0.93	NA
MS-#4-4.0%	4.0	2.9	57.2	94.6	0.092	0.92	0.93	0.57
MS-#4-4.4%	4.4	2.2	58.0	95.3	0.104	0.93	0.94	0.65
MS-#4-4.8%	4.8	1.6	57.4	94.1	0.122	0.92	0.93	0.76
MS-#4-7.1%	7.1	1.9	55.0	89.5	0.103	0.89	0.88	0.64
MS-#4-9.6%	9.6	2.3	55.0	77.9	NA	0.89	0.77	NA
MS-#4-10.3%	10.3	2.1	48.0	75.8	0.064	0.77	0.75	0.40
MS-#4-14.3%	14.3	2.2	47.8	70.1	0.046	0.77	0.69	0.28
MS-#4-17.5%	17.5	1.6	40.2	65.7	NA	0.65	0.65	NA

Table 4-2: Summary of accelerated corrosion test on high chromium steel rebar

Designation	Mass Loss %	Pitting Factor (PF)	Yield Strength ( $f_y$ ) ksi	Ultimate Strength ( $f_u$ ) ksi	Strain at Rupture ( $\epsilon_u$ ) in./in.	( $f_{y,Corr.}/f_{y,Ctr.}$ )	( $f_{u,Corr.}/f_{u,Ctr.}$ )	( $\epsilon_{u,Corr.}/\epsilon_{u,Ctr.}$ )
HC-#3-0% Ctrl	0.0	1.0	142.0	176.6	0.069	1.00	1.00	1.00
HC-#3-3.1%	3.1	2.4	126.0	151.4	0.042	0.89	0.86	0.61
HC-#3-5%	5.0	2.9	135.5	163.1	0.035	0.95	0.92	0.51
HC-#3-5.9%	5.9	2.2	121.0	145.1	0.048	0.85	0.82	0.70
HC-#3-7.5%	7.5	2.0	115.0	139.7	0.042	0.81	0.79	0.61
HC-#3-7.7%	7.7	2.8	113.8	128.0	0.018	0.80	0.72	0.26
HC-#3-8.9%	8.9	2.0	117.0	133.6	0.025	0.82	0.76	0.37
HC-#3-9.2%	9.2	2.4	111.0	118.9	0.023	0.78	0.67	0.34
HC-#3-15.4%	15.4	1.4	95.0	100.7	0.020	0.67	0.57	0.29
HC-#3-16.7%	16.7	2.2	68.3	69.8	0.010	0.48	0.39	0.15
HC-#4-0% Ctrl	0.0	1.0	127.4	162.4	0.085	1.00	1.00	1.00
HC-#4-2.0%	2.0	2.2	122.0	156.8	0.057	0.96	0.97	0.67
HC-#4-2.9%	2.9	2.9	121.0	153.7	0.054	0.95	0.95	0.63
HC-#4-3.1%	3.1	2.5	118.0	154.1	0.069	0.93	0.95	0.81
HC-#4-4.8%	4.8	2.4	119.3	143.0	NA	0.94	0.88	NA
HC-#4-6.1%	6.1	1.5	115.7	146.3	0.066	0.91	0.90	0.78
HC-#4-9.0%	9.0	1.6	108.6	128.4	0.026	0.85	0.79	0.31
HC-#4-9.4%	9.4	2.1	106.0	111.3	0.021	0.83	0.69	0.25
HC-#4-9.8%	9.8	3.5	107.0	108.3	NA	0.84	0.67	NA
HC-#4-10.5%	10.5	2.0	93.3	102.2	0.016	0.73	0.63	0.19
HC-#4-14.7%	14.7	2.6	70.0	75.8	0.005	0.55	0.47	0.06

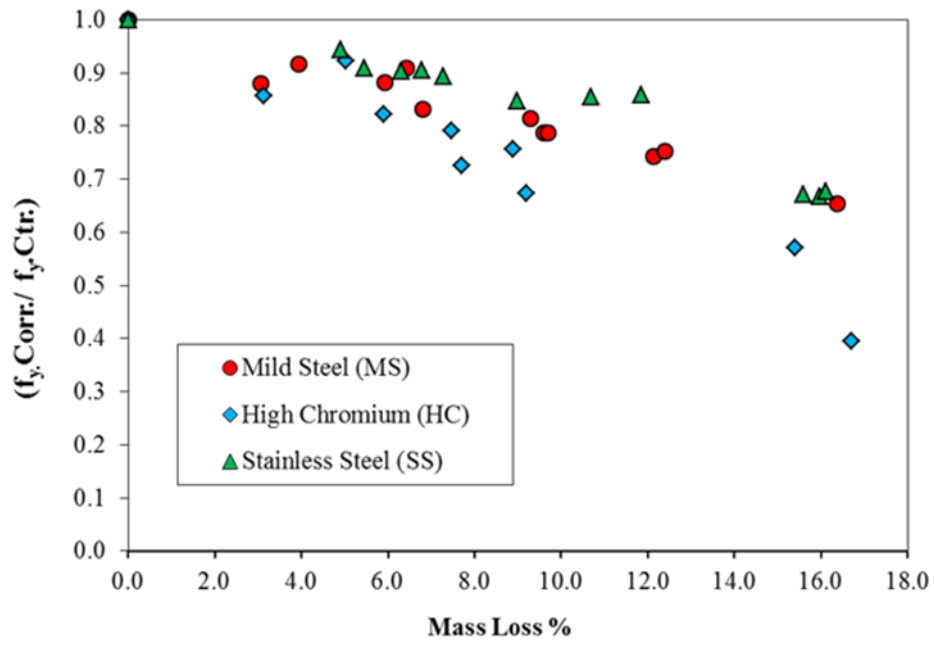
Table 4-3: Summary of accelerated corrosion test on stainless steel rebar

Designation	Mass Loss %	Pitting Factor (PF)	Yield Strength ( $f_y$ ) ksi	Ultimate Strength ( $f_u$ ) ksi	Strain at Rupture ( $\epsilon_u$ ) in./in.	( $f_{y,Corr.}/f_{y,Ctr.}$ )	( $f_{u,Corr.}/f_{u,Ctr.}$ )	( $\epsilon_{u,Corr.}/\epsilon_{u,Ctr.}$ )
SS-#3-0% Ctrl	0.0	1.0	85.0	115.1	0.232	1.00	1.00	1.00
SS#3-4.9%	4.9	3.6	80.3	101.3	0.099	0.94	0.88	0.43
SS#3-5.5%	5.5	2.6	77.3	101.8	0.144	0.91	0.88	0.62
SS#3-6.3%	6.3	2.2	76.8	100.4	0.111	0.90	0.87	0.48
SS-#3-6.8%	6.8	1.8	77.0	99.1	0.136	0.91	0.86	0.58
SS-#3-7.3%	7.3	1.7	76.0	101.2	0.132	0.89	0.88	0.57
SS#3-9.0%	9.0	2.2	72.0	91.1	0.072	0.85	0.79	0.31
SS#3-10.7%	10.7	1.8	72.7	87.7	0.073	0.86	0.76	0.31
SS#3-11.9%	11.9	1.7	73.0	87.1	0.076	0.86	0.76	0.33
SS#3-15.6%	15.6	1.9	57.0	67.5	0.040	0.67	0.59	0.17
SS#3-16%	16.0	1.6	56.8	69.9	0.066	0.67	0.61	0.29
SS#3-16.1%	16.1	2.3	57.5	65.3	0.033	0.68	0.57	0.14
SS-#4-0% Ctrl	0.0	1.0	90.0	114.6	0.244	1.00	1.00	1.00
SS-#4-1.0%	1.0	1.7	83.0	111.3	0.198	0.92	0.97	0.81
SS-#4-3.2%	3.2	2.6	78.5	106.9	0.196	0.87	0.93	0.80
SS-#4-4.3%	4.3	1.4	80.7	105.1	0.176	0.90	0.92	0.72
SS-#4-7.6%	7.6	3.4	72.5	92.1	0.093	0.81	0.80	0.38
SS-#4-7.7%	7.7	3.6	64.6	76.8	0.048	0.72	0.67	0.20
SS-#4-9.2%	9.2	1.9	69.5	82.1	0.052	0.77	0.72	0.21
SS-#4-10.1%	10.1	2.4	66.0	78.0	0.047	0.73	0.68	0.19
SS-#4-11.3%	11.3	2.5	62.8	75.6	NA	0.70	0.66	NA
SS-#4-13.8%	13.8	2.4	60.4	66.0	0.024	0.67	0.58	0.10

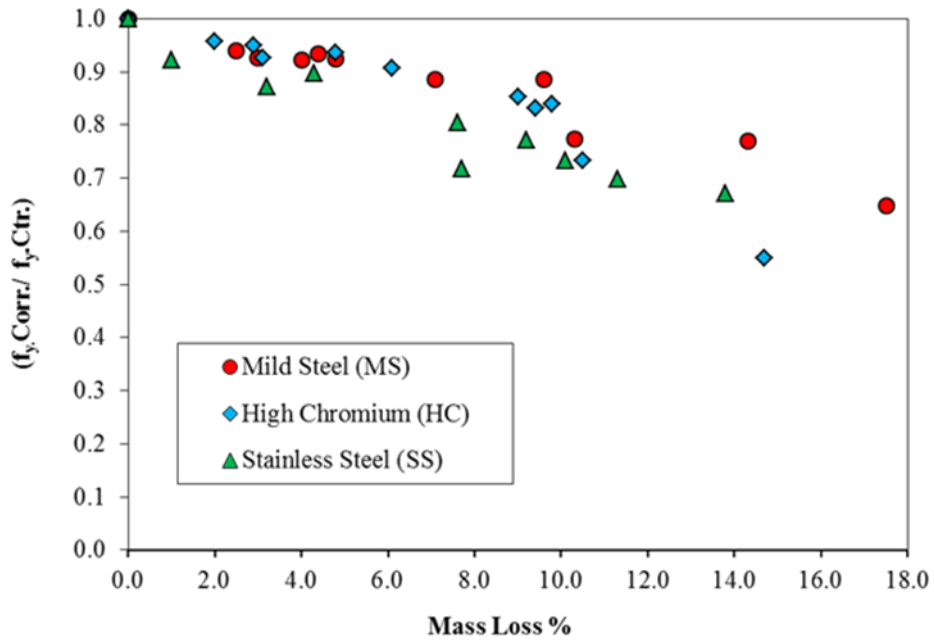
### 4.3.2 Yield strength

The effect of steel type on the yield strength of corroded steel rebar is shown in Fig.4-4, in which the ratio of residual yield strengths of corroded rebars to the yield strength of the uncorroded ones are plotted against mass loss levels for both No. 3 and No. 4 rebar. It can be seen from Fig.4-4(a), that with increasing the corrosion level (mass loss), yield strength, of all types of steel rebar (No. 3) decreases significantly. The extent

of yield strength reduction for mild steel is similar to that of high chromium and stainless steel with slight variation for mass loss up to 10%. This variation increases in the case of high chromium steel especially for mass loss beyond 12%. Furthermore, when the mass loss is above 16%, mild and stainless steels show 32% reduction in the yield strength, compared to 40% reduction in the case of high chromium steel. Overall, mild and stainless steels show less degradation in the yield strength as compared to high chromium steel. While No. 4 stainless steel exhibits a higher reduction in yield strength in all mass loss levels as compared to the mild and high chromium steels as shown in Fig. 4-4(b).



(a) Rebar size No. 3

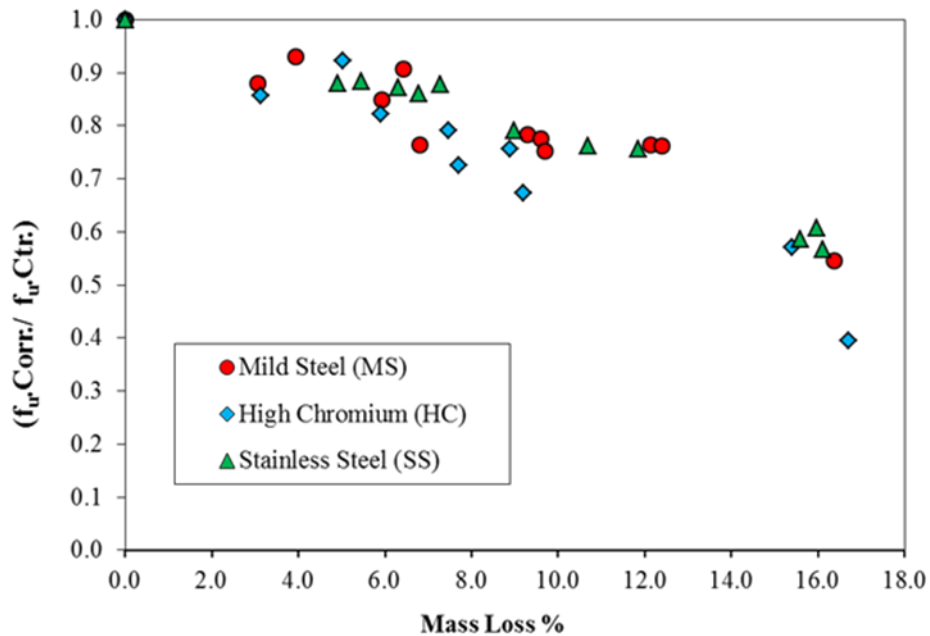


(b) Rebar size No. 4

Fig. 4-4: Effect of steel type on the yielding strength of corroded rebars

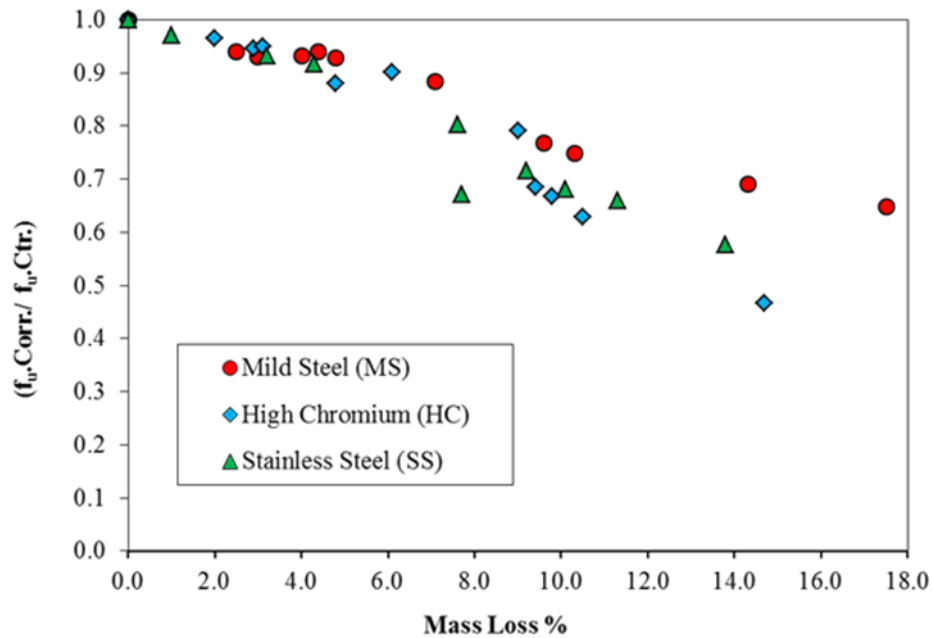
### 4.3.3 Ultimate strength

The trend of residual ultimate strength for three types of corroded steel is plotted in Fig. 4-5, in which the ratio of the ultimate strength of corroded rebar to the ultimate strength of uncorroded ones is presented against mass loss levels for both No. 3 and No. 4 rebar. It can be seen that there is less variation in the ultimate reductions for all three types of steel, compared to yield strength. However, the ultimate strength of these types of steel is more influenced by the mass loss than the yield strength. All three types of steel rebar (No. 3 and No. 4) experienced a reduction of the ultimate strength by about 45% for mass loss of 15%.



(a) Rebar size No. 3

Fig. 4-5 (continued on the next page)



(b) Rebar size No. 4

Fig. 4-5: Effect of steel type on the ultimate strength of corroded rebar

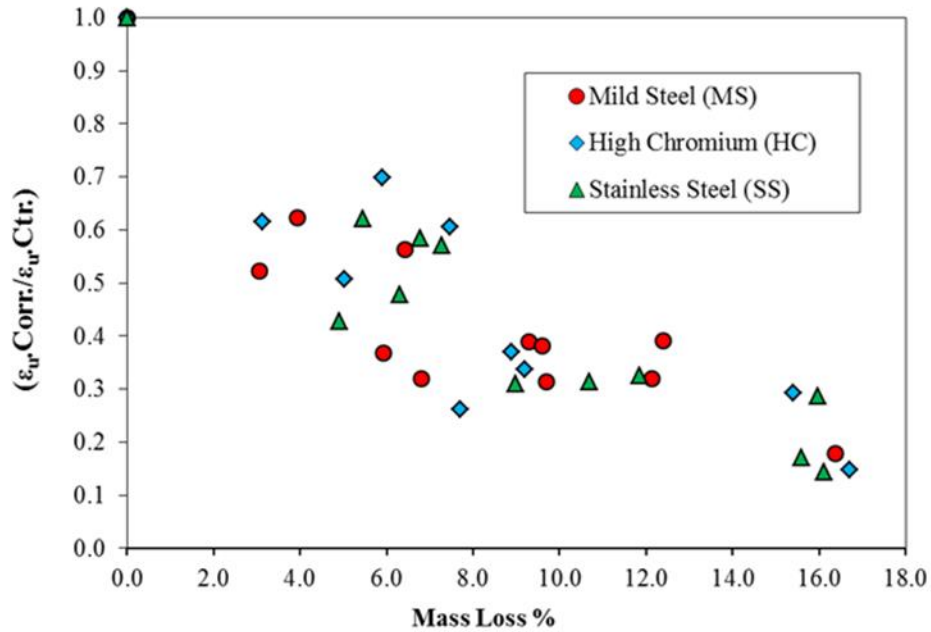
#### 4.3.4 Ductility (ultimate strain)

The effect of corrosion level (mass loss) on the ductility (ultimate strain) for mild steel, high chromium, and stainless steel for both rebar size (No. 3 and No. 4) is shown in Fig. 4-6 in which the ductility ratio deduction was plotted versus the mass loss levels. It can be seen, generally, the ductility ratio of all three types of steels decreases with the increasing of the mass loss level. The relative increasing in ductility observed with increasing mass loss levels (between 4%-10% mass loss) can be attributed to the fact that increasing mass loss is not the only factor that affects the ductility response of these three types of steel.

The other factor that influences the ductility of these steel types is the pitting factor of the tested steel rebars and this can be well seen from Tables 4-1, 4-2, and 4-3. It

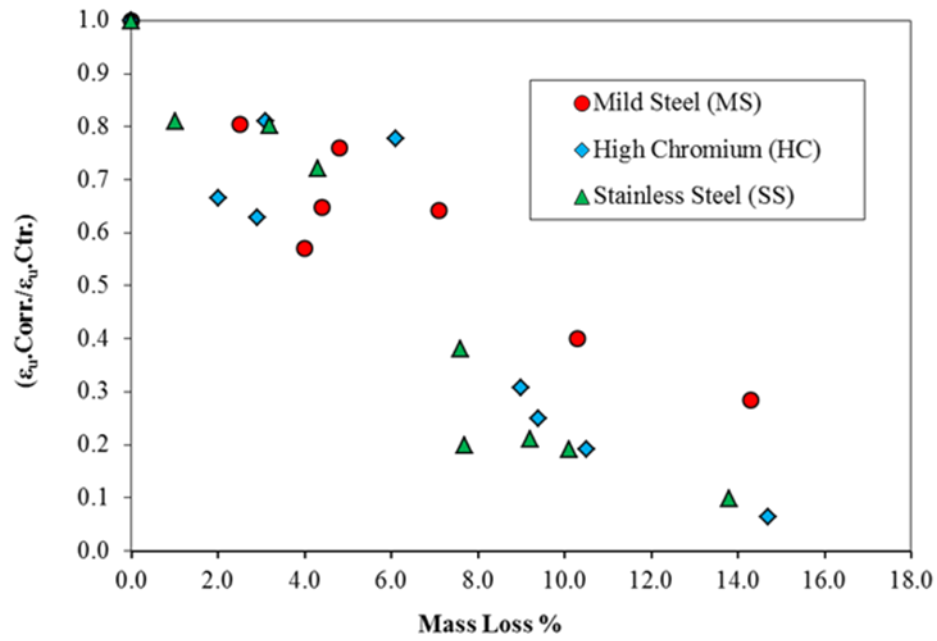
can be noted that the ductility of any of these types of steel decreases with increasing mass loss level when the pitting factor at that mass loss level is high for example specimen MS-#3-12.1% (ML=12.1% and PF=2.8) exhibited lower ductility compared with specimen MS#3-12.4 (ML=12.4% and PF=1.6) despite that both specimens were from the same mass loss range.

The pitting factor reflects the extent of the localized corrosion. For some of the specimens, the corrosion is almost uniformly distributed along the rebar, while for some other specimens; the reduction in the diameter of the specimen due to corrosion is concentrated at certain locations. Such locations create weak points for the specimen to rupture with lower ultimate strains. This can be seen clearly in the failure modes of the specimens that are shown in Fig. 4-7. The failure mode of corroded mild steel (MS), high chromium (HC), and stainless steel (SS) specimens are shown in Fig. 4-8, Fig. 4-9, and Fig. 4-10 respectively.



(a) Rebar size No. 3

Fig. 4-6 (continued on the next page)



(b) Rebar size No. 4

Fig. 4-6: Effect of steel type on the ultimate strength of corroded rebars

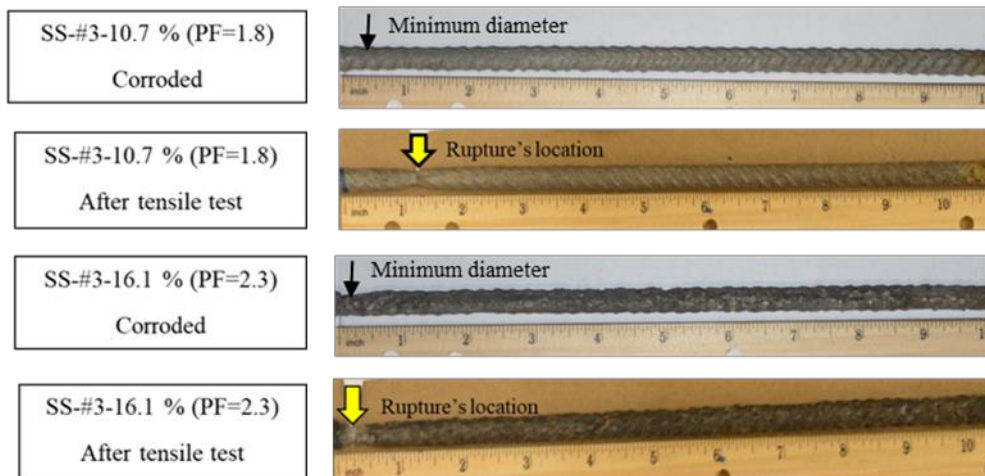
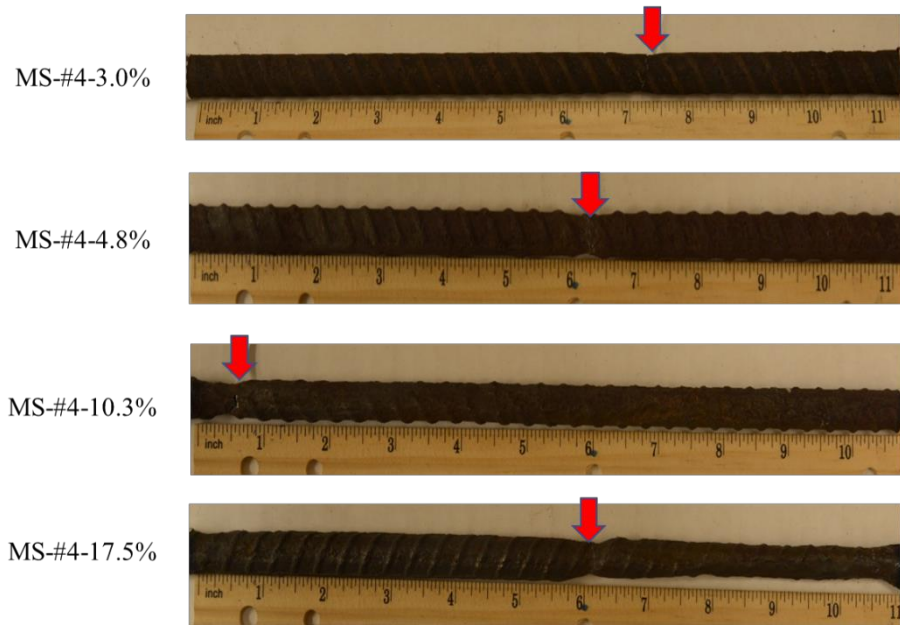
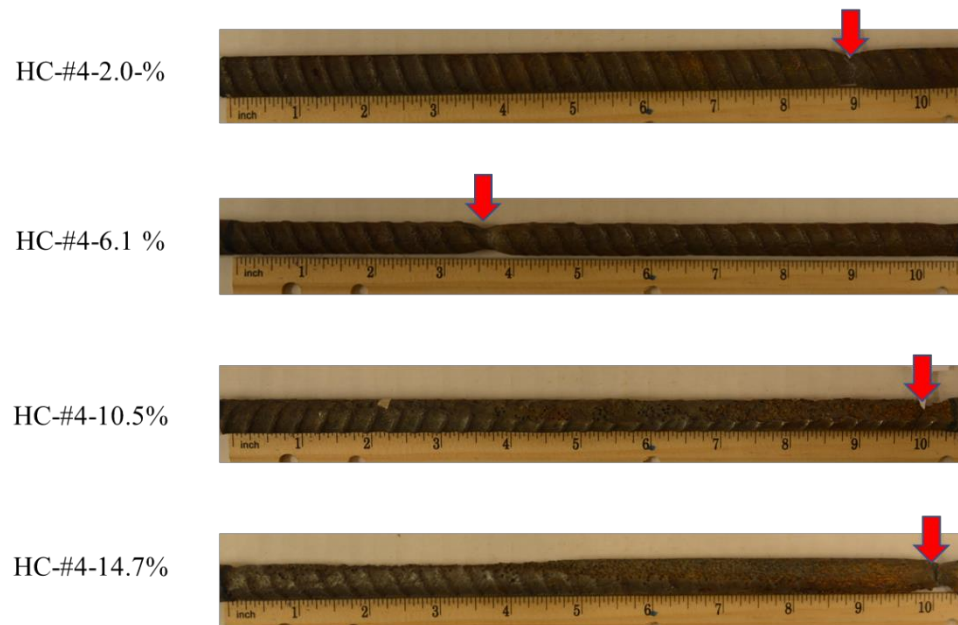


Fig. 4-7: Effect of pitting attack on failure mode of mild steel rebars



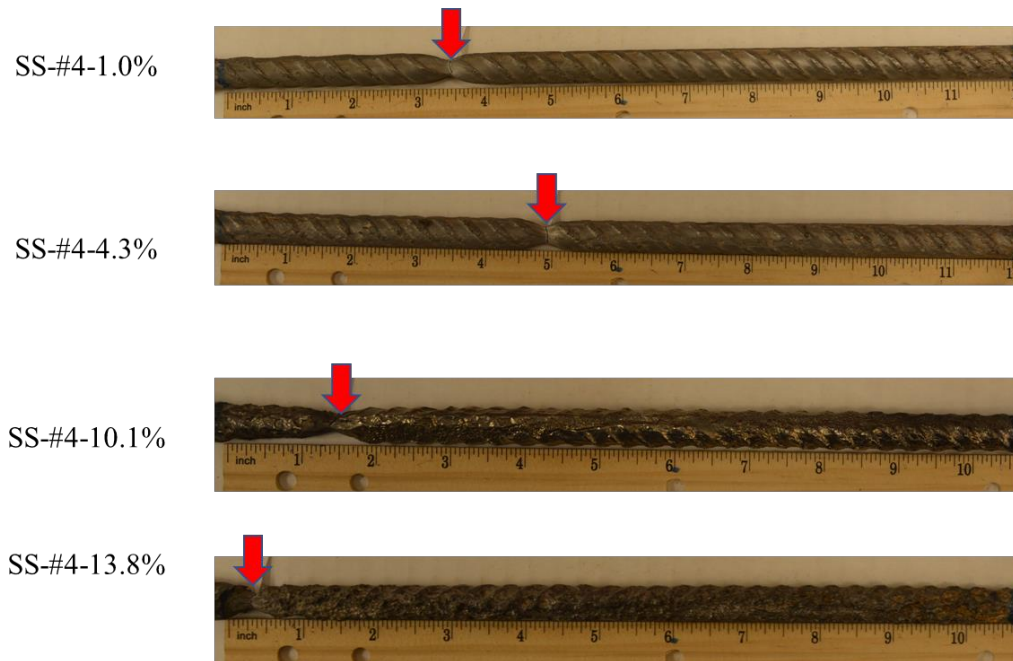
The given arrows represent the location of rupture

Fig. 4-8: Failure modes of corroded mild steel rebar



The given arrows represent the location of rupture

Fig. 4-9: Failure modes of corroded high chromium steel rebar



The given arrows represent the location of rupture

Fig. 4-10: Failure modes of corroded stainless steel rebar

In addition to the effect of the type of the rebar on the engineering properties, it can be seen in Table 4-1 to Table 4-3 that pitting factors are varied among the rebar types. Generally, pitting factors in stainless steel rebar had smaller values compared to high chromium and mild steel rebar. This could be attributed to the high level of chromium and nickel in stainless steel compositions that give it an excellent resistance against corrosion.

#### 4.4 Effect of Rebar Size on the Engineering Properties

To investigate the effect of rebar size on the engineering properties of corroded steel rebar, the yield strength factors are plotted in terms of mass loss levels for both rebar sizes (No. 3, and No. 4) for mild steel, high chromium, and stainless steel as shown in Fig. 4-

11. This figure shows that the variation in the yield strength reduction ratio of different rebar sizes (No. 3 vs. No. 4) is insignificant. Therefore, the rebar size has little influence on the yield strength of corroded steel rebar. Similarly, the rebar size shows little effect on the ultimate strength ratio and ductility ratio for all three types of steel as shown in Figs 4-12 and 4-13.

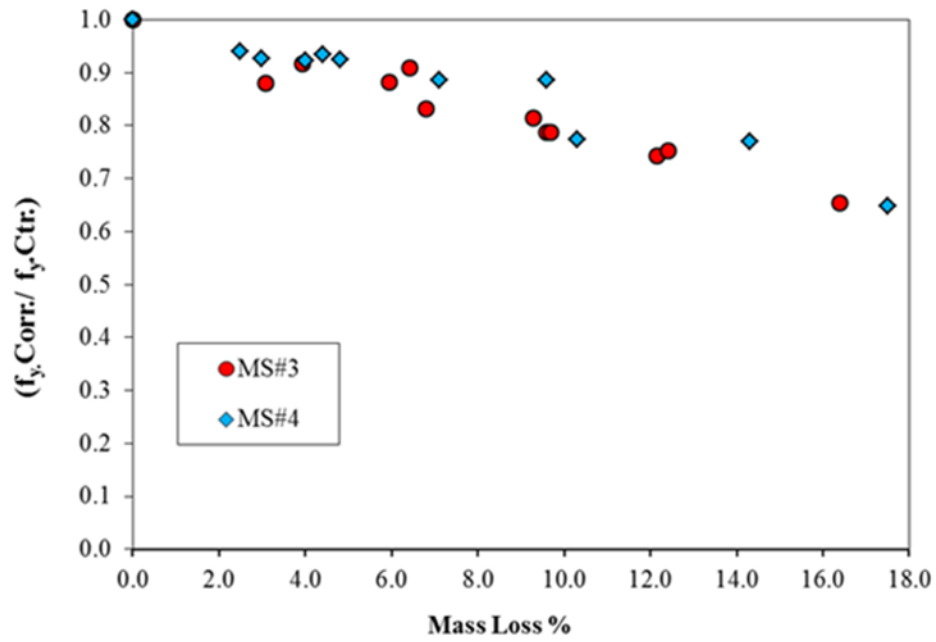


Fig. 4-11 (continued on the next page)

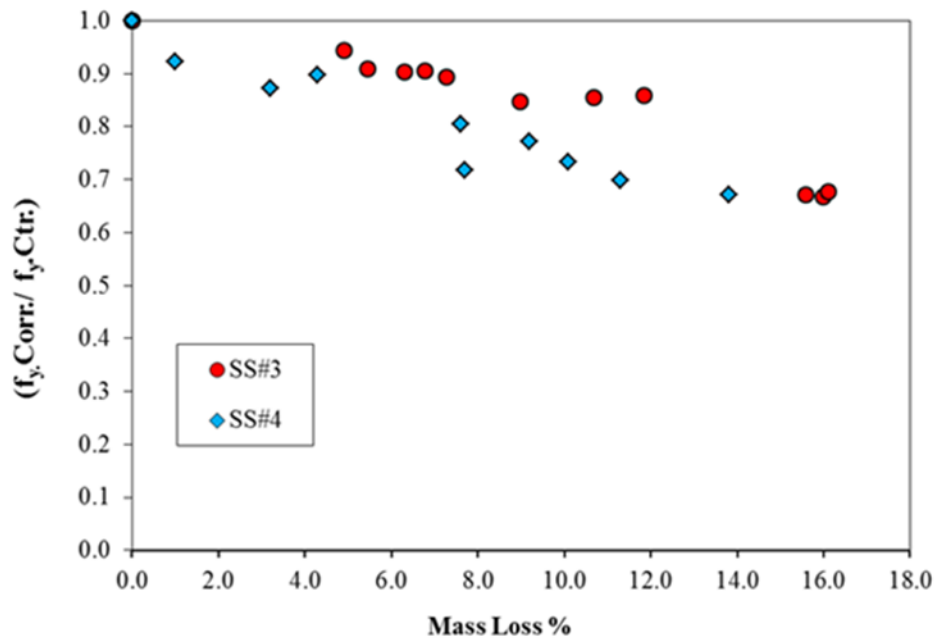
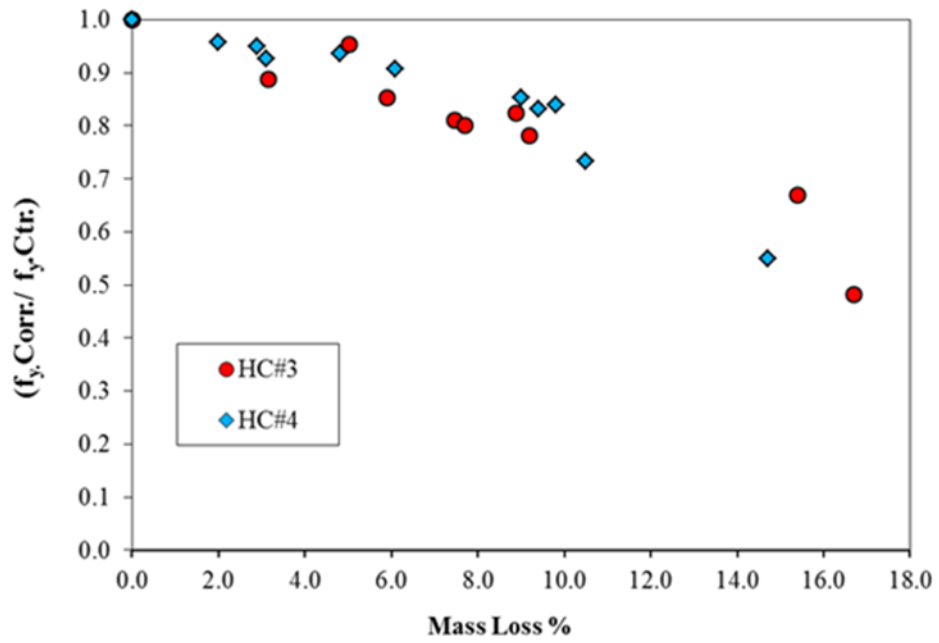


Fig. 4-11: Effect of rebar size on the yielding strength of mild, high chromium, and stainless steels

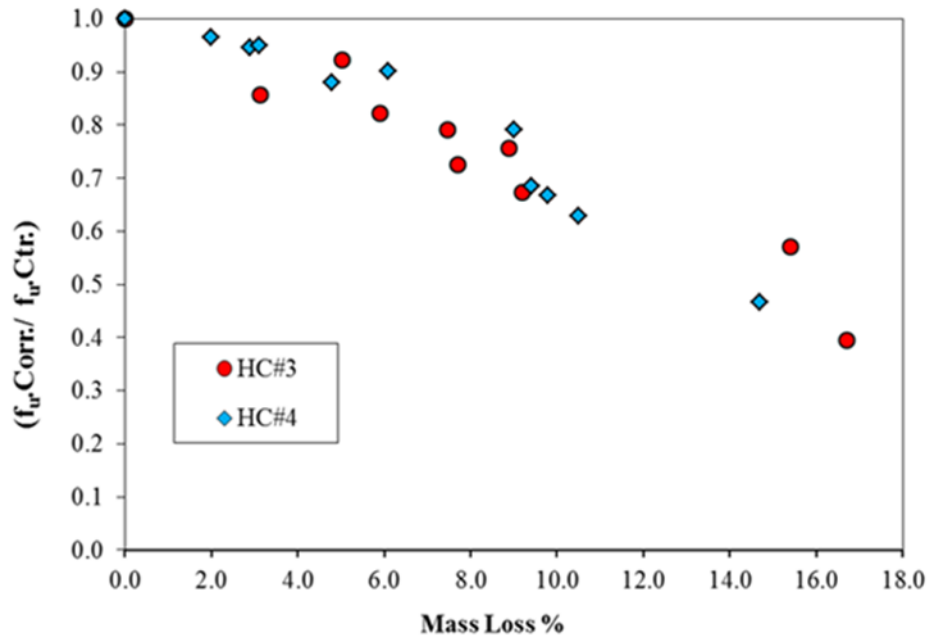
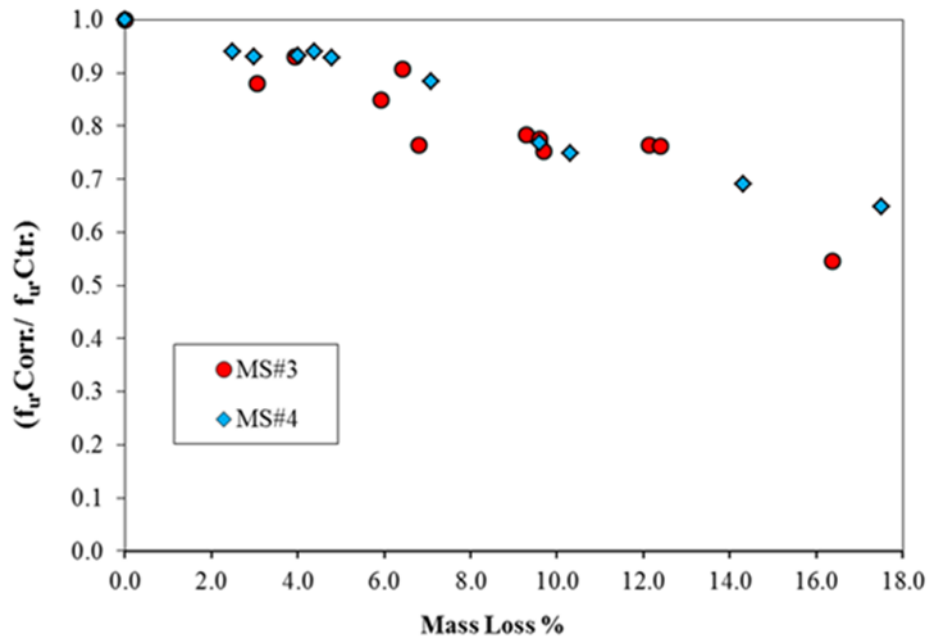


Fig. 4-12 (continued on the next page)

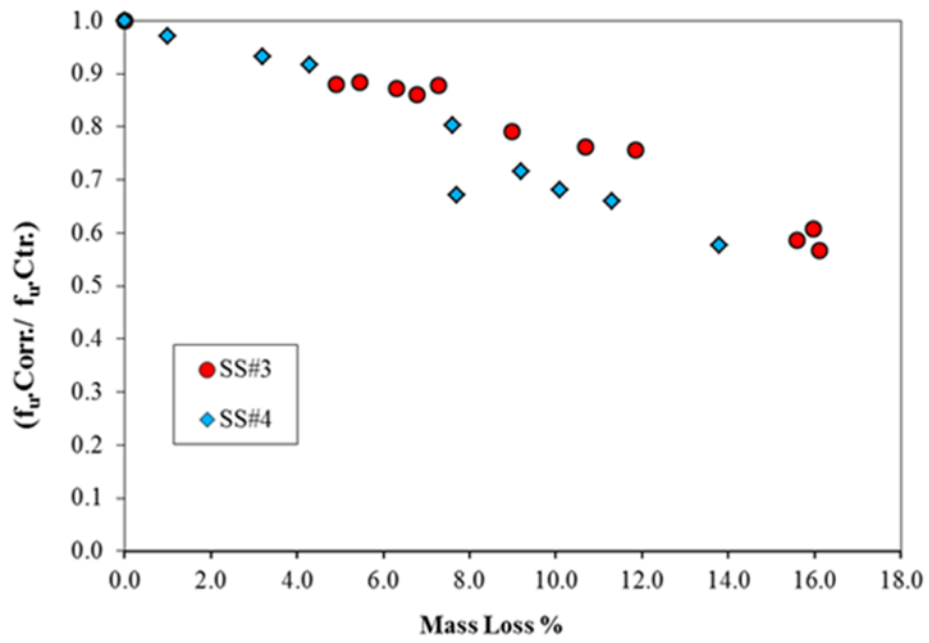


Fig. 4-12: Effect of rebar size on the ultimate strength of mild, high chromium, and stainless steels

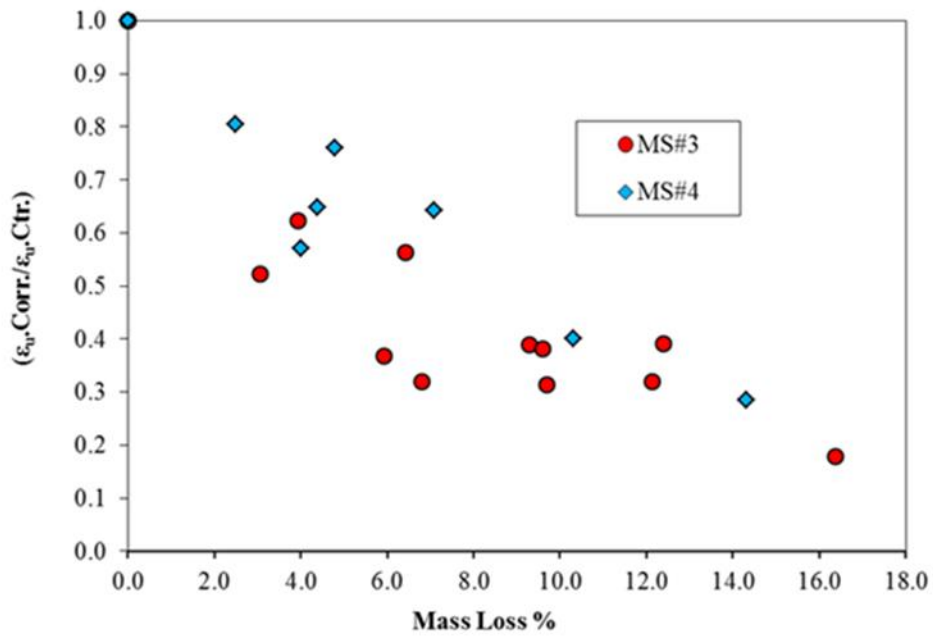


Fig. 4-13 (continued on the next page)

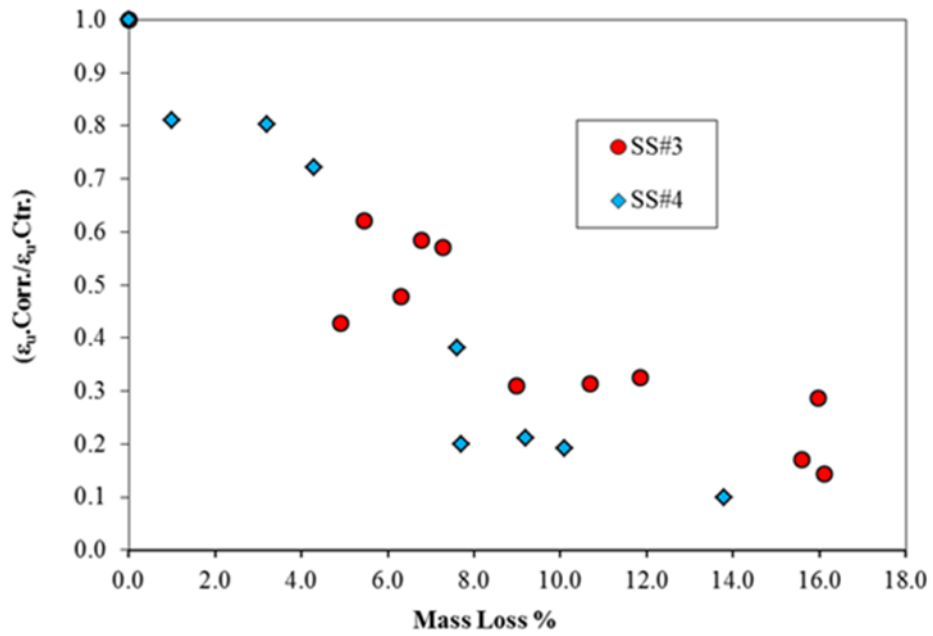
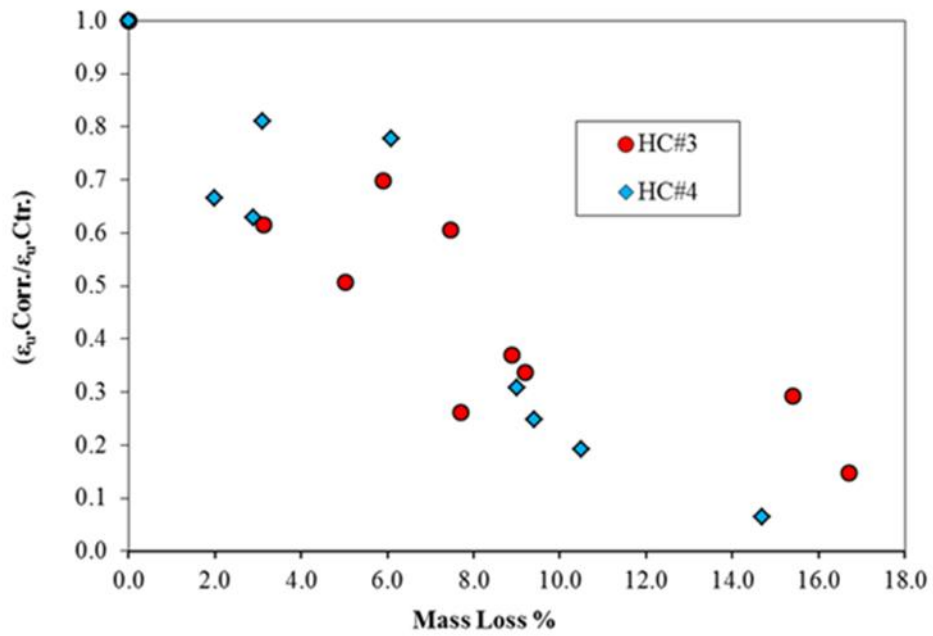


Fig. 4-13: Effect of rebar size on the ductility of mild, high chromium, and stainless steels

## 4.5 Proposed Equations for Corroded Steel Rebars

Engineering properties of corroded steel reinforcement are crucial for undertaking structural analysis to evaluate the response of concrete structure members subjected to corrosion. However, these properties vary with the high mass loss level. For deriving engineering properties specific to steel reinforcement used in concrete structures, a linear and multi regression analysis, with least sum of squares of errors, is carried out on the data generated from the tensile test of corroded steel rebar. Due to the slight variation in the reduction factors between the rebar sizes (No. 3 and No. 4) used in this work, the following unified relations are proposed for yield strength, ultimate strength, and ductility reduction factors for each type of steel rebar, for mass loss level up to 17%.

### 4.5.1 Mild steel rebar

#### 4.5.1.1 Yield strength reduction factor

For evaluating the yield strength of corroded mild steel reinforcement of rebar size (No. 3 and No. 4), the following relation for mass loss level up to 17% is proposed

$$\frac{f_{y\text{ Corr.}}}{f_{y\text{ Ctrl}}} = 1 - 0.0197(\text{Mass loss \%}). \quad (4-7)$$

#### 4.5.1.2 Ultimate strength reduction factor

For evaluating the ultimate strength of corroded mild steel reinforcement of rebar size (No. 3 and No.4), the following relation for mass loss level up to 17% is proposed

$$\frac{f_{u\text{ Corr.}}}{f_{u\text{ Ctrl}}} = 1 - 0.0225(\text{Mass loss \%}). \quad (4-8)$$

#### 4.5.1.3 Ductility reduction factor

For evaluating the ultimate strength of corroded mild steel reinforcement of rebar size (No. 3 and No. 4), the following relation for mass loss level up to 17% and corresponding pitting factor is proposed

$$\frac{\epsilon_{u\text{ Corr.}}}{\epsilon_{u\text{ Ctrl}}} = 1 - 0.038(\text{Mass loss \%}) - 0.098(\text{Pitting factor}). \quad (4-9)$$

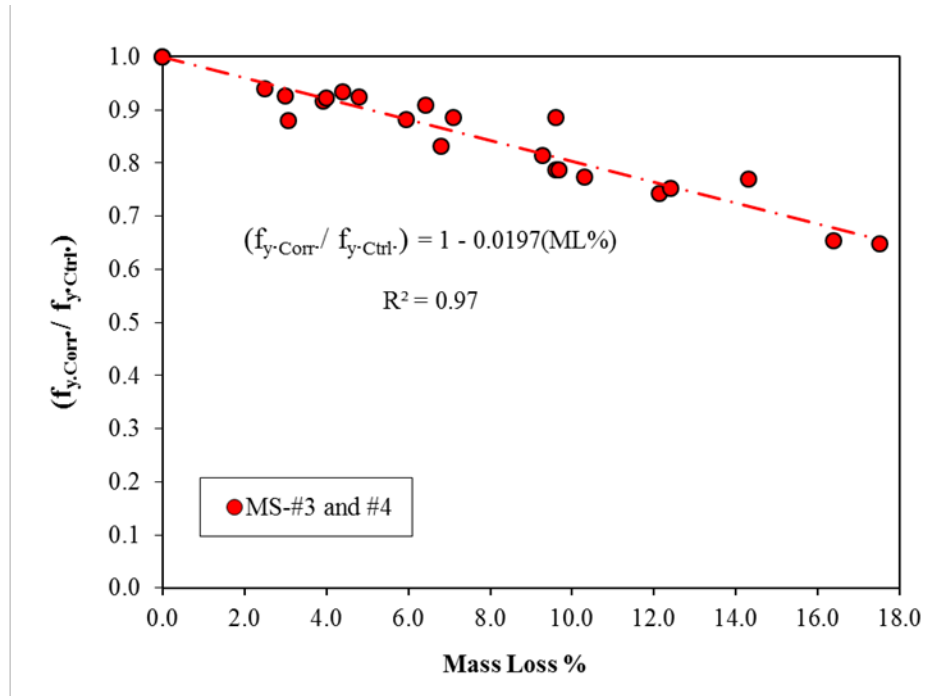


Fig. 4-14: Linear regression of yield strength of mild steel (MS)

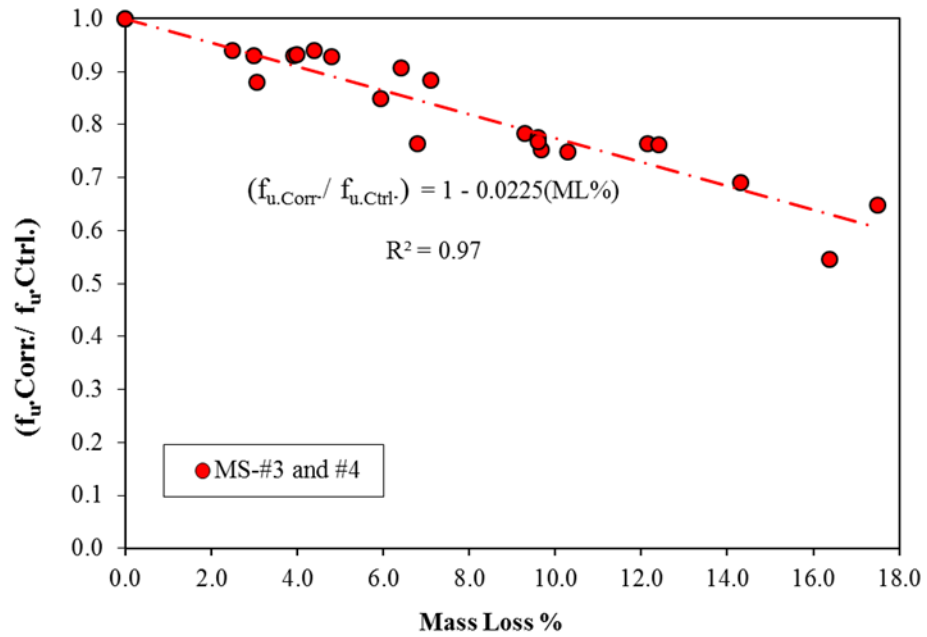


Fig. 4-15: Linear regression of ultimate strength of mild steel (MS)

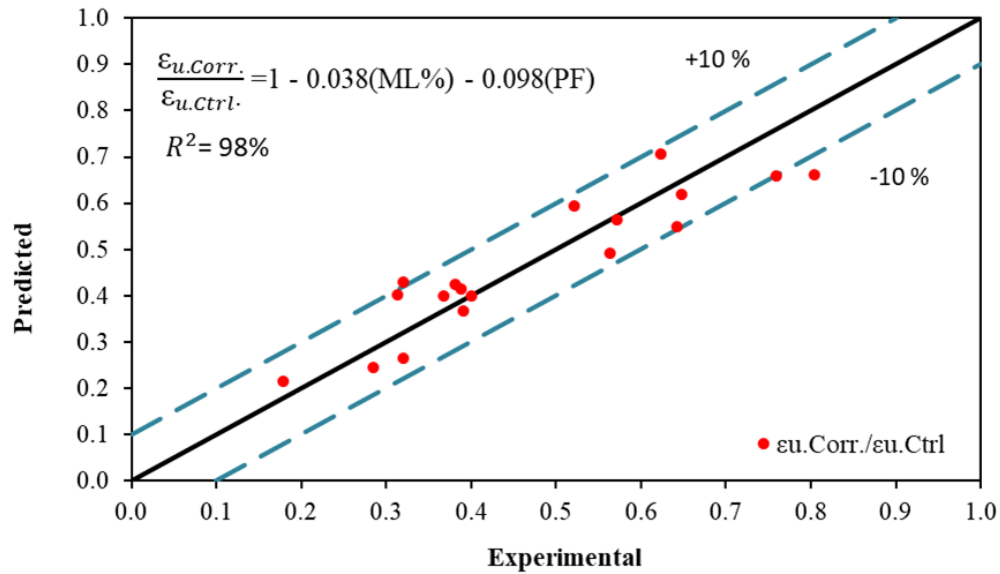


Fig. 4-16: Multi-regression of ductility of mild steel (MS)

## 4.5.2 High chromium steel rebar

### 4.5.2.1 Yield strength reduction factor

For evaluating the yield strength of corroded high chromium steel reinforcement of rebar size (No. 3 and No. 4), the following relation for mass loss level up to 17% is proposed

$$\frac{f_{y\text{ Corr.}}}{f_{y\text{ Ctrl}}} = 1 - 0.0240(\text{Mass loss } \%). \quad (4-10)$$

### 4.5.2.2 Ultimate strength reduction factor

For evaluating the ultimate strength of corroded high chromium steel reinforcement of rebar size (No. 3 and No. 4), the following relation for mass loss level up to 17% is proposed

$$\frac{f_{u\text{ Corr.}}}{f_{u\text{ Ctrl}}} = 1 - 0.0318(\text{Mass loss \%}). \quad (4-11)$$

#### 4.5.2.3 Ductility reduction factor

For evaluating the ultimate strength of corroded high chromium steel reinforcement of rebar size (No. 3 and No. 4), the following relation for mass loss level up to 17% and corresponding pitting factor is proposed

$$\frac{\epsilon_{u\text{ Corr.}}}{\epsilon_{u\text{ Ctrl}}} = 1 - 0.046(\text{Mass loss \%}) - 0.088(\text{Pitting factor}). \quad (4-12)$$

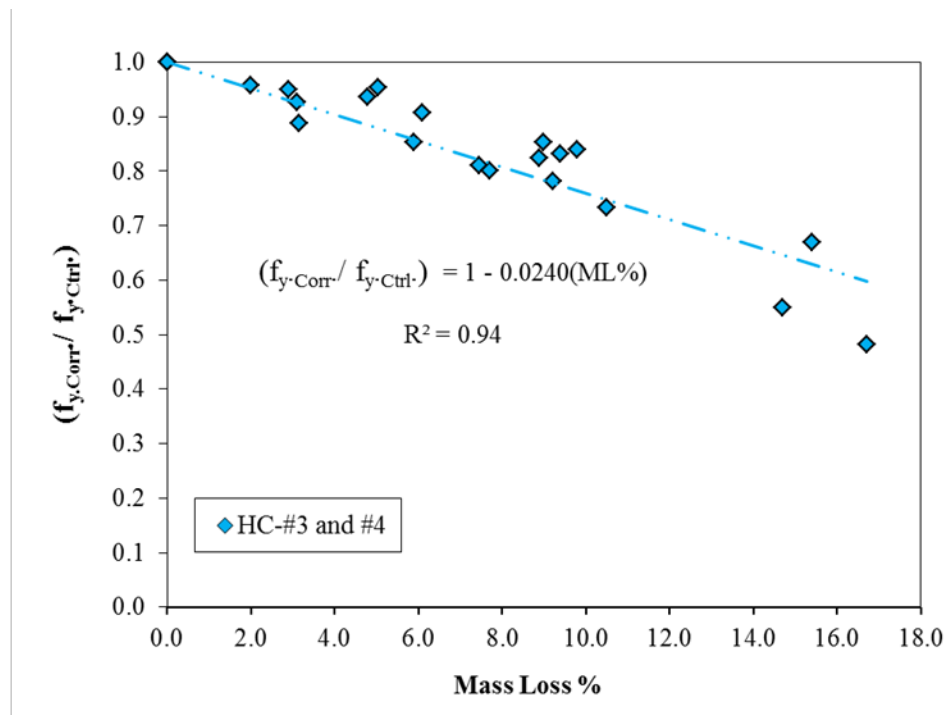


Fig. 4-17: Linear regression of yield strength of high chromium steel (HC)

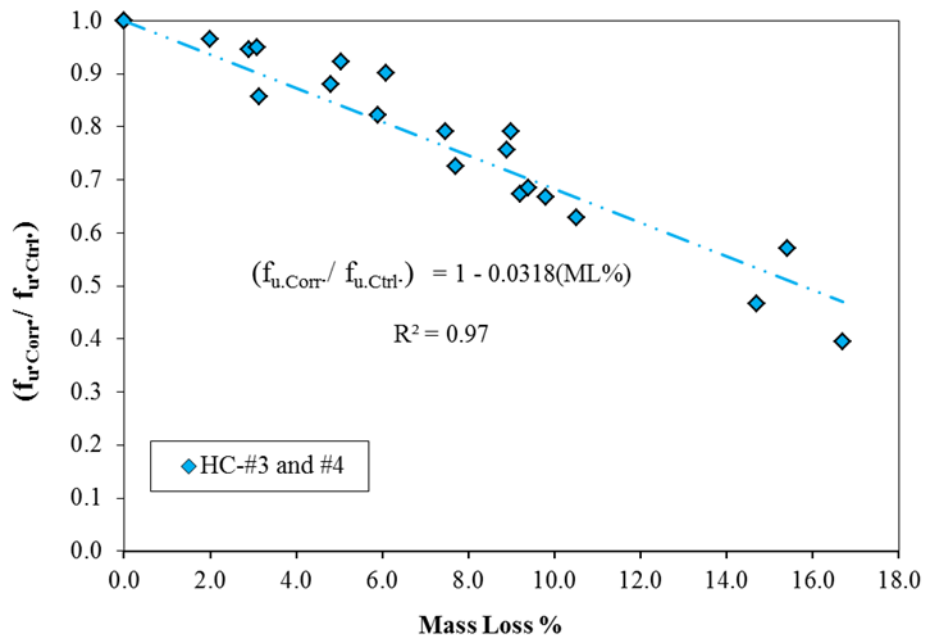


Fig. 4-18: Linear regression of ultimate strength of high chromium steel (HC)

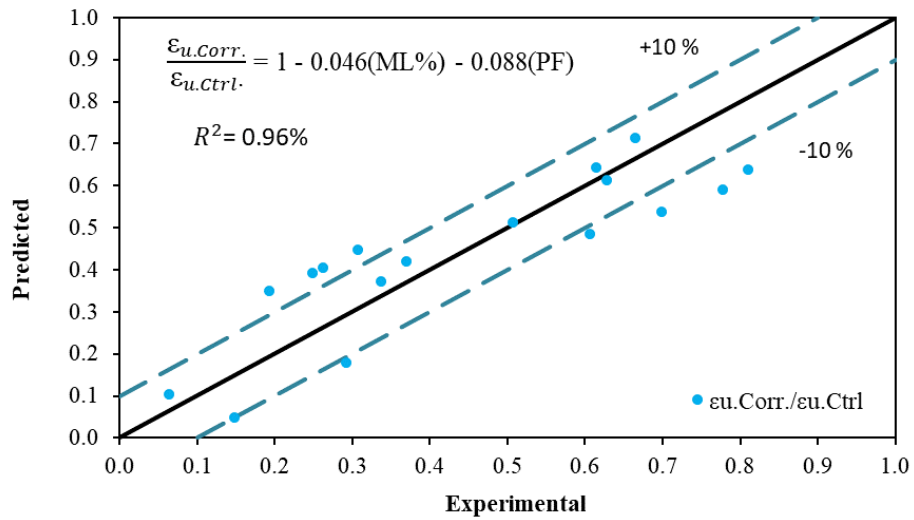


Fig. 4-19: Multi-regression of ductility of high chromium steel (HC)

### 4.5.3 Stainless steel rebar

#### 4.5.3.1 Yield strength reduction factor

For evaluating the yield strength of corroded stainless steel reinforcement of rebar size (No. 3 and No. 4), the following relation for mass loss level up to 17% is proposed

$$\frac{f_{y\text{ Corr.}}}{f_{y\text{ Ctrl}}} = 1 - 0.0208(\text{Mass loss \%}). \quad (4-12)$$

#### 4.5.3.2 Ultimate strength reduction factor

For evaluating the ultimate strength of corroded stainless steel reinforcement of rebar size (No. 3 and No. 4), the following relation for mass loss level up to 17% is proposed

$$\frac{f_{u\text{ Corr.}}}{f_{u\text{ Ctrl}}} = 1 - 0.0263(\text{Mass loss \%}). \quad (4-13)$$

#### 4.5.3.3 Ductility reduction factor

For evaluating the ultimate strength of corroded stainless steel reinforcement of rebar size (No. 3 and No. 4), the following relation for mass loss level up to 17% and corresponding pitting factor is propose

$$\frac{\varepsilon_{u\text{ Corr.}}}{\varepsilon_{u\text{ Ctrl}}} = 1 - 0.044(\text{Mass loss \%}) - 0.096(\text{Pitting factor}). \quad (4-14)$$

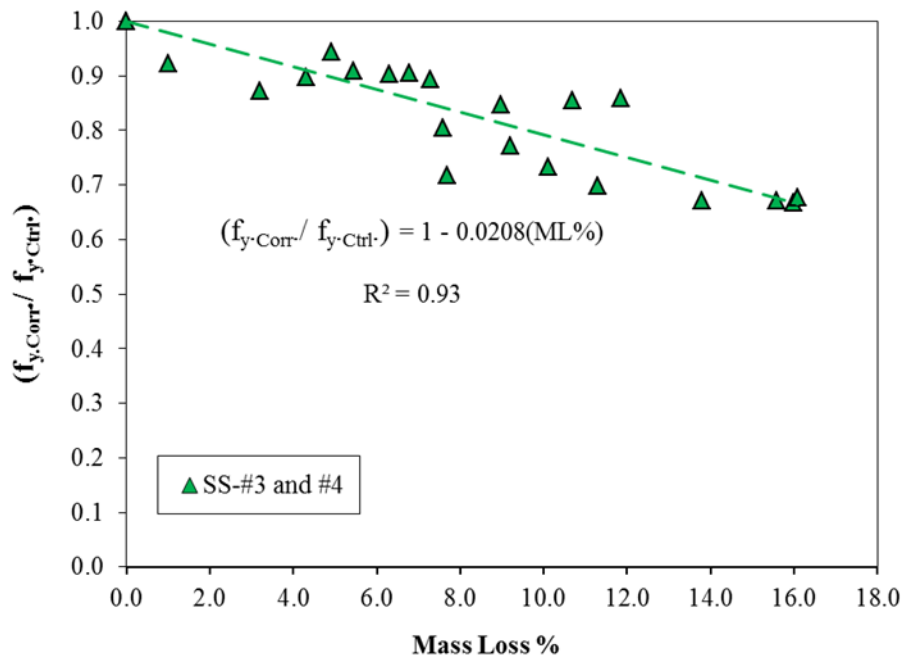


Fig. 4-20: Linear regression of yielding strength of stainless steel (SS)

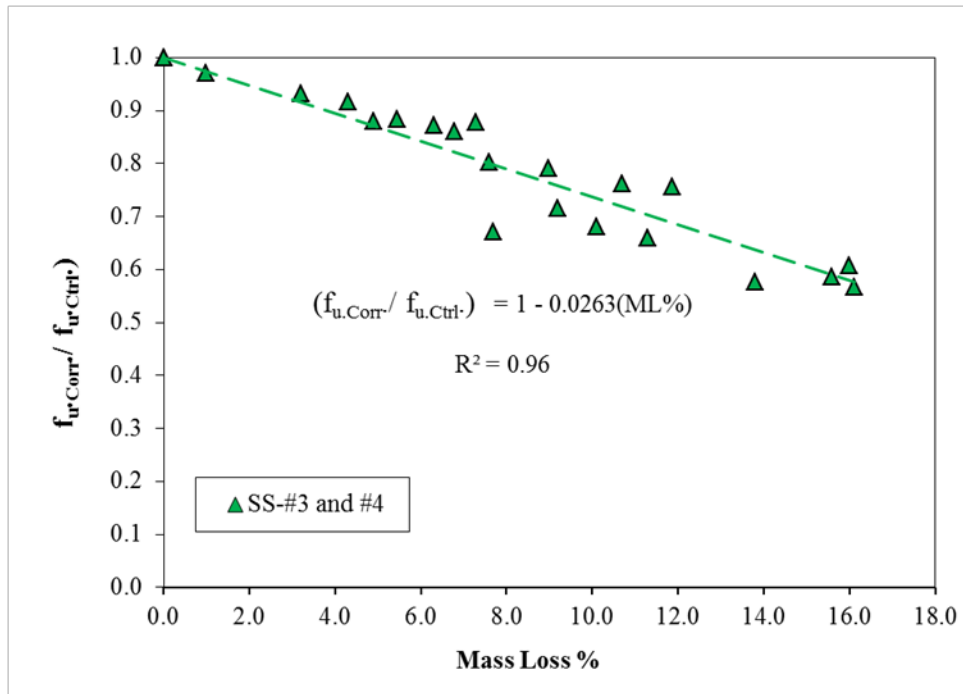


Fig. 4-21: Linear regression of ultimate strength of stainless steel (SS)

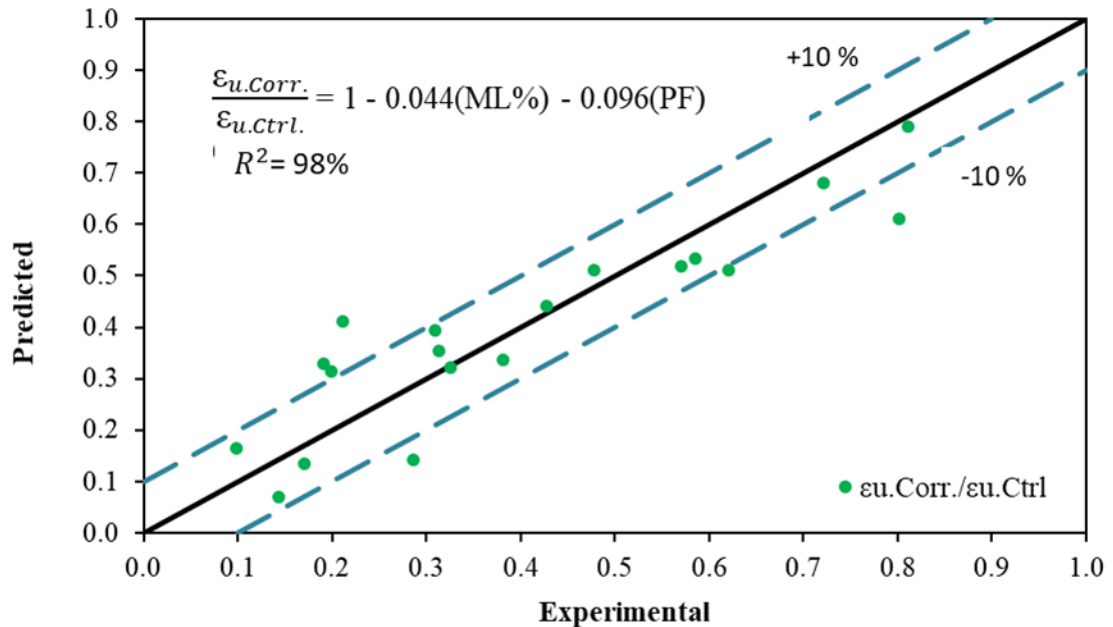


Fig. 4-22: Multi-regression of ductility of stainless steel (SS)

As shown in Figs. 4-14, 4-17, and 4-20, the linear regression is a good fit for yield strength predictions with  $R^2 = 97\%$ ,  $94\%$ , and  $93\%$  for MS, HC, and SS steels, respectively. Similarly, it can be seen from Figs. 4-15, 4-18, and 4-21, that the linear regression is a good fit for ultimate strength predictions with  $R^2 = 97\%$ ,  $97\%$ , and  $96\%$  for MS, HC and SS steels, respectively. However, to predict the ductility(ultimate strain) , multi-regression is required to find the best fit for the test data. This is due to the fact that both mass loss and pitting factor influence the prediction of ductility. In Figs. 4-16, 4-19, and 4-22, the predicated ductility from multi- regression is plotted against the corresponding experimental result data. The linear line represents the perfect predictions while the two dashed lines (+10% and -10%) represent the margin of 10% deviation from the perfect predictions. It can be seen from these figures that the vast majority of the predicated values of ductility are within the 10% margin deviation and with  $R^2 = 98\%$ ,  $96\%$ , and  $98\%$  for MS, HC and SS steels respectively. The proposed relations can be

utilized for evaluating the residual carrying capacity of concrete structural members exposed to corrosion. Summary of the statistical analysis for the equations proposed is listed in Table 4-4 and Table 4-5. It is worth to mention that  $R^2$  was calculated for yield and ultimate tensile strength and ultimate strain in Table 4-4, and Table 4-5 based on equating the intercept to be equal to 1.0 exactly with zero standard error.

Table 4-4: Summary of the statistical analysis of the yield and ultimate strength of mild steel (MS), high chromium steel (HC), and stainless steel (SS)

Rebar Type		Mild Steel (MS)		High Chromium (HC)		Stainless Steel (SS)	
		( $f_{y,Corr}/f_{y,Ctrl}$ )	( $f_{u,Corr}/f_{u,Ctrl}$ )	( $f_{y,Corr}/f_{y,Ctrl}$ )	( $f_{u,Corr}/f_{u,Ctrl}$ )	( $f_{y,Corr}/f_{y,Ctrl}$ )	( $f_{u,Corr}/f_{u,Ctrl}$ )
Intercept	Value	1.0	1.0	1.0	1.0	1.0	1.0
	Standard Error	0.0	0.0	0.0	0.0	0.0	0.0
Slope	Value	-0.0197	-0.0225	-0.0240	-0.318	-0.0208	-0.263
	Standard Error	0.0006	0.0009	0.0013	0.0013	0.0012	0.0010
Statistics	$R^2$	0.97	0.97	0.94	0.97	0.93	0.96
	Adjusted- $R^2$	0.93	0.92	0.89	0.91	0.88	0.92
	P-Value	6.41E-19	9.83E-18	6.35E-14	1.34E-16	9.07E-14	3.67E-17
	Test Significance	2.52E-38	3.42E-17	1.72E-13	4.88E-16	2.26E-13	1.30E-16

Table 4.5: Summary of the statistical analysis of ultimate strain of mild steel(MS),highchromium steel(HC), and stainless steel (SS)

		Value	Standard Error	R <sup>2</sup>	Adjusted R <sup>2</sup>	P-Value	Test Significance
(ε <sub>u.Corr.</sub> /ε <sub>u.Ctrl.</sub> )-MS	Intercept	1.0	0.0	0.98	0.92	-	1.81E-14
	ML %	-0.038	0.00358			1.26E-08	
	PF	-0.098	0.01305			1.25E-06	
(ε <sub>u.Corr.</sub> /ε <sub>u.Ctrl.</sub> )-HC	Intercept	1.0	-	0.96	0.90	-	4.75E-11
	ML %	-0.046	0.00575			9.83E-07	
	PF	-0.088	0.02328			1.88E-03	
(ε <sub>u.Corr.</sub> /ε <sub>u.Ctrl.</sub> )-SS	Intercept	1.0	0.0	0.98	0.92	-	3.88E-14
	ML %	-0.044	0.00440			1.68E-08	
	PF	-0.096	0.01834			6.48E-05	

#### 4.6 Summary

The load-displacement data from tensile tests on corroded steel rebar is employed to plot the residual stress-strain response for mild steel, high chromium, and stainless steels for both rebar sizes No. 3 and No. 4 and for mass loss levels 1%-17%. Also, the significant points of the stress-strain curve,( namely yield strength, ultimate strength and ductility) are recorded. These points are utilized to calculate the reduction factors for residual yield, ultimate strength and ductility as compared to corresponding values from control specimens. The yield, ultimate strength and ductility reduction factors for mild, high chromium, and stainless steels are plotted and compared in figures for both rebar sizes No. 3 and No. 4 and the general trends is traced and explained. Then, the tests data are utilized to derive relations to predict the residual yield, ultimate strength and ductility using linear and multi-regressions. The reduction factor prediction relations for yield and ultimate strength are derived in term moss loss level, while the ductility prediction relations are derived in term of mass loss level and pitting factors. Conclusions on the results data are presented in next chapter.

## Chapter Five

### CONCLUSIONS AND RECOMMENDATIONS

#### 5.1 General

The effect of corrosion in the engineering properties of steel reinforcement is investigated to develop an understanding on the extent of the reduction in the engineering properties, namely; yield ultimate strength and ductility due to corrosion. In the experimental work, three sets of steel reinforcement embedded in concrete specimens of mild, high chromium, and stainless steel rebar with two rebar sizes No. 3 and No. 4 are subjected to accelerated corrosion then tested for tensile strength. The main parameters were mass loss, steel rebar type, and steel rebar size. Results from tensile strength tests are utilized to derive relations for the reduction factors of yielding, ultimate strength and ductility of corroded steel rebars.

#### 5.2 Conclusions

Based on the results generated from this study, the following conclusion can be drawn:

- The yield strength, ultimate strength, and ductility decrease significantly due to corrosion. with increasing mass loss (corrosion) in embedded steel reinforcement
- Steel types have a slight influence on the engineering properties of corroded reinforcement. The reductions in yield strength and tensile strength of corroded HC is the highest, followed by SS, and these reductions of corroded MS are the lowest among the three steel types. These differences in the reduction might also come from the differences in the steel grades. However, the difference in the

reductions of the engineering properties of different types of rebar is not significant, especially when the mass loss level is smaller than 10%. Additionally, steel types did not show a significant influence on the ductility of corroded rebar.

- Rebar size has no influence on the reduction of the engineering properties and ductility of the corroded rebar.
- Mass loss is the most dominant factor that influences the reduction of yield and ultimate strength
- Mass loss and pitting factor are the main parameters that influence the ductility reduction in corroded steel rebars
- For practice use, the effect of rebar types and rebar sizes can be neglected and the following unified equations can be utilized to predict the residual capacity of corroded reinforcement rebar in reinforced concrete structures:

$$\frac{f_{y\text{Corr.}}}{f_{y\text{Ctrl}}} = 1 - 0.0214(\text{Mass loss \%}), \quad (5-1)$$

$$\frac{f_{u\text{Corr.}}}{f_{u\text{Ctrl}}} = 1 - 0.0266(\text{Mass loss \%}), \quad (5-2)$$

and

$$\frac{\epsilon_{u\text{Corr.}}}{\epsilon_{u\text{Ctrl}}} = 1 - 0.0428(\text{Mass loss \%}) - 0.0927(\text{Pitting factor}). \quad (5-3)$$

### 5.3 Recommendations for Future Work

While this study has expanded the scope of the study of the influence of the corrosion levels on the engineering properties of conventional and resistant corrosion reinforcement steel rebar, further research is required to extend the understanding of the

effect of corrosion on engineering properties of steel reinforcement in a real structure subjected to a corrosive environment. The following are some of the recommendations for further research in this area:

- Experimental studies can be extended to include the effect of electrical accelerated corrosion on engineering properties of other types of resistant corrosion reinforcements such as epoxy coated reinforcement rebar with different levels of surface damage.
- In this study, the corrosion was induced in reinforcement rebar embedded in concrete by electrical accelerated corrosion test. This can be extended by testing resistant corrosion reinforcement rebar extracted from real corroded structures.

## REFERENCES

- ACI 222R, (2001). "Protection of Metals in Concrete Against corrosion." *American Concrete Institute*, Farmington Hills, MI.
- ACI 309.2R-98, (2002). "Building Code Requirements for Structural." *American Concrete Institute*, Farmington Hills, MI.
- ACI 318-02, (2002). "Building Code Requirements for Structural Concrete." *American Concrete Institute*, Farmington Hills, MI.
- Almusallam A. A., (2001). "Effect of degree of corrosion on the properties of reinforcing steel bars." *Construction and Building Materials*, 15(8), pp. 361-368.
- Angst U., (2018). "Challenges and Opportunities in Corrosion of Steel in Concrete." *Materials and Structures*, 51(1), pp. 1–20.
- Angst U., Elsener B., Larsen C. & Vennesland O., (2009). "Critical chloride content in reinforced concrete — A review." *Cement and Concrete Research*, 39(12), pp. 1122–1138
- ASTM A1035, (2019). "Standard Specification for Deformed and Plain, Low-Carbon, Chromium, Steel Bars for Concrete Reinforcement." West Conshohocken, PA.
- ASTM A615, (2018). "Standard Specification for Deformed and Plain Carbon-Steel Bars for Concrete Reinforcement1." West Conshohocken, PA.

- ASTM A955, (2018).” Standard Specification for Deformed and Plain Stainless Steel Bars for Concrete Reinforcement.” West Conshohocken, PA.
- Barr P. & Wixom K., (2011). " Feasibility of using high-strength steel and MMFX rebar in bridge design." *Utah. Department of Transportation*. UDOT Report No. UT-09.09
- Broomfield J., (1997). “Corrosion of Steel in Concrete : Understanding, Investigation and Repair.” (1st. Edition.). London: E & FN Spon.
- Broomfield J., (2003). “Corrosion of Steel in Concrete. Understanding, Investigation and Repair.” Spon Press, London, UK.
- Cairns J., Gehlen C., Andrade C., Bartholomew M., Gulikers J., Leon F., Javier M., Stuart, McKenna P., Osterminski K., Paeglitis A. & Straub D., (2011). “Condition Control and Assessment of Reinforced Concrete Structures Exposed to Corrosive Environments.” International Federation for Structural Concrete (fib), Vol. 59, Lausanne, Switzerland.
- Cairns J., Plizzari, G. A., Du Y., Law D. W. & Franzoni, C., (2005). “Mechanical properties of corrosion-damaged reinforcement.” *ACI Materials Journal*, 102(4), 256.
- Du Y. G., Clark, L. A., & Chan, A. H. C., (2005). “Residual capacity of corroded reinforcing bars.” *Magazine of Concrete Research*, 57(3), pp. 135-147.
- Heusler K., Landolt D. & Trasatti S., (1989). “Electrochemical corrosion nomenclature.” *Journal of Electroanalytical Chemistry*, 274(1), pp. 345–348.

- Hyzak M., (2018). "Seamless Bridges". *TX Bridge Webnar, Texas Department of Transportation*. Retrieved from <http://ftp.dot.state.tx.us/pub/txdot-info/brg/webinars/2018-0913/05.pdf>
- Imperatore S., & Rinaldi Z., (2008). "Mechanical behaviour of corroded rebars and influence on the structural response of R/C elements." *2nd International Conference on Concrete Repair, Rehabilitation and Retrofitting, ICCRRR-2*, November 2008, Cape Town, South Africa.
- Imperatore S., Rinaldi Z., & Drago, C., (2017). "Degradation relationships for the mechanical properties of corroded steel rebars." *Construction and Building Materials*, 148, pp. 219-230.
- Koch G., Brongers PH & Thompson N., (2002). "Corrosion Cost and Preventive Strategies in the United States." NACE International.
- Landolt D., (2007). "Corrosion and Surface Chemistry of Metals." 1st. Edition, Lausanne, Switzerland, EPFL Press, distributed by CRC Press.
- Lee H. S. & Cho Y. S., (2009). "Evaluation of the mechanical properties of steel reinforcement embedded in concrete specimen as a function of the degree of reinforcement corrosion." *International journal of fracture*, 157(1-2), pp. 81-88.
- Markeset G., & Mvr dal R., (2008) "Modelling of reinforcement corrosion in concrete- State of the art." *Technical Report COIN Project report 7. SINTEF Building and Infrastructure Research Institute*, Oslo, Norway.

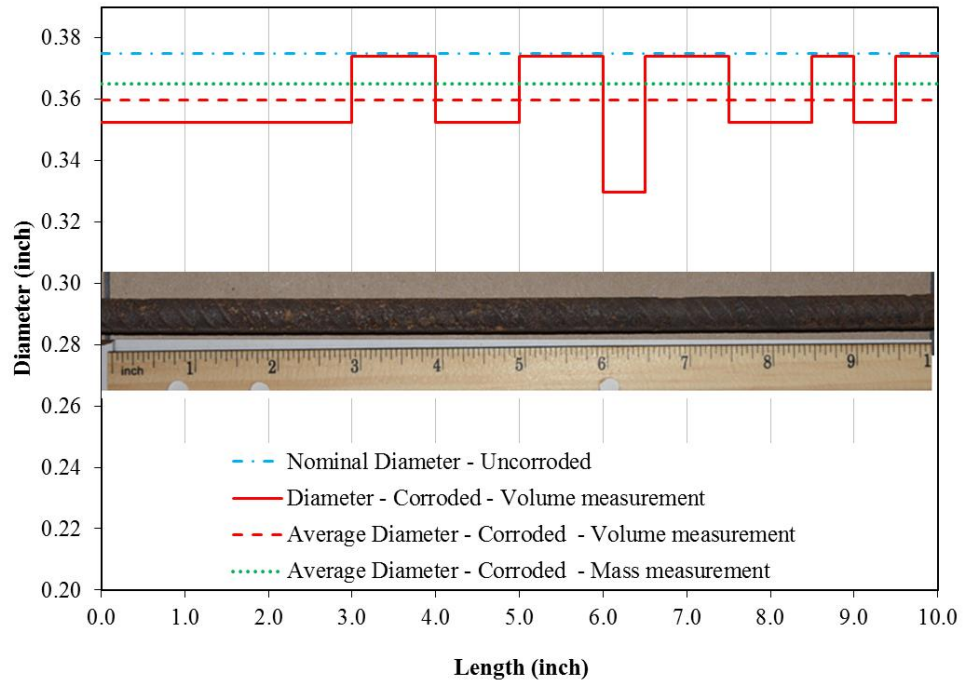
- McDonald B., Pefifer D., & Sherman M., (1998). "Corrosion evaluation in epoxy coated rebar, metallic clad, and solid metallic reinforcing bar in concrete." FHWA-RD-98-153.
- Morinaga, S., (1996). "Remaining life of reinforced concrete structures after corrosion cracking." *Durability of building materials and components* 7, 127.
- Moser R., Brett H., Lawrence K., Preet S. & Kimberly K., (2011). "Durability of Precast Prestressed Concrete Piles in Marine Environment: Reinforcement Corrosion and Mitigation." *Research Project No. 07-30*. Georgia Department of Transportation
- Ou Y. C., Susanto Y. T. T., & Roh H. (2016). "Tensile behavior of naturally and artificially corroded steel bars." *Construction and Building Materials*, 103, pp. 93-104.
- PCA, (2002). "Types and Causes of Concrete Deterioration." Serial No. 2617. Portland Cement Association. Skokie, Illinois.
- Speller F., (1922). "Control of Corrosion By Deactivation Of Water." *Journal of Franklin Institute*, 193,515-542.
- Speller F., (1951). "Corrosion, Causes and Prevention." 3rd. Edition, New York: McGraw-Hill.
- Sun X., Kong H., Wang H., & Zhang Z. (2018). "Evaluation of corrosion characteristics and corrosion effects on the mechanical properties of reinforcing steel bars based on three-dimensional scanning." *Corrosion Science*, 142, pp. 284-294.

Walker, Cederholm A. & Bent L., (1907). "The Corrosion Of Iron And Steel." *American Chemical Society*, 29, pp. 1251-1264.

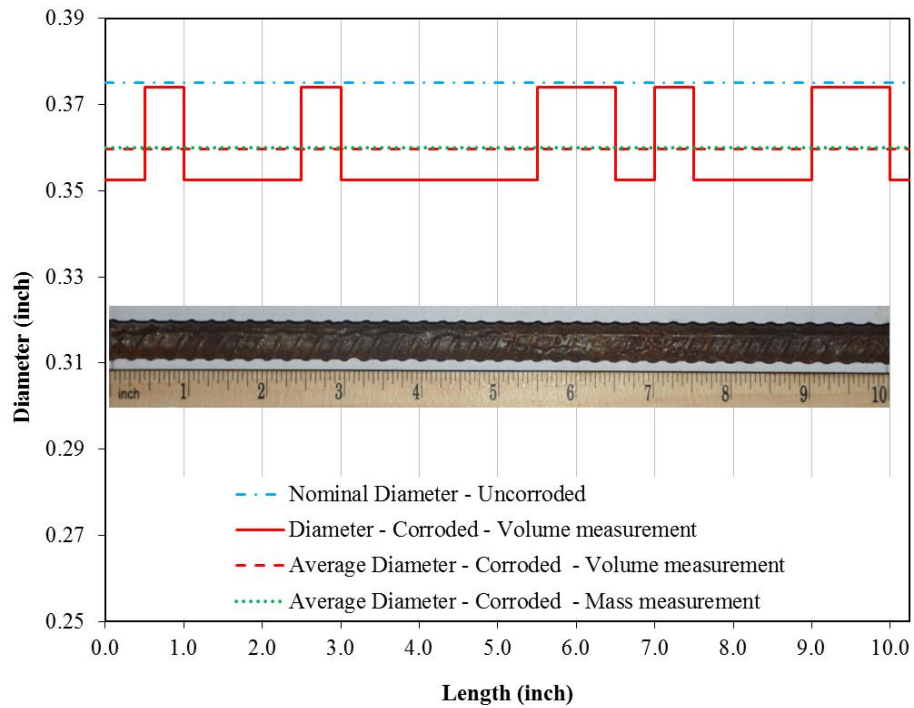
Wilson C. & Oates J., (1969). "Corrosion and the maintenance engineer." New York. Hart Publishing Company Inc.

Zhang P. S., Lu M. & Li X. Y., (1995) "The mechanical behavior of corroded bar." *Journal of Industrial Buildings*, 25, No.257, pp.41-44.

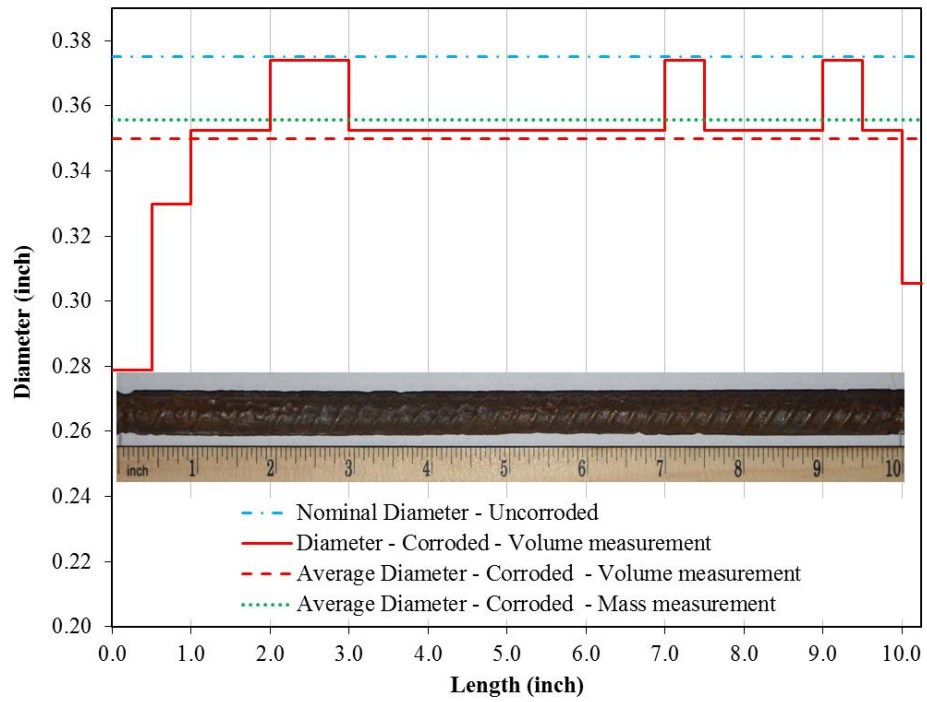
## APPENDIX



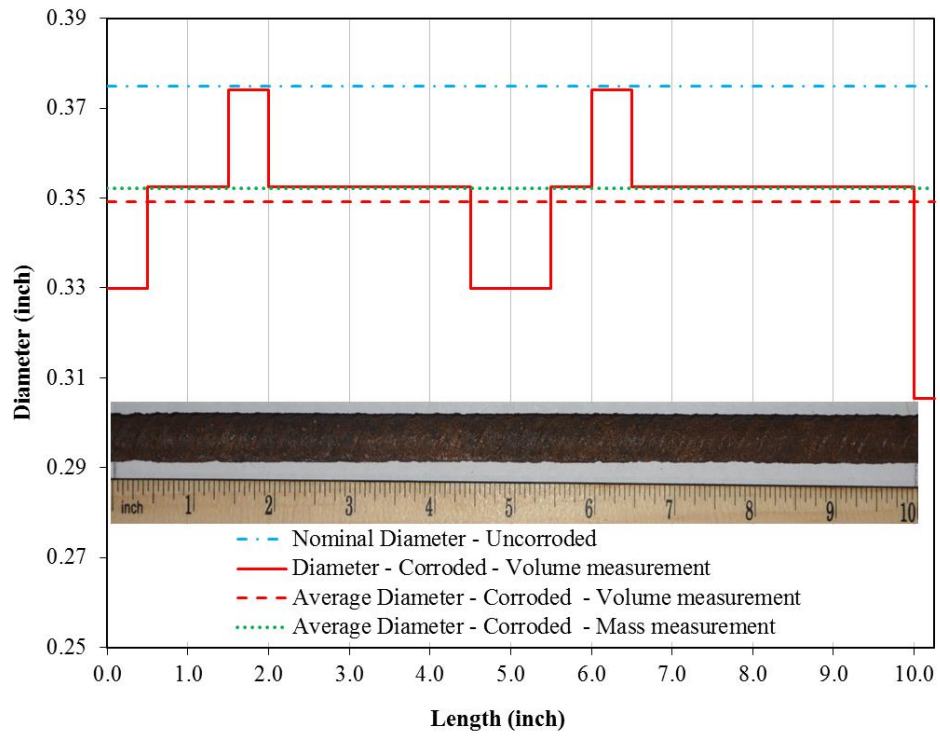
Cross section profile of MS-#3-3.1%



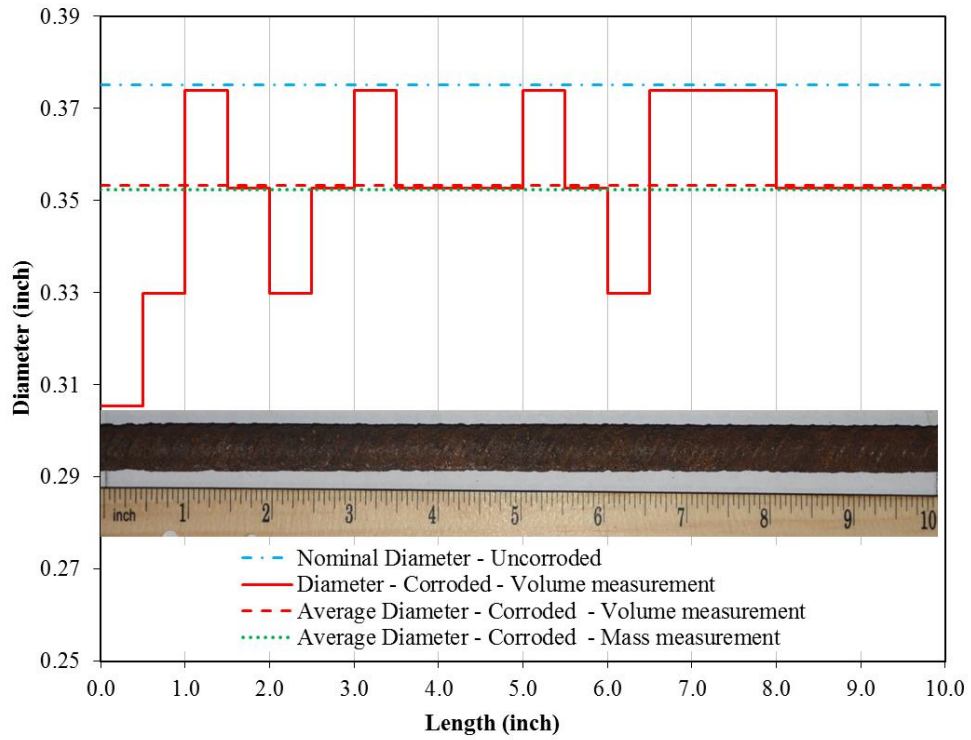
Cross section profile of MS-#3-3.9%



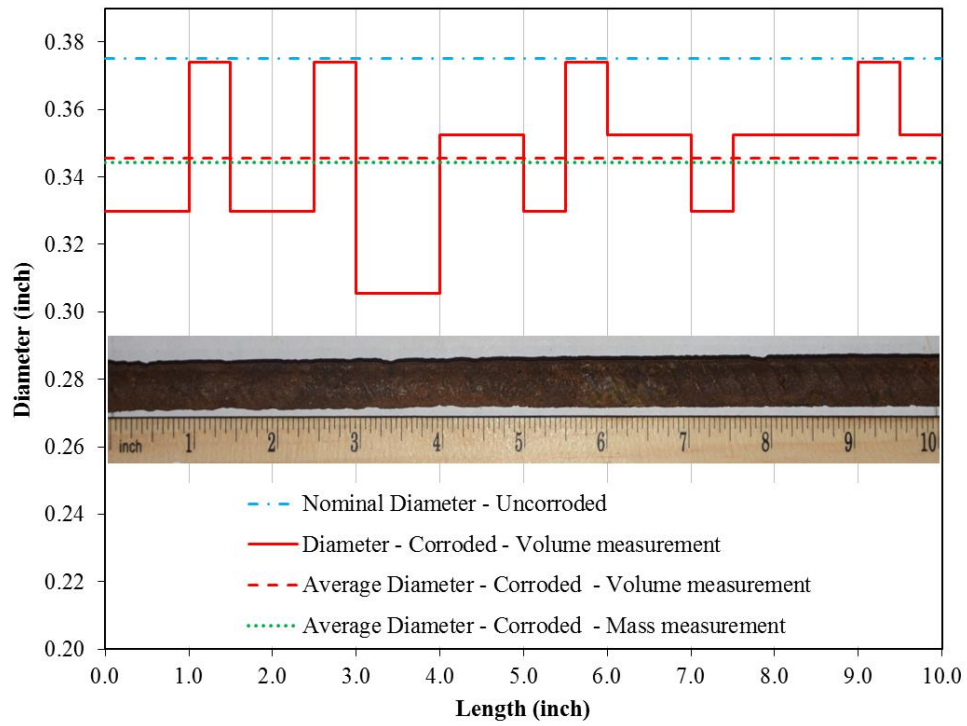
Cross section profile of MS-#3-5.9%



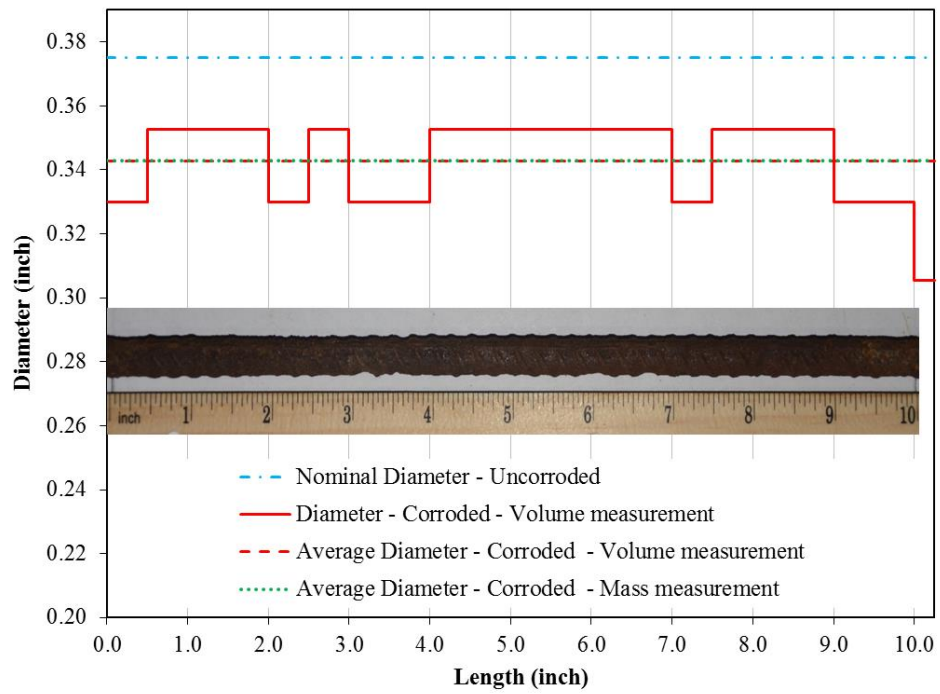
Cross section profile of MS-#3-6.4%



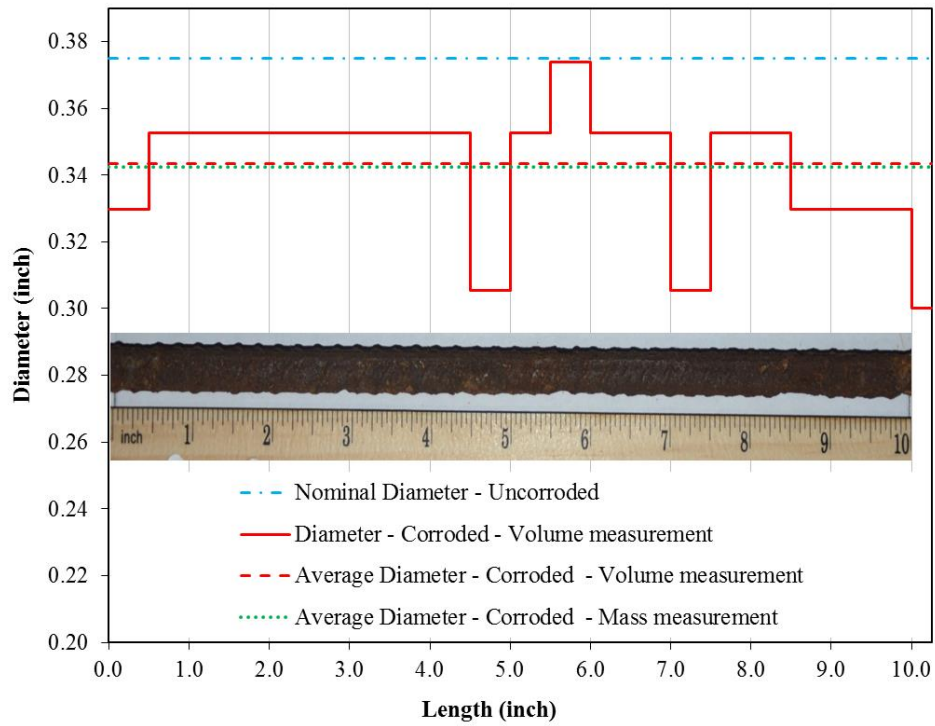
Cross section profile of MS-#3-6.8%



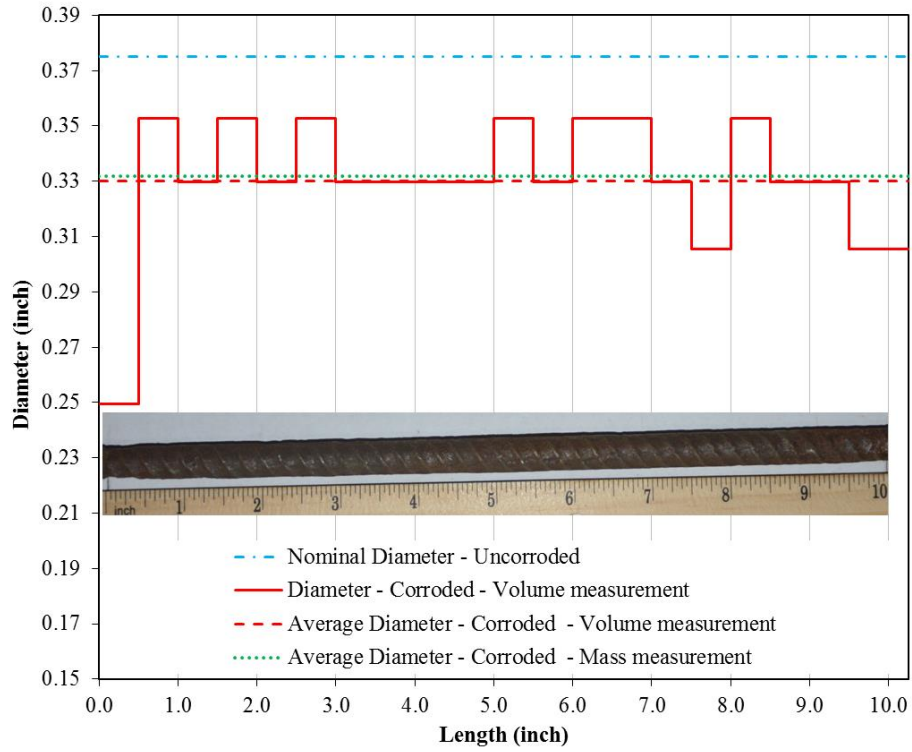
Cross section profile of MS-#3-9.3%



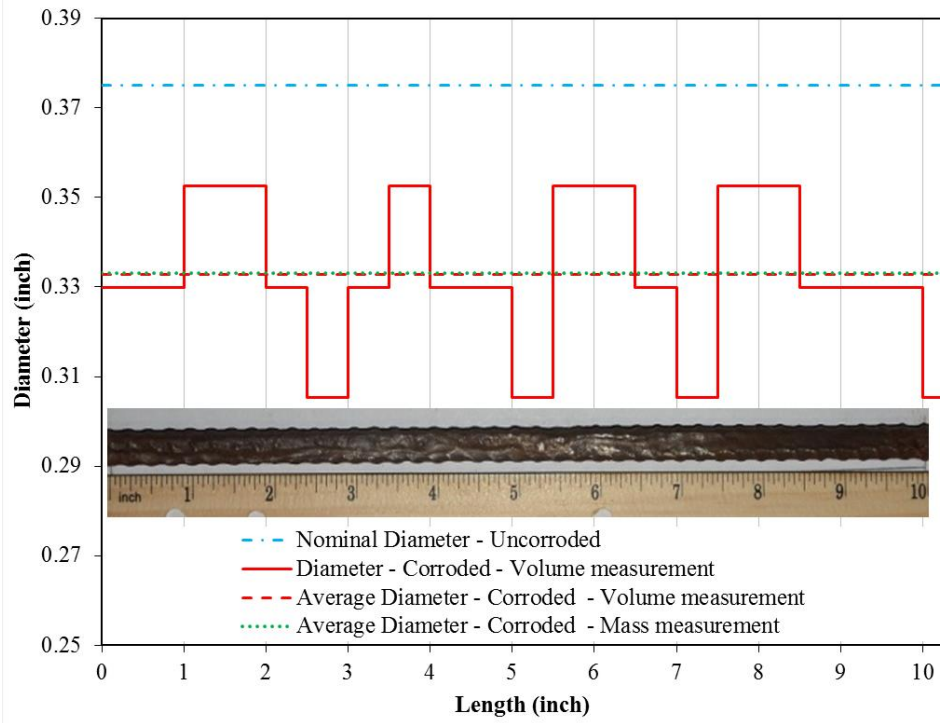
Cross section profile of MS-#3-9.6%



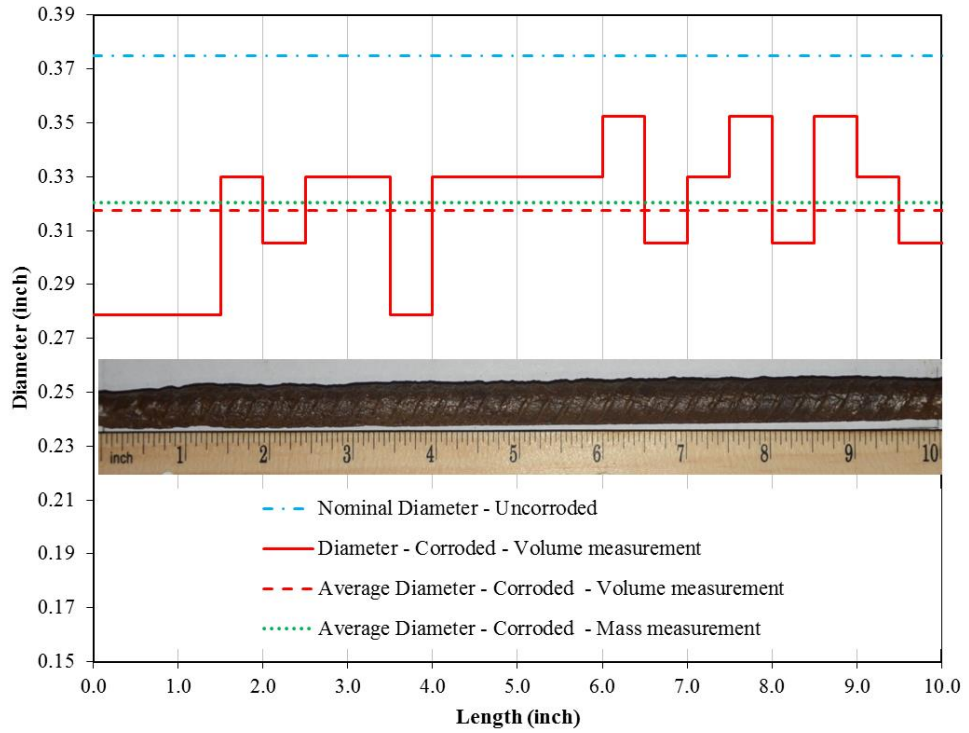
Cross section profile of MS-#3-9.7%



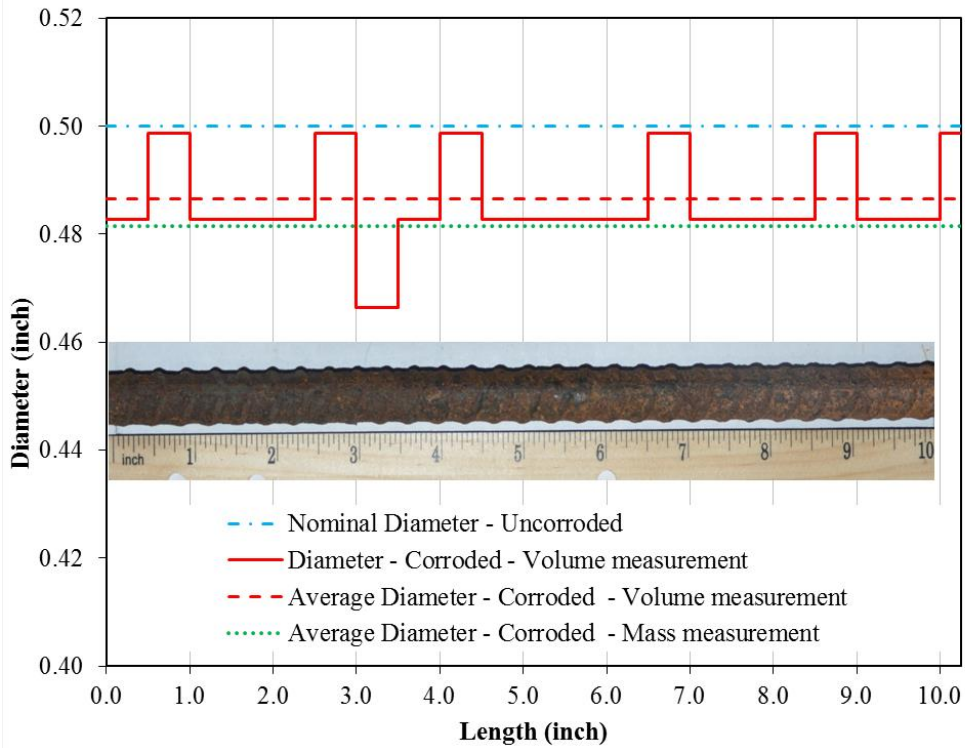
Cross section profile of MS-#3-12.1%



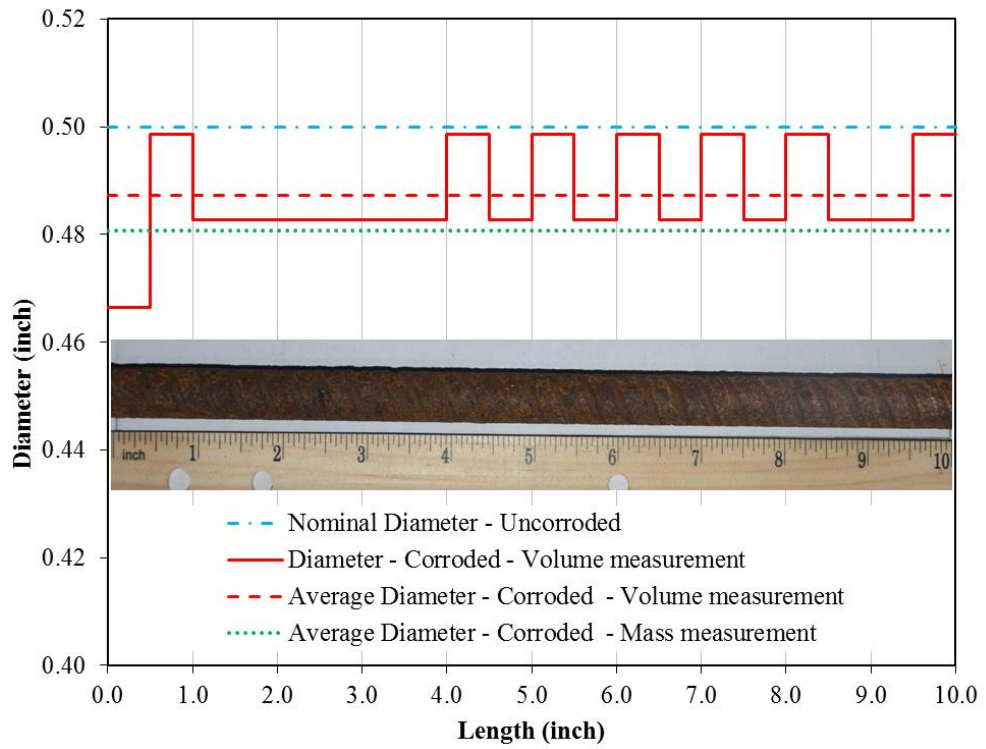
Cross section profile of MS-#3-12.4%



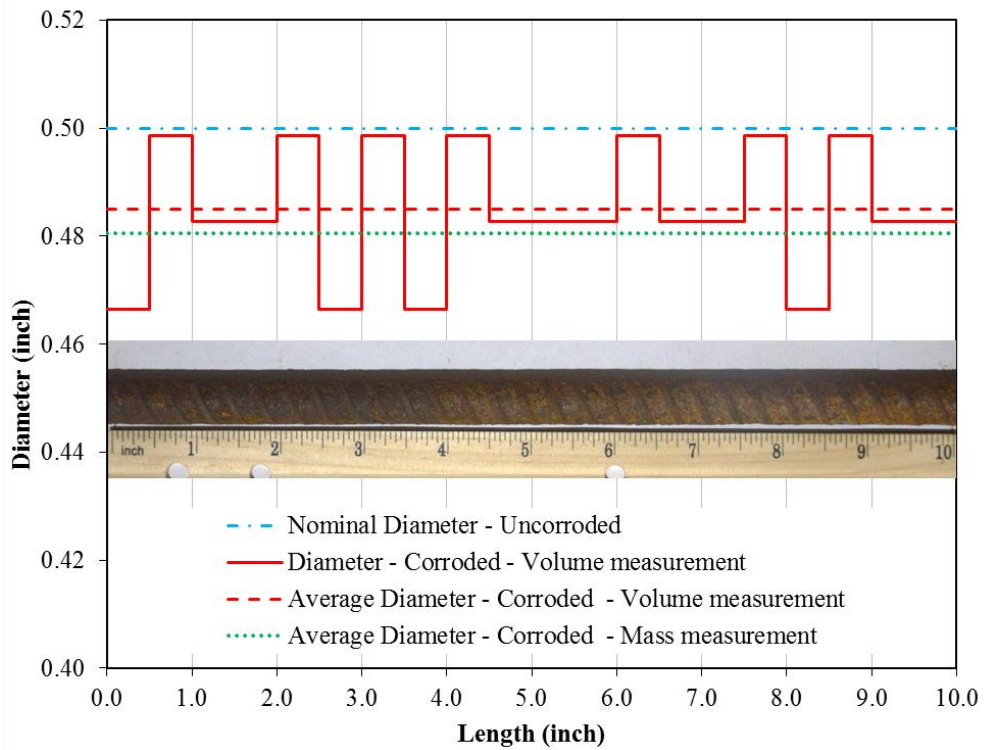
Cross section profile of MS-#3-16.4%



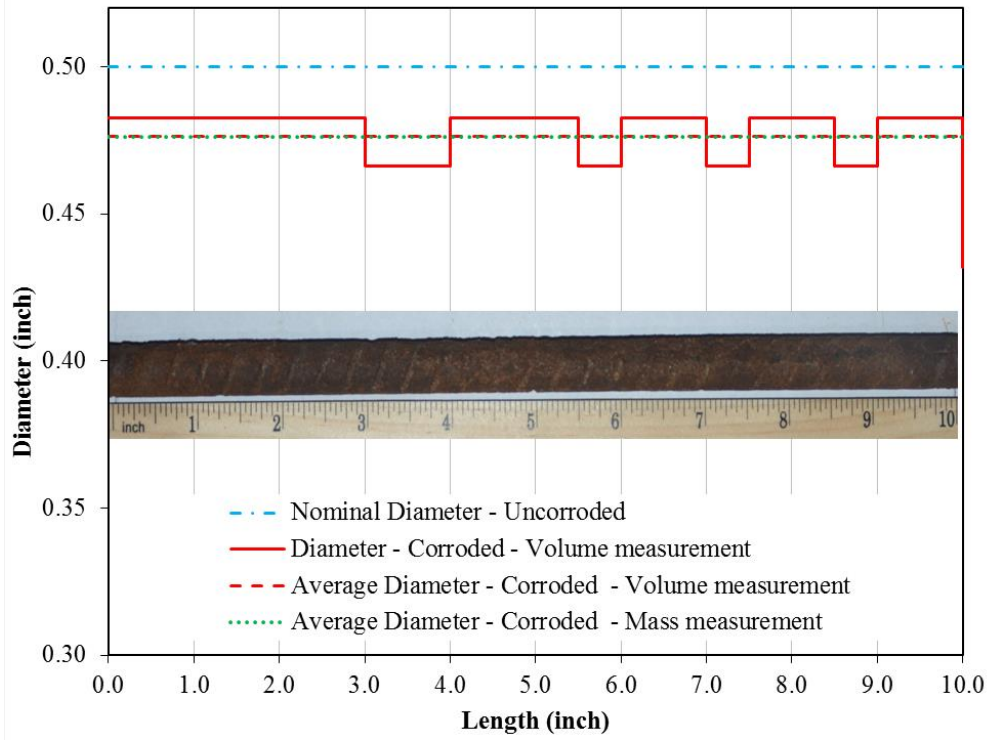
Cross section profile of MS-#4-2.5%



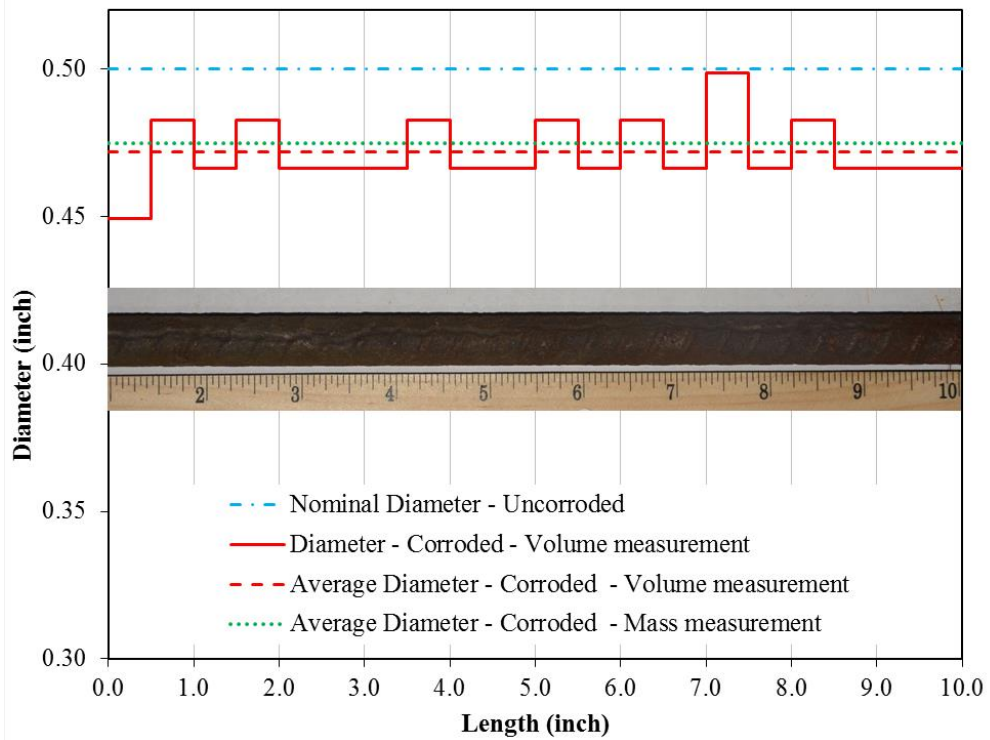
Cross section profile of MS-#4-2.8%



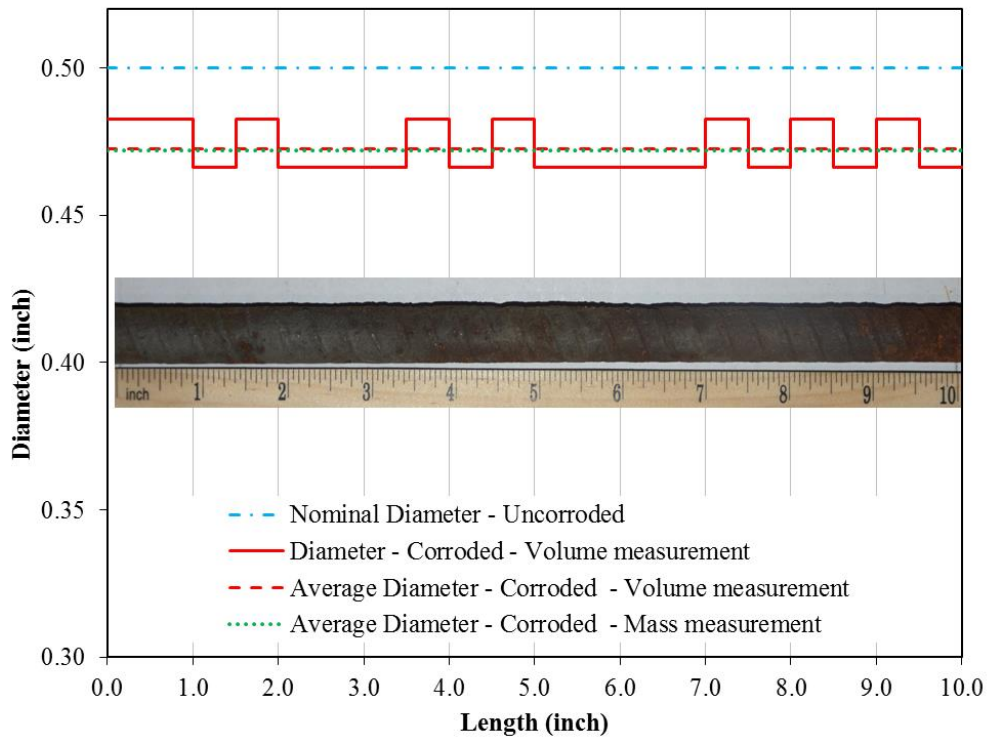
Cross section profile of MS-#4-3.0%



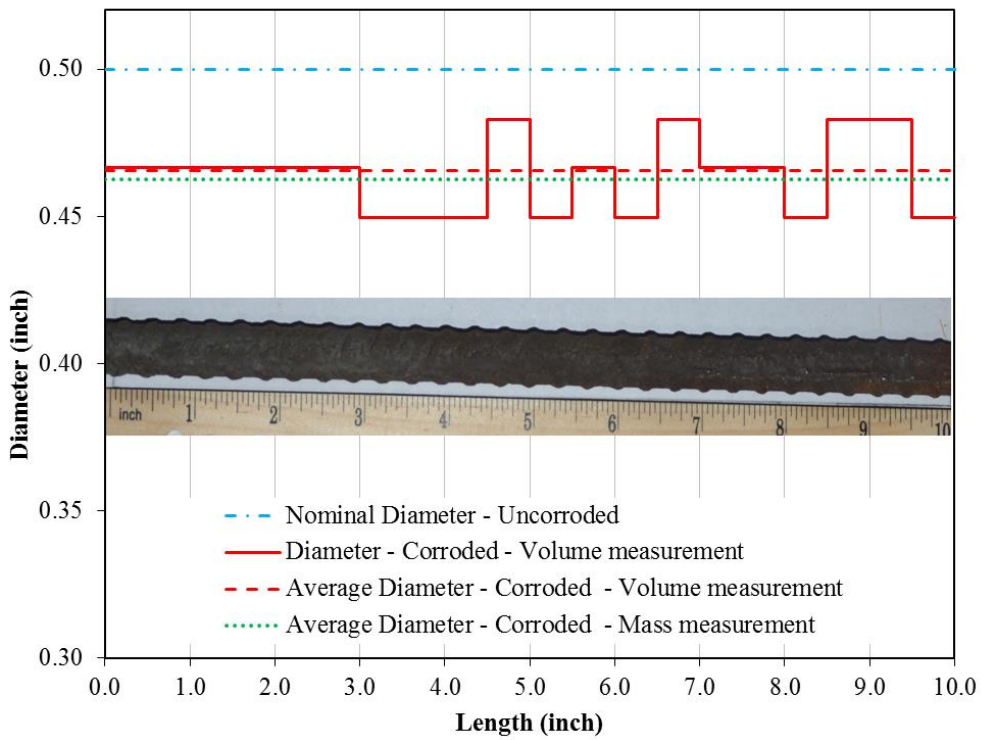
Cross section profile of MS-#4-4.0%



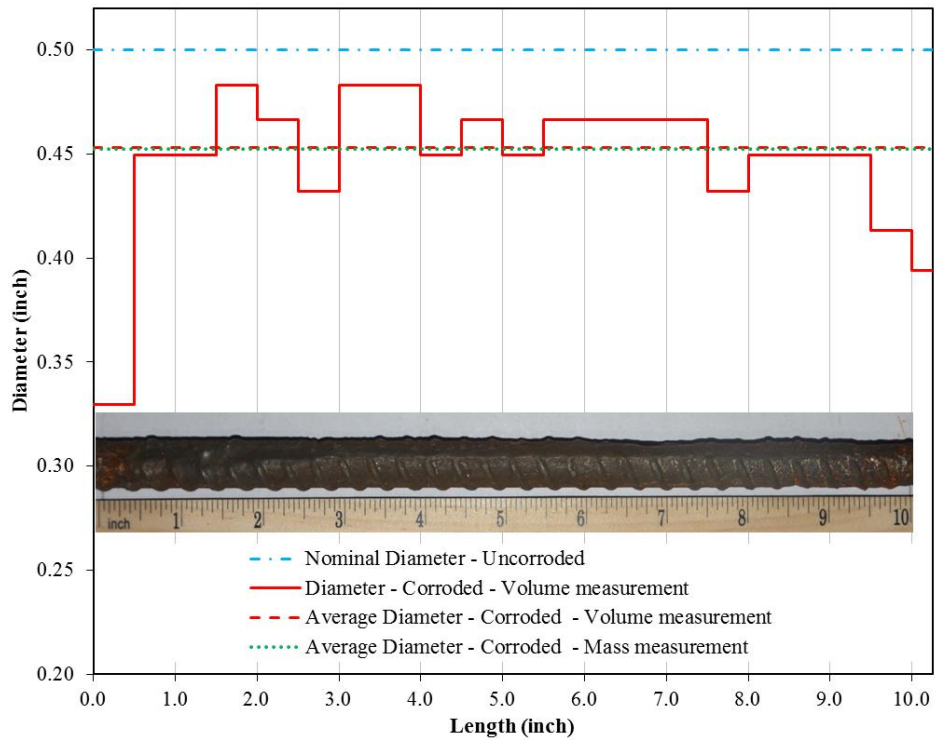
Cross section profile of MS-#4-4.4%



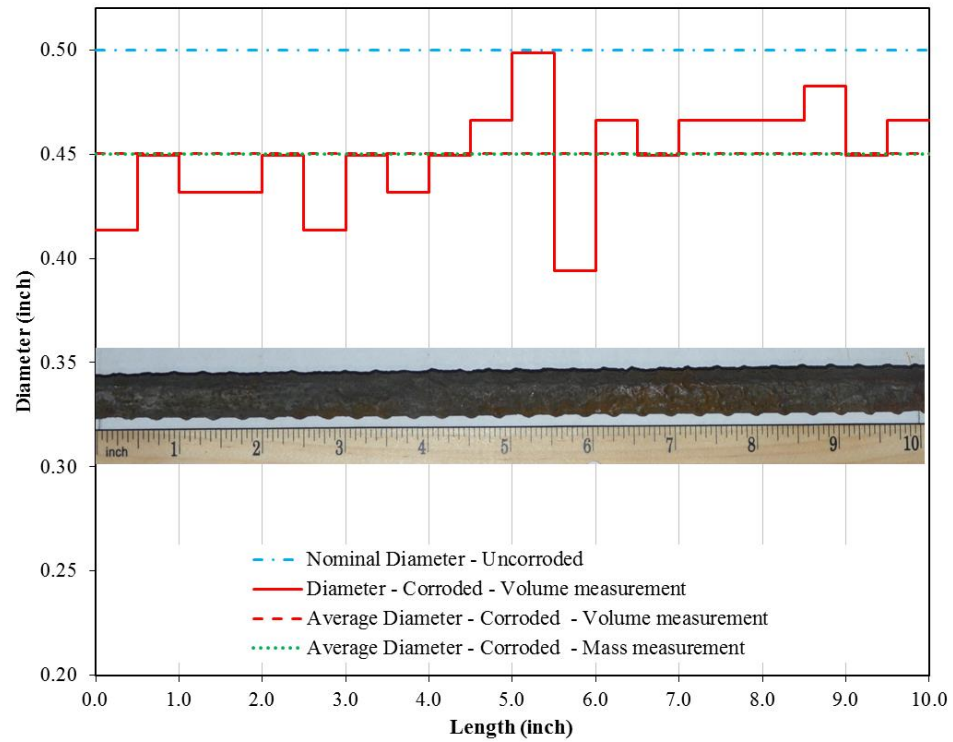
Cross section profile of MS-#4-4.8%



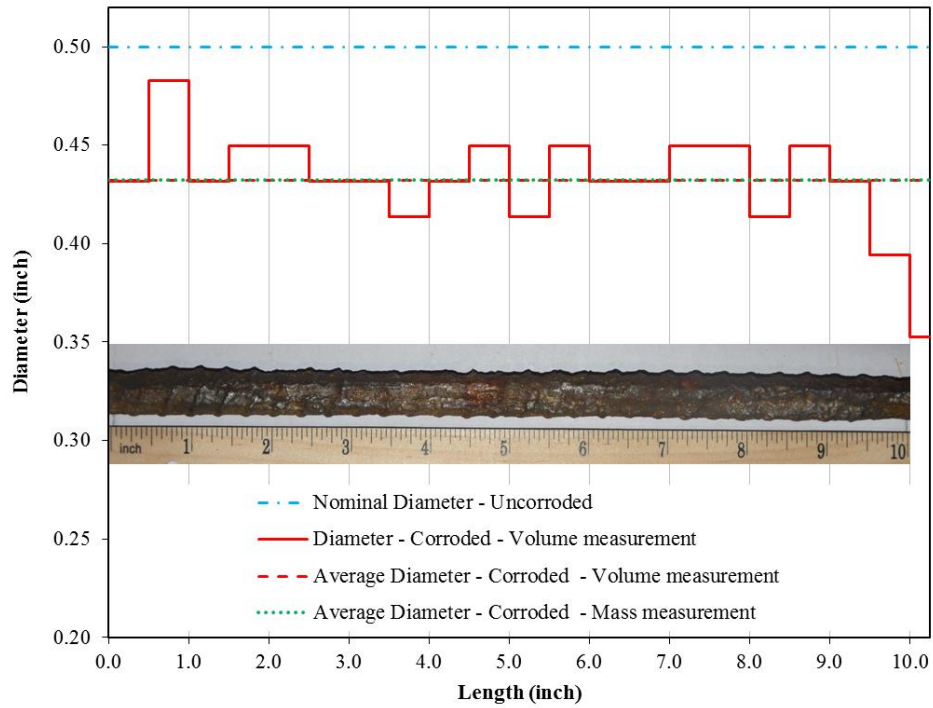
Cross section profile of MS-#4-7.1%



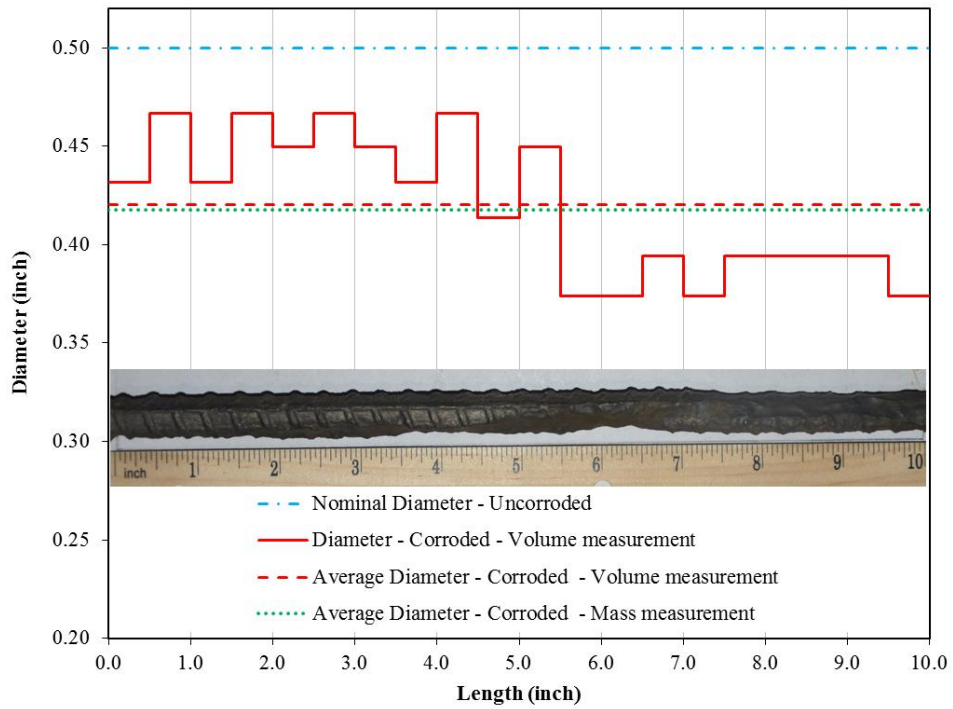
Cross section profile of MS-#4-9.6%



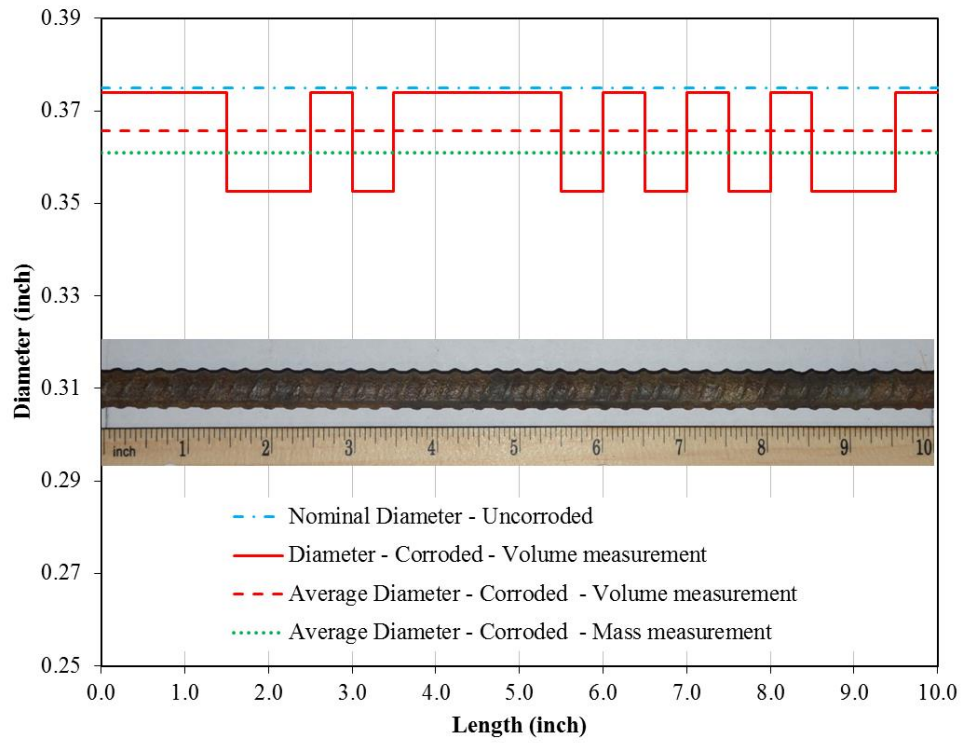
Cross section profile of MS-#4-10.3%



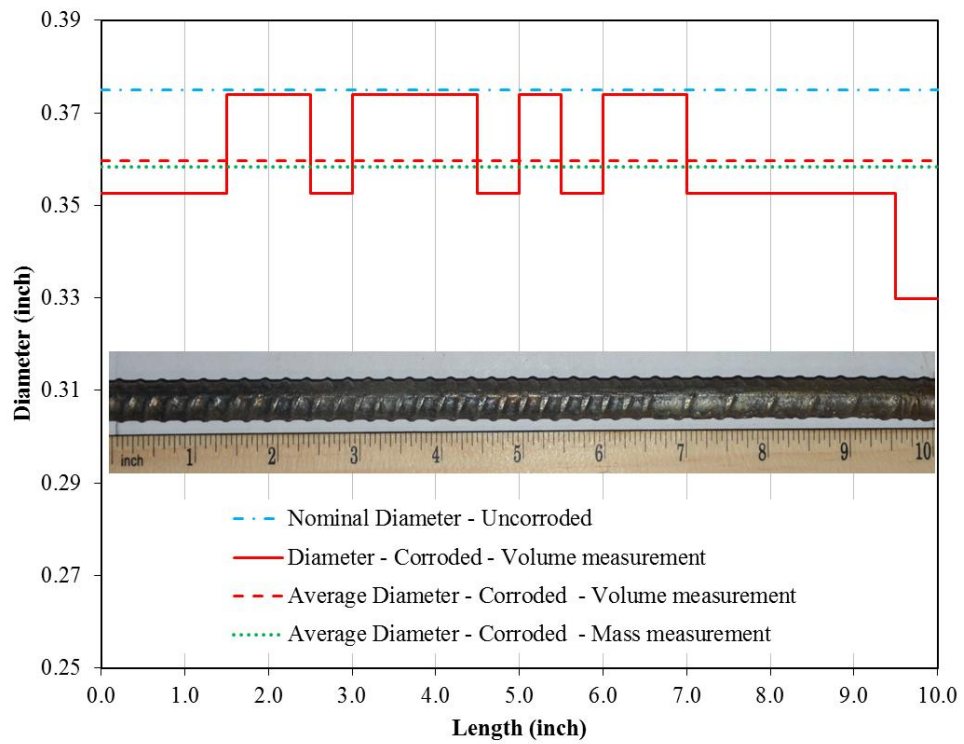
Cross section profile of MS-#4-14.3%



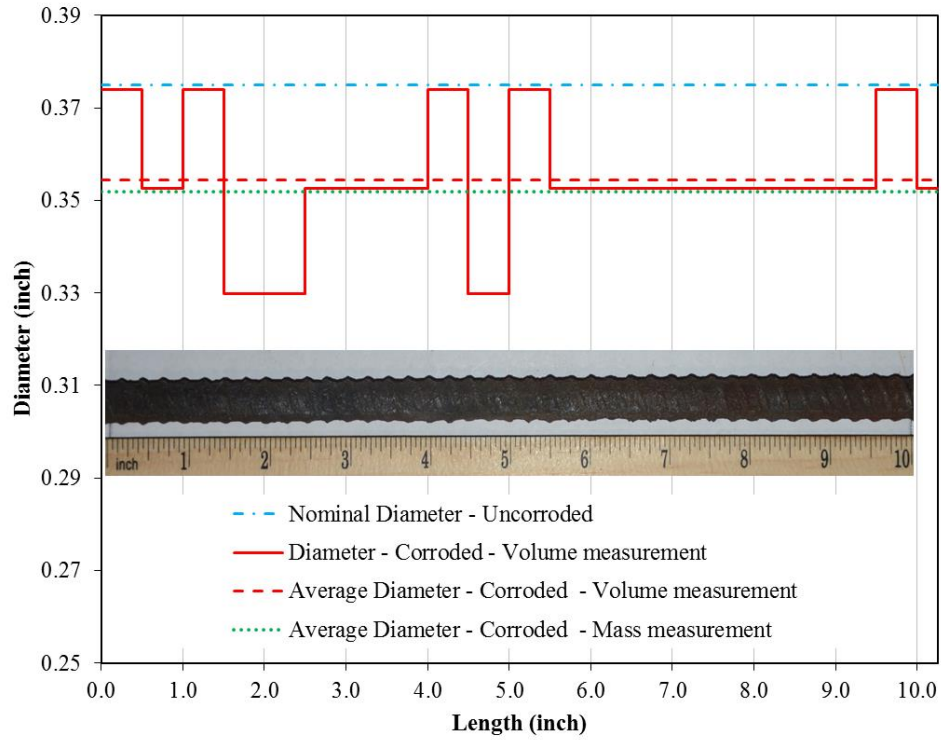
Cross section profile of MS-#4-17.5%



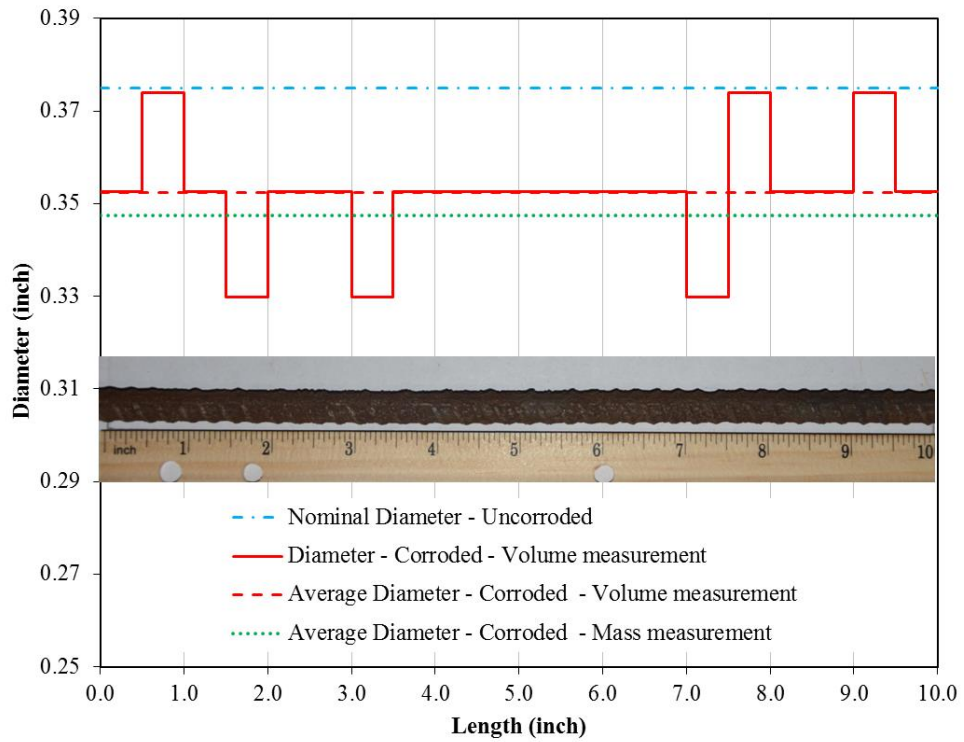
Cross section profile of HC-#3-3.1%



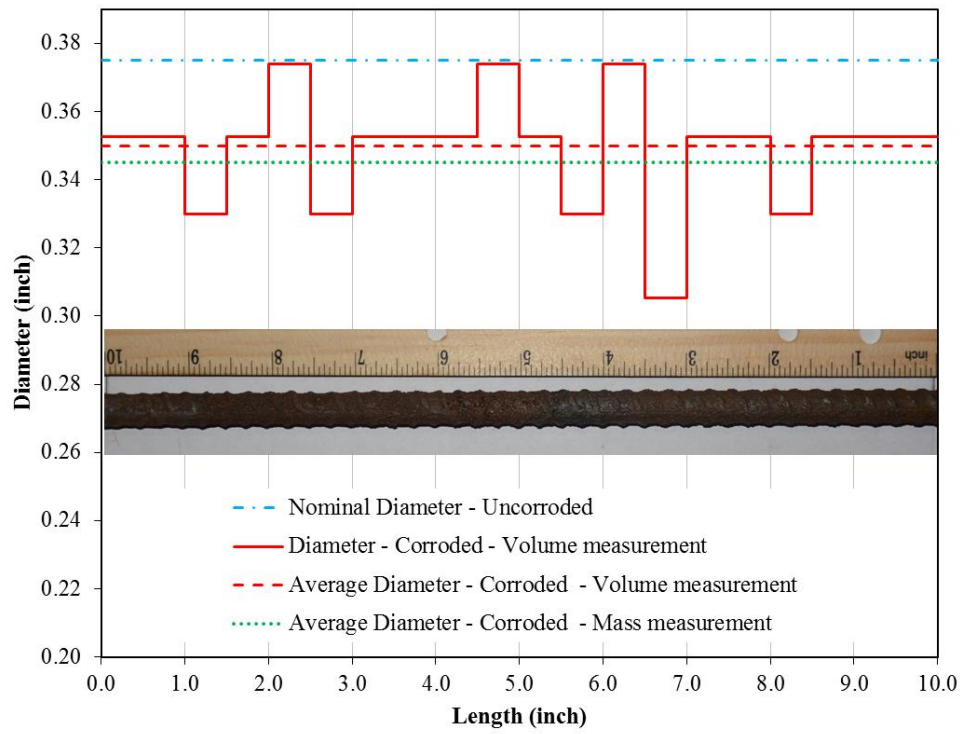
Cross section profile of HC-#3-5.0%



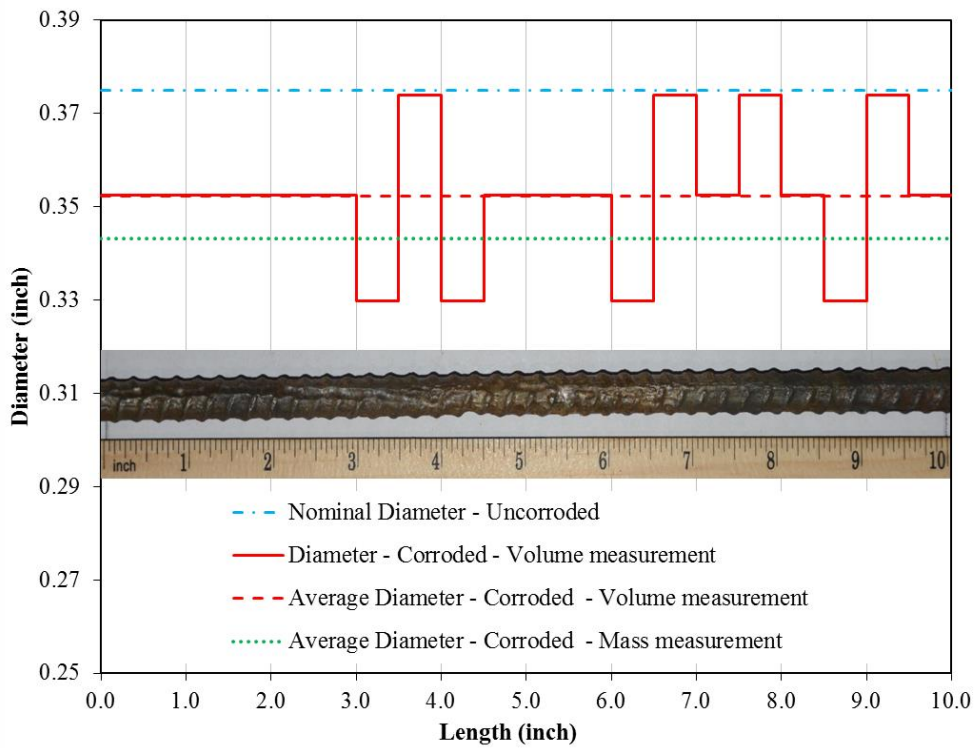
Cross section profile of HC-#3-5.9%



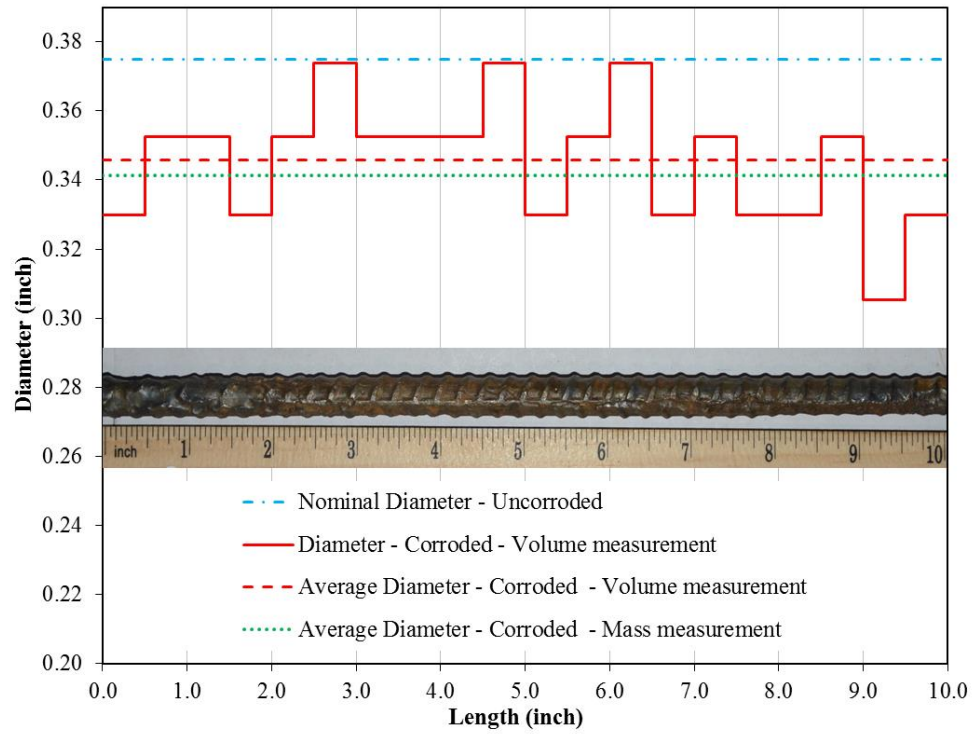
Cross section profile of HC-#3-7.5%



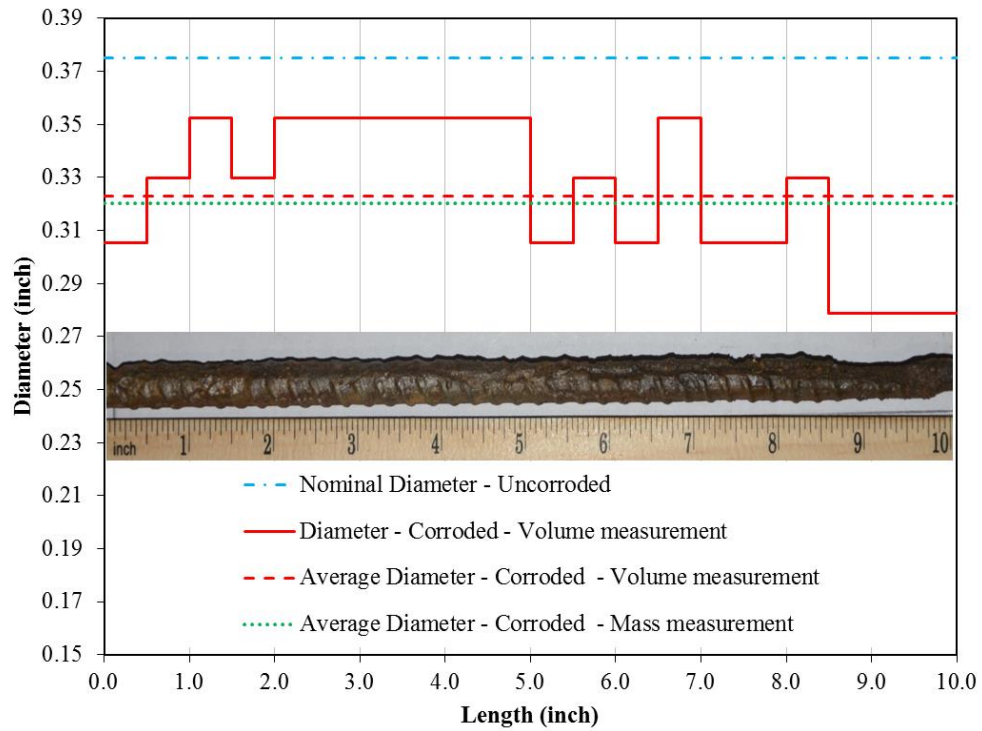
Cross section profile of HC-#3-7.7



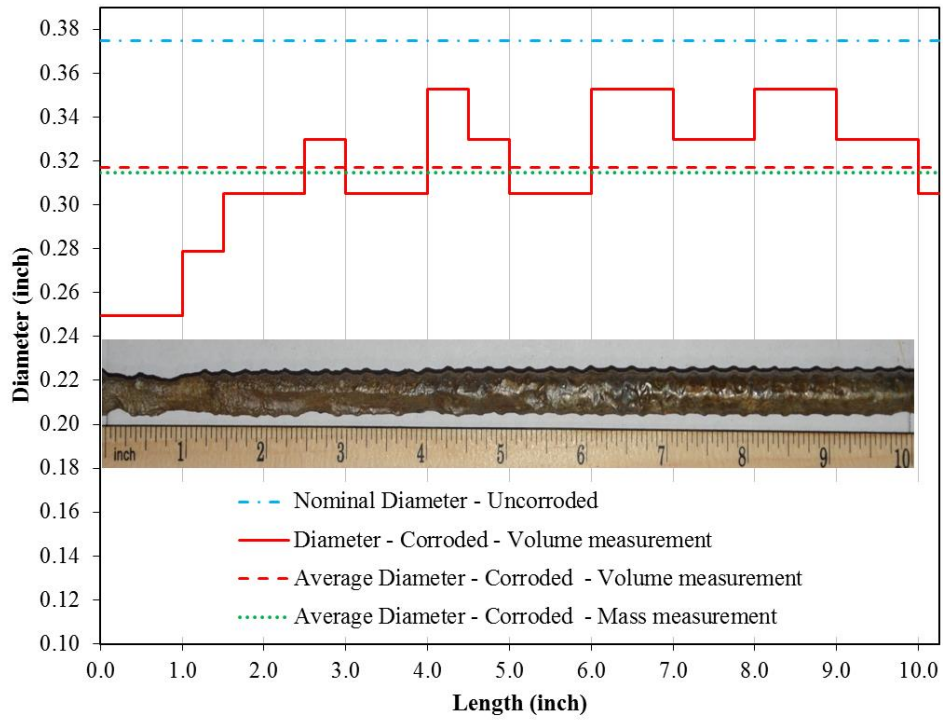
Cross section profile of HC-#3-8.9%



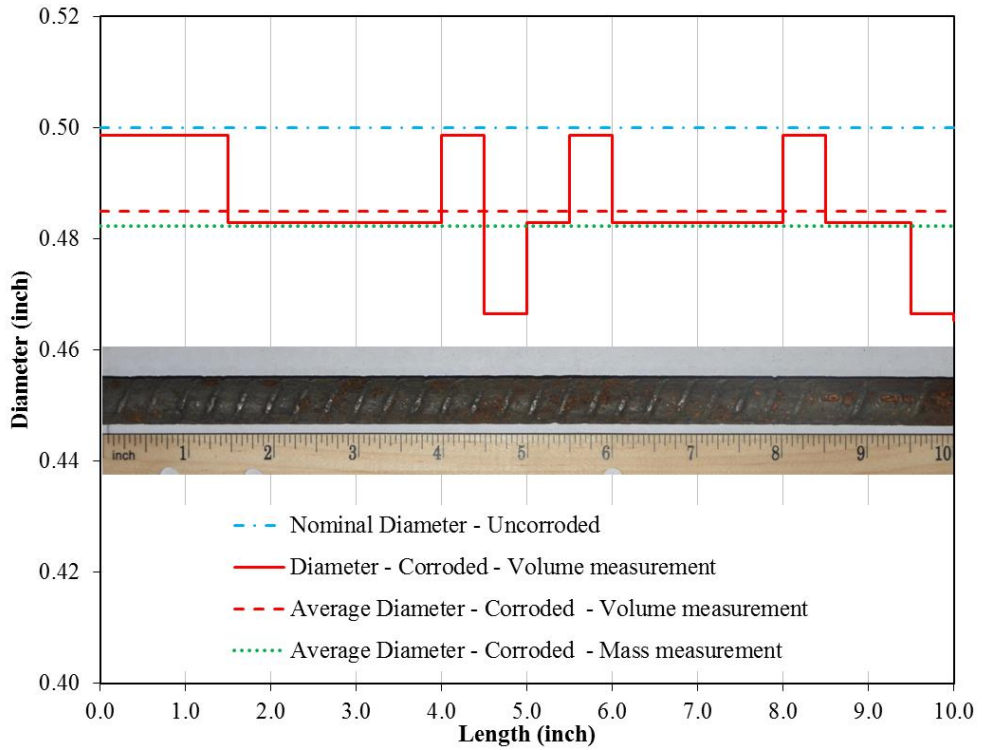
Cross section profile of HC-#3-9.2%



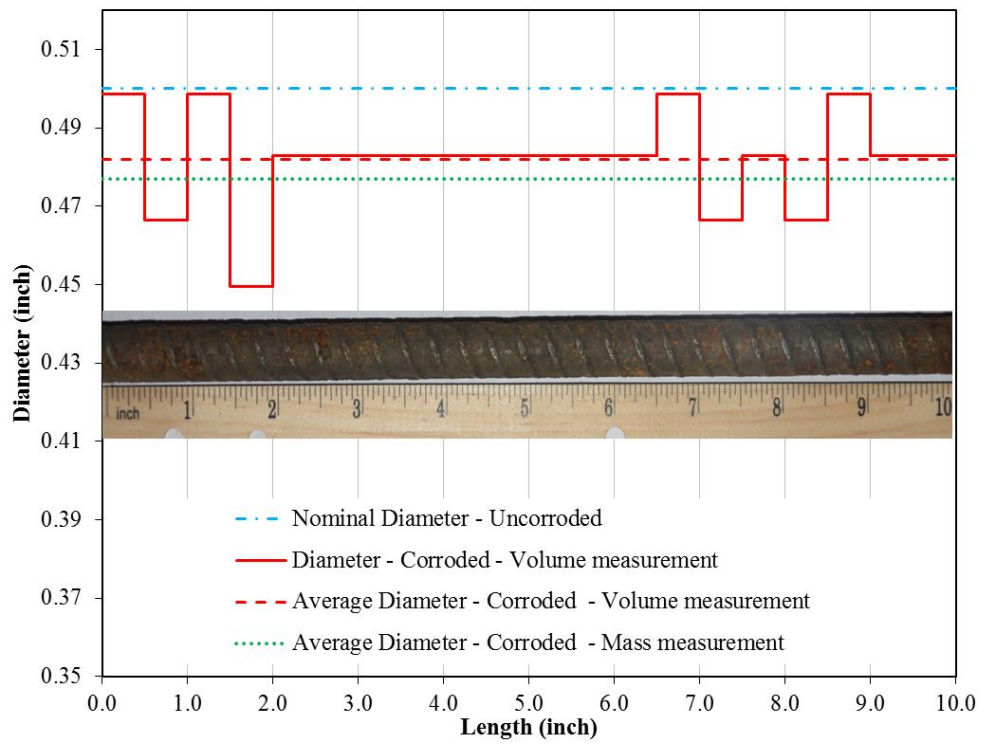
Cross section profile of HC-#3-15.4%



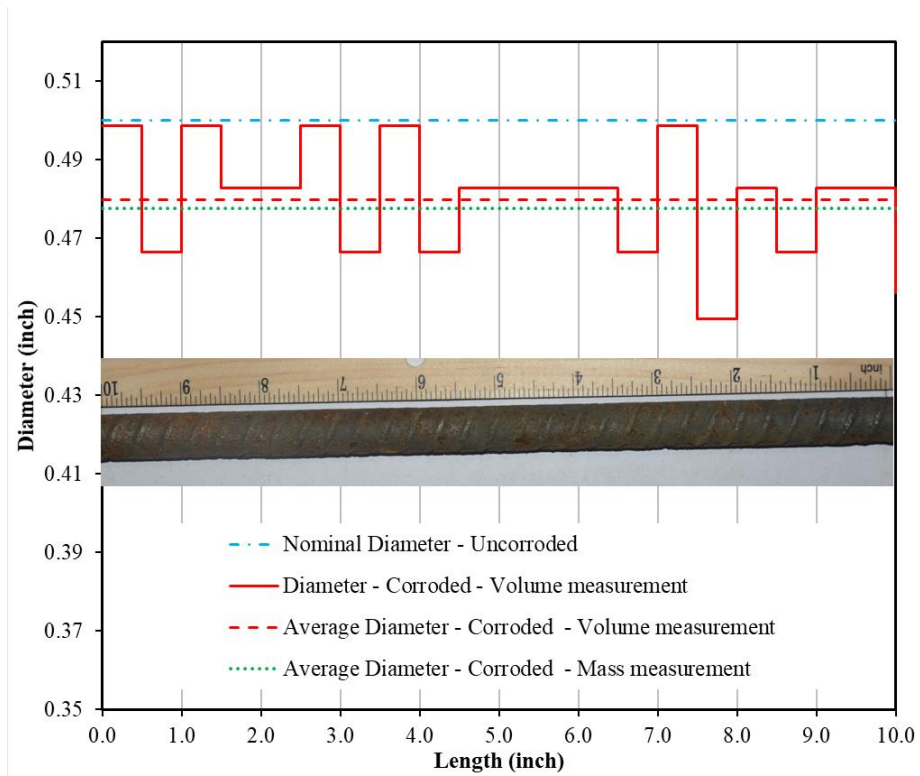
Cross section profile of HC-#3-16.7%



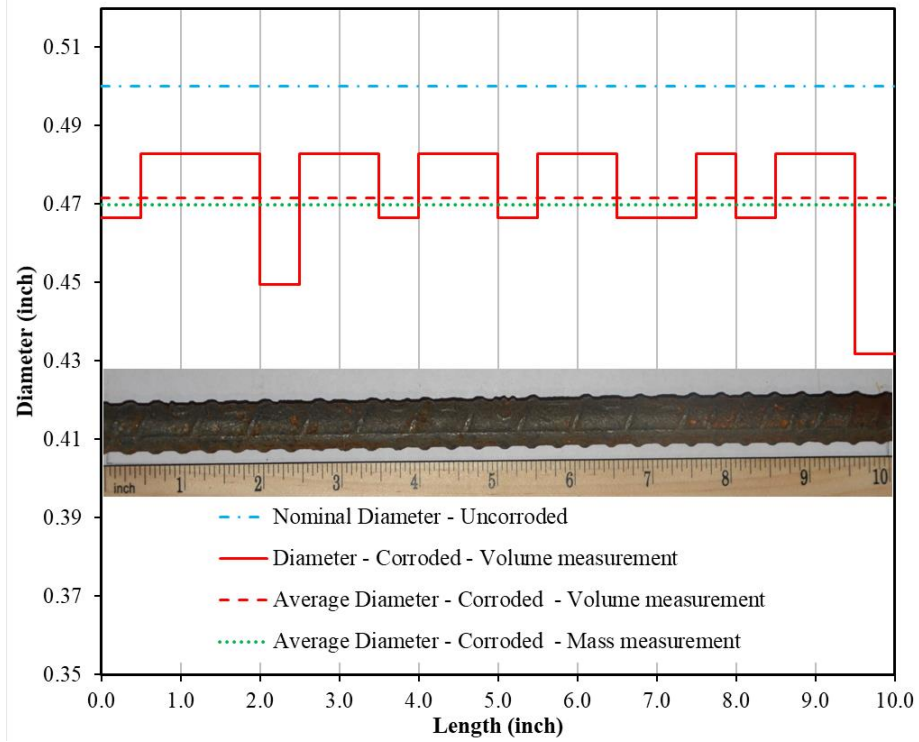
Cross section profile of HC-#4-2.0%



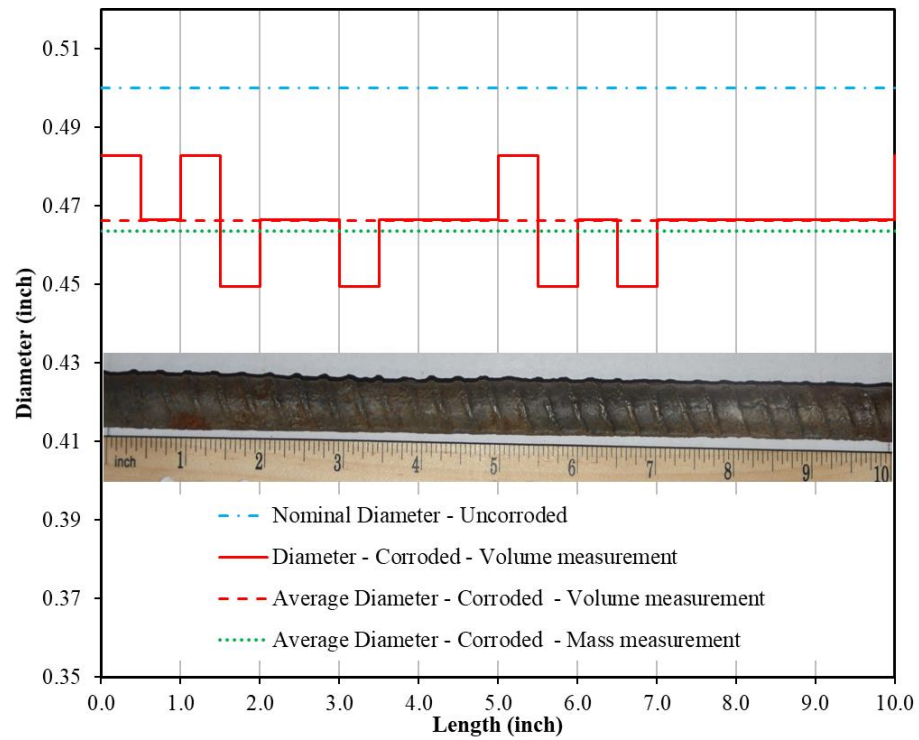
Cross section profile of HC-#4-2.9%



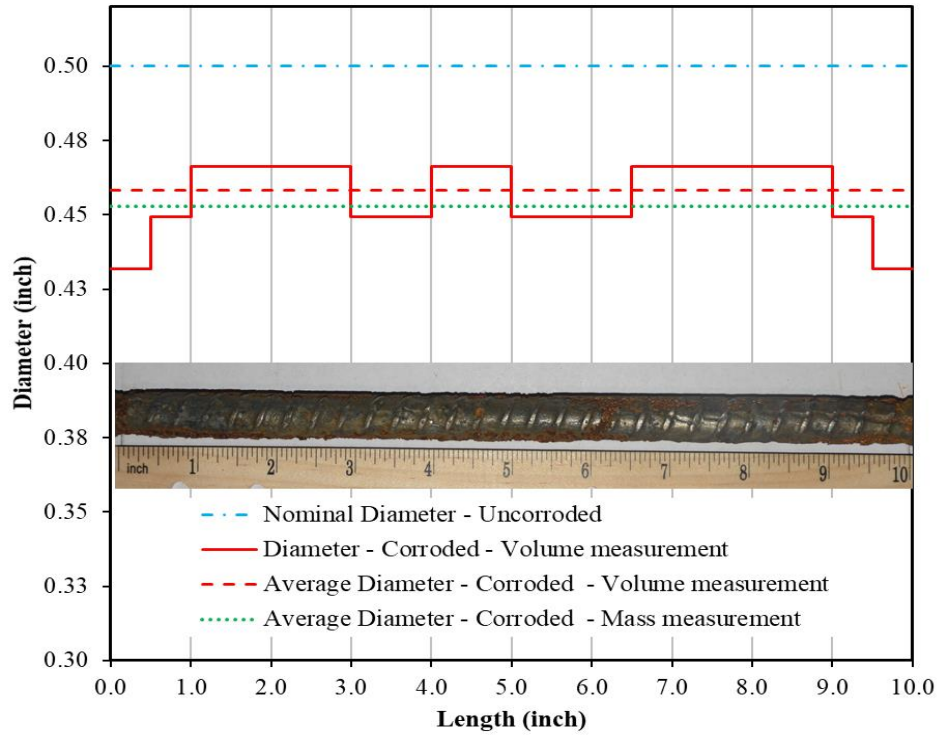
Cross section profile of HC-#4-3.1 %



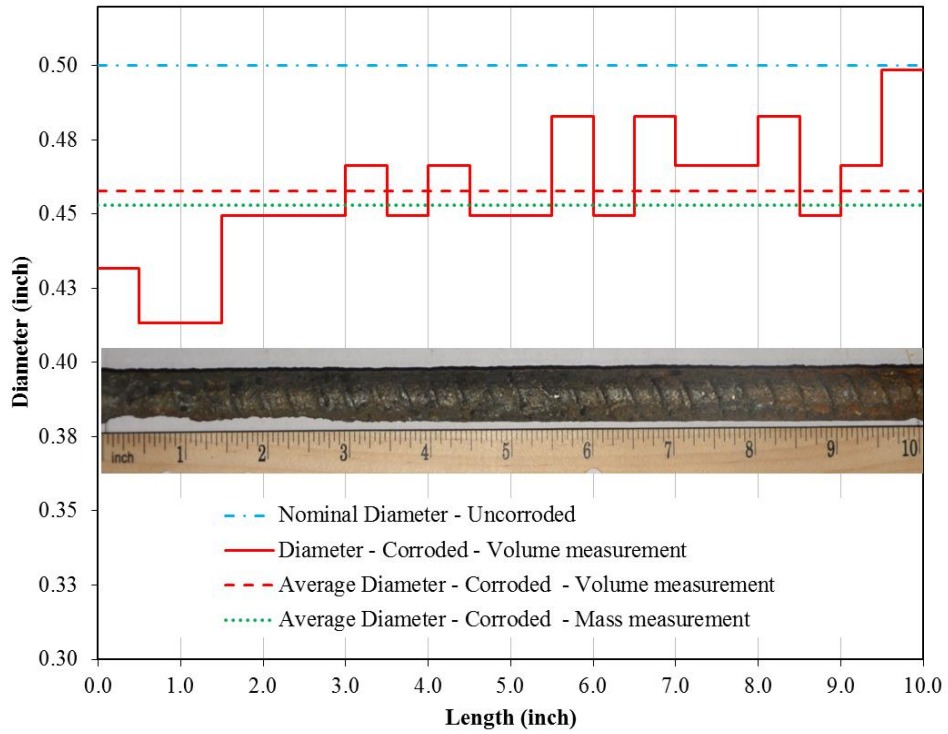
Cross section profile of HC-#4-4.8%



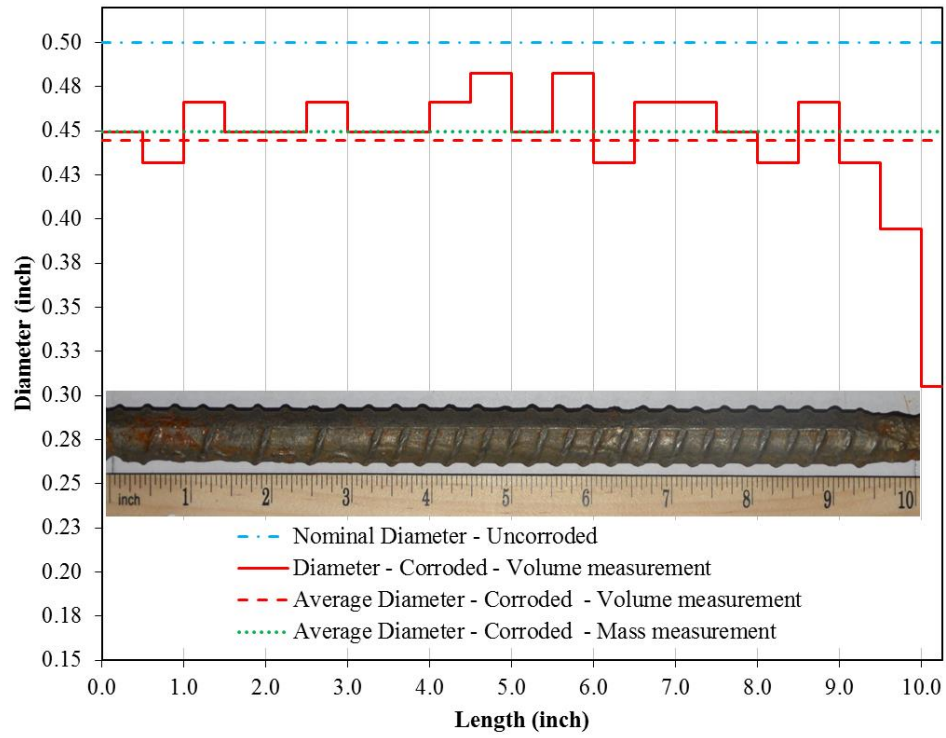
Cross section profile of HC-#4-6.1%



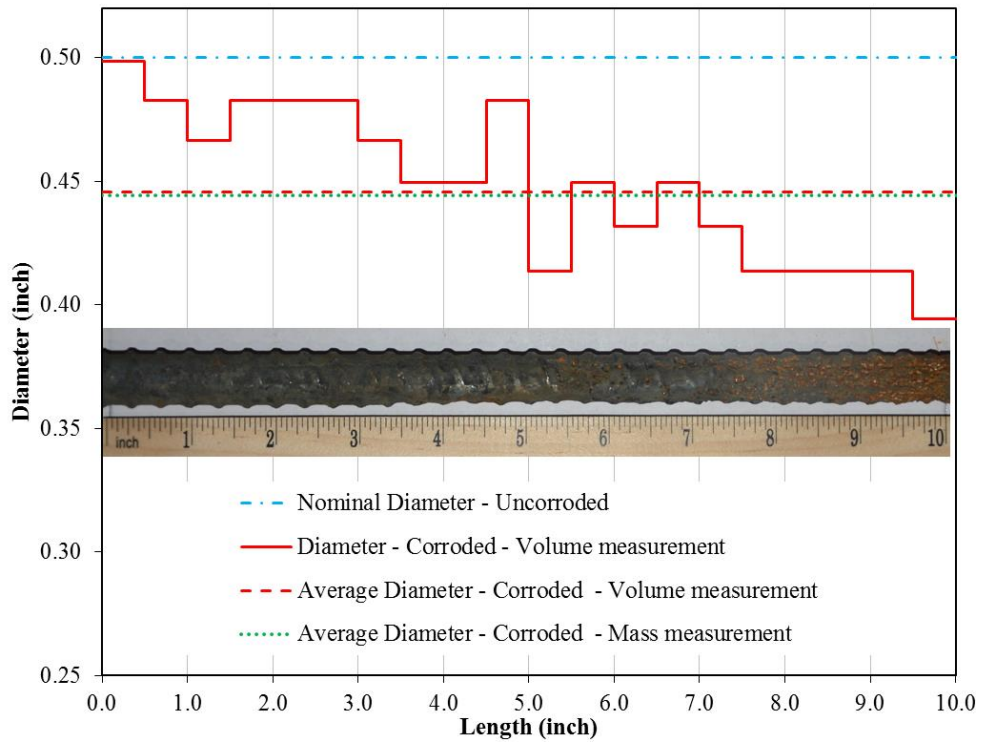
HC-#4-9.0% -Cross Section Profile



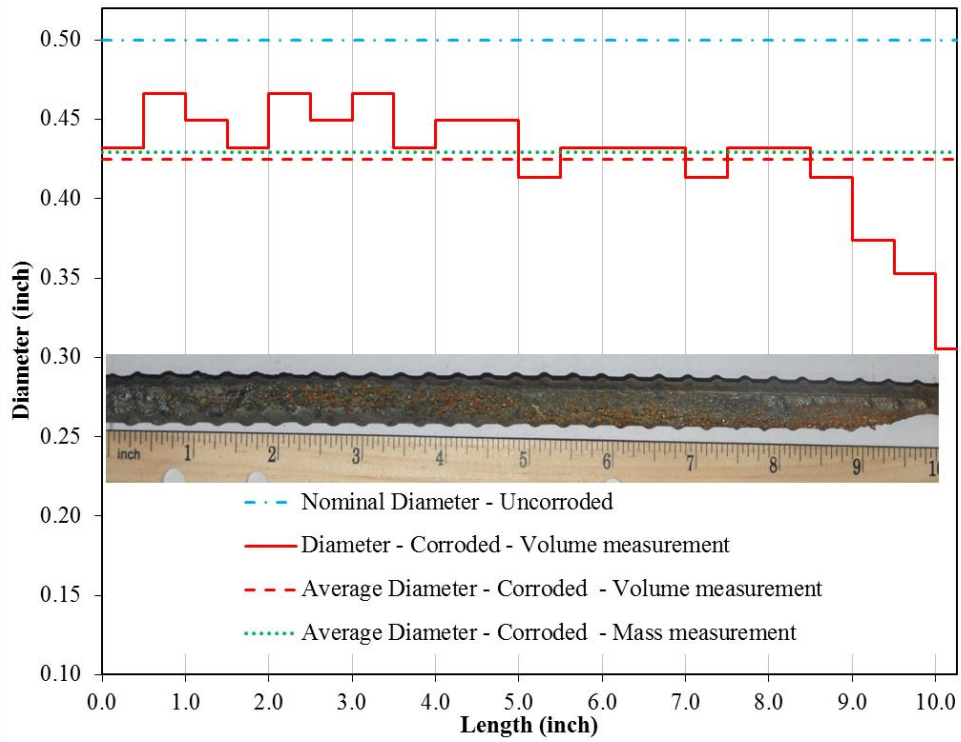
Cross section profile of HC-#4-9.4%



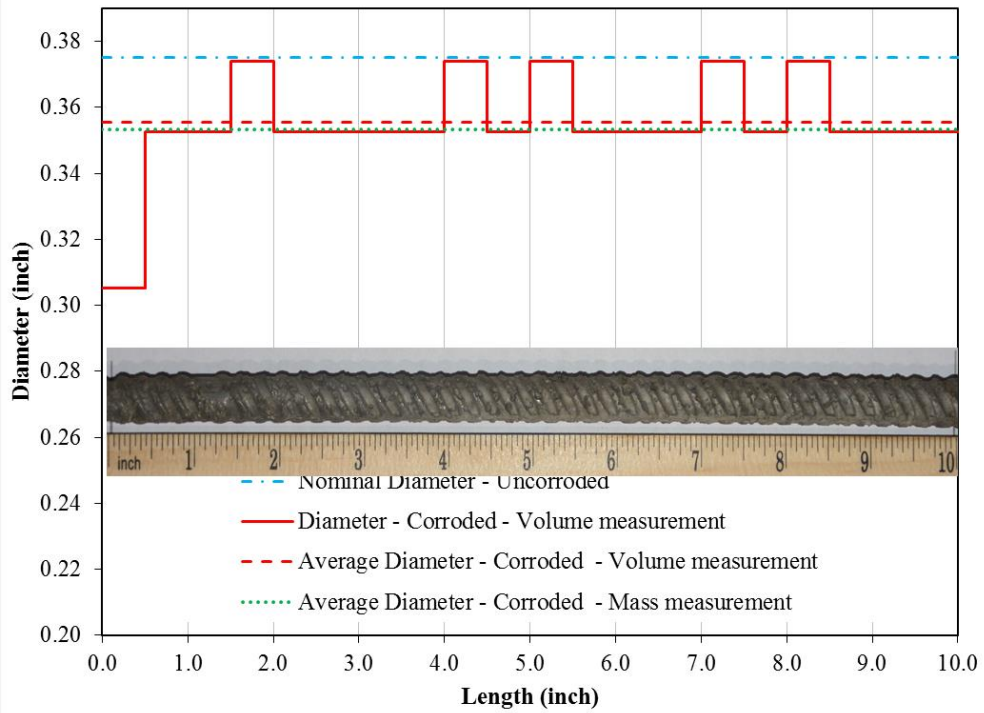
Cross section profile of HC-#4-9.8%



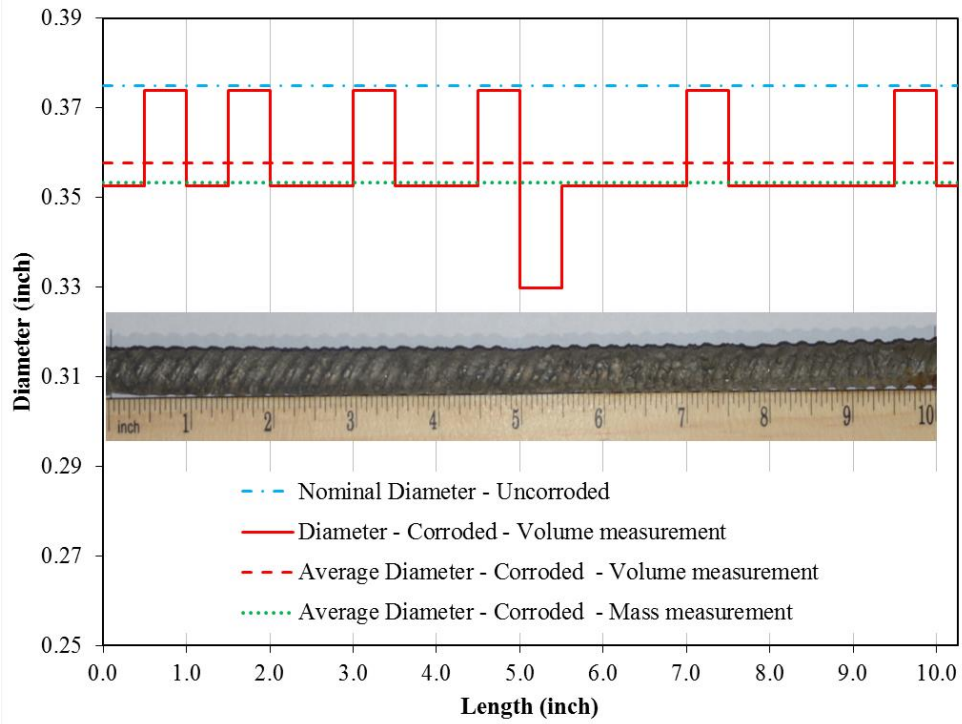
Cross section profile of HC-#4-10.5%



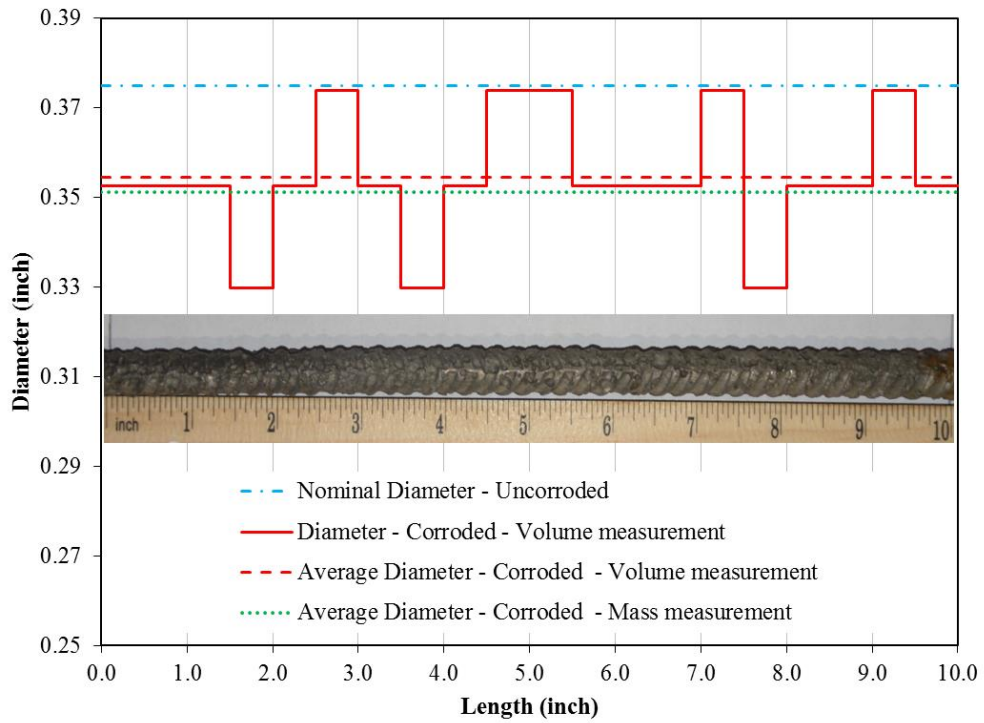
Cross section profile of HC-#4-14.7%



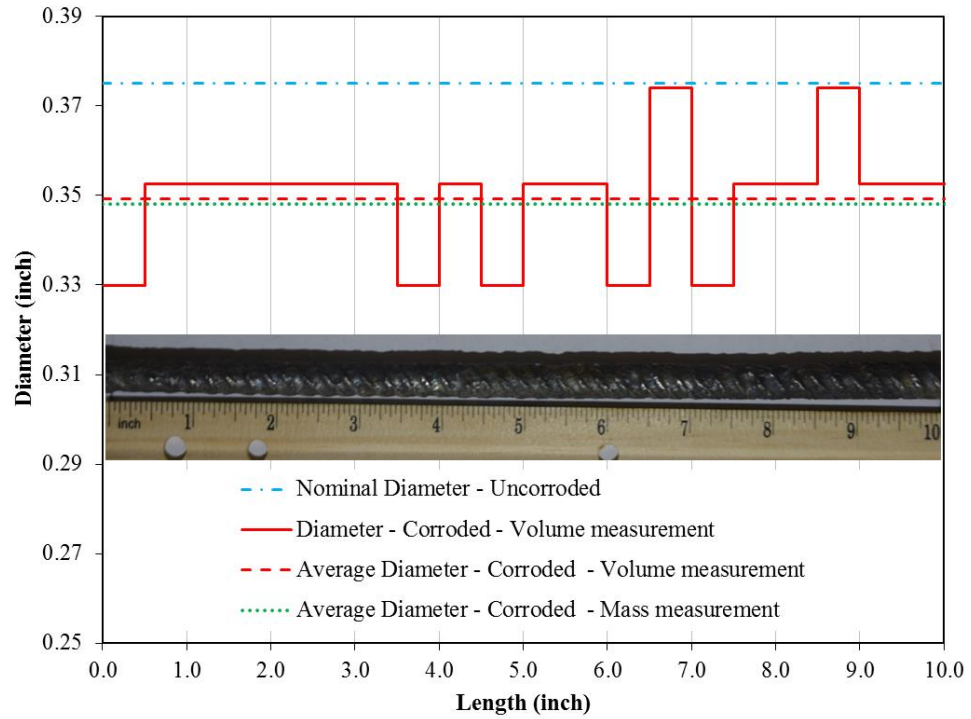
Cross section profile of SS-#3-4.9%



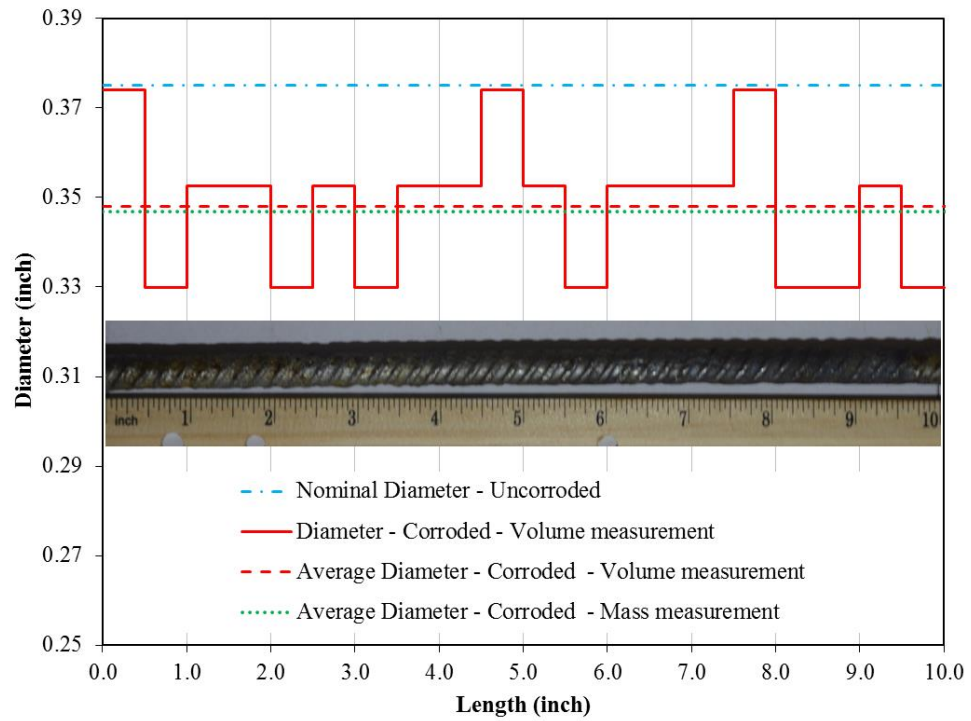
Cross section profile of SS-#3-5.5%



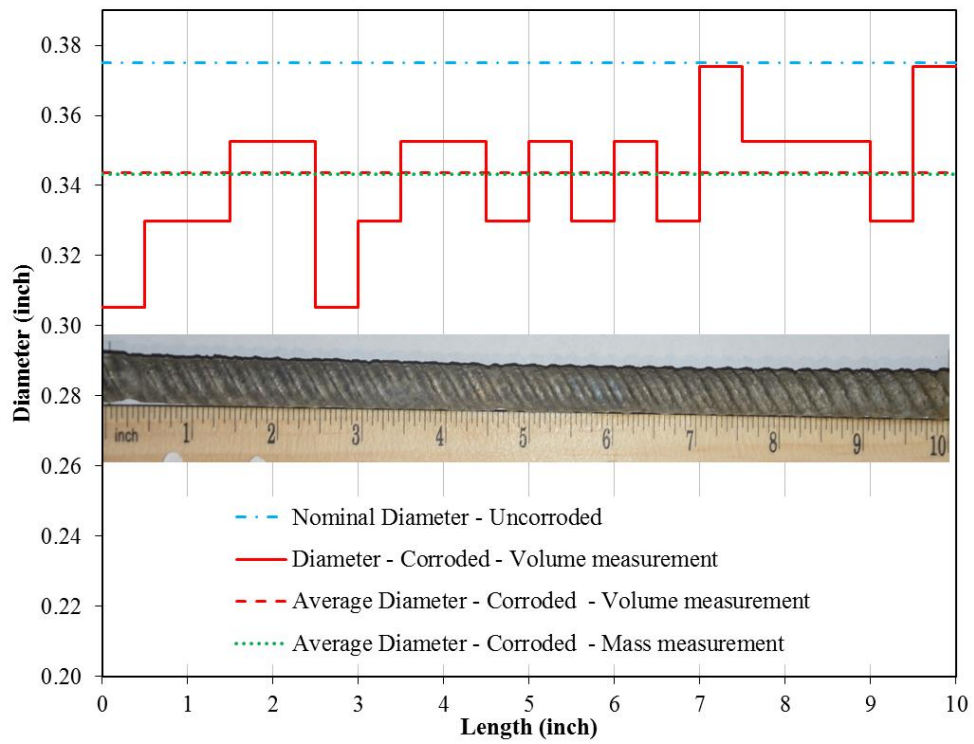
Cross section profile of SS-#3-6.3%



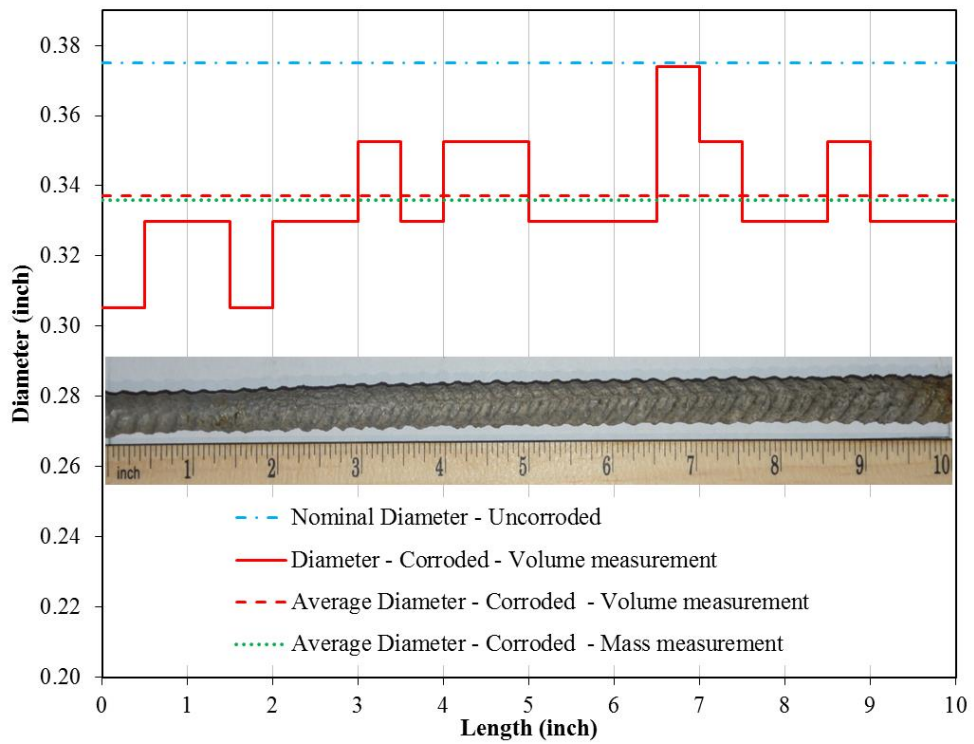
Cross section profile of SS-#3-6.8%



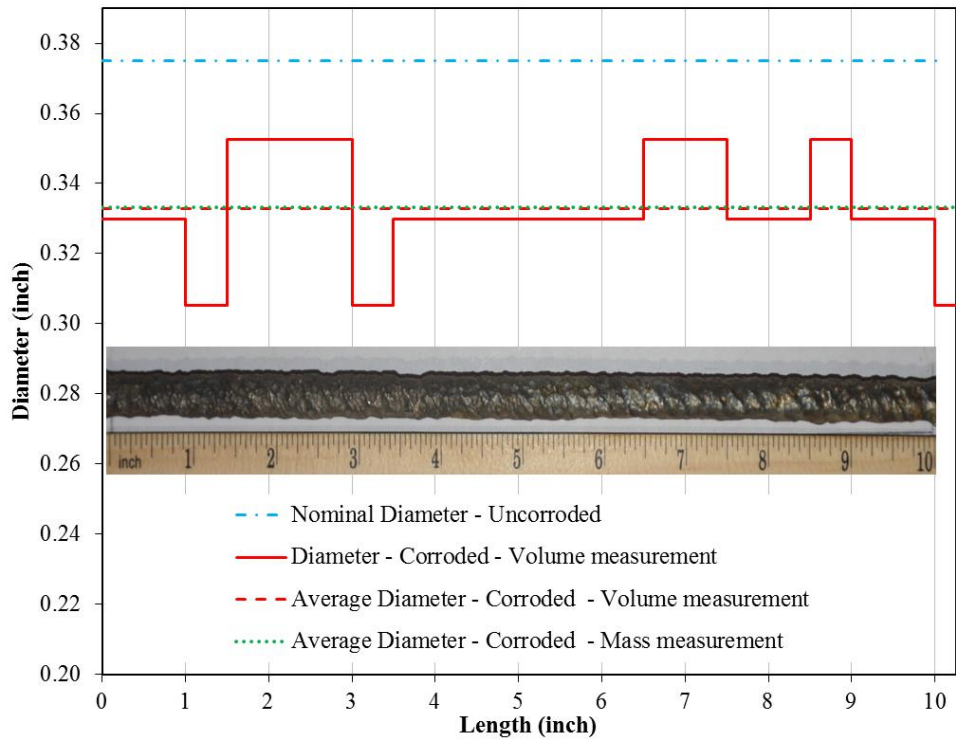
Cross section profile of SS-#3-7.3%



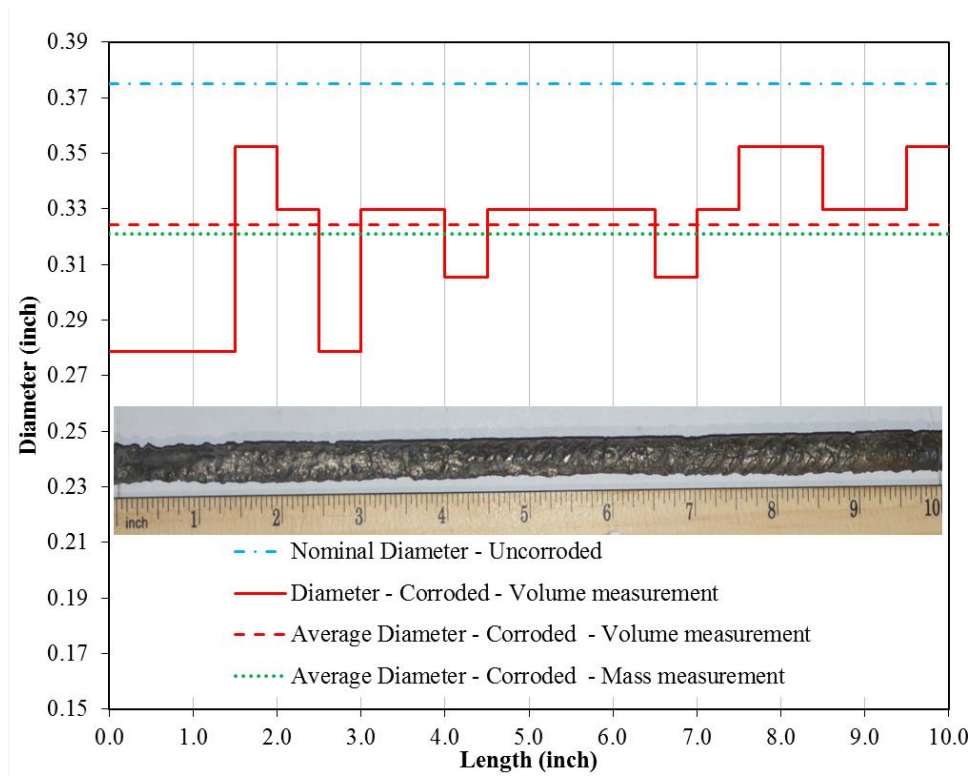
Cross section profile of SS-#3-9.0%



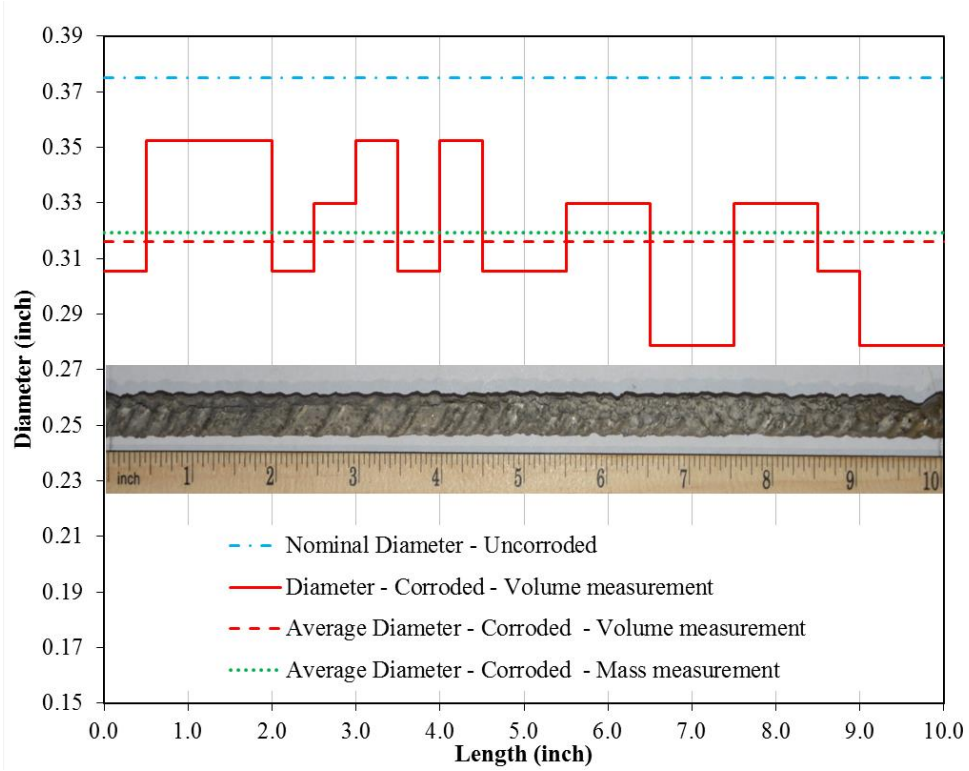
Cross section profile of SS-#3-10.7%



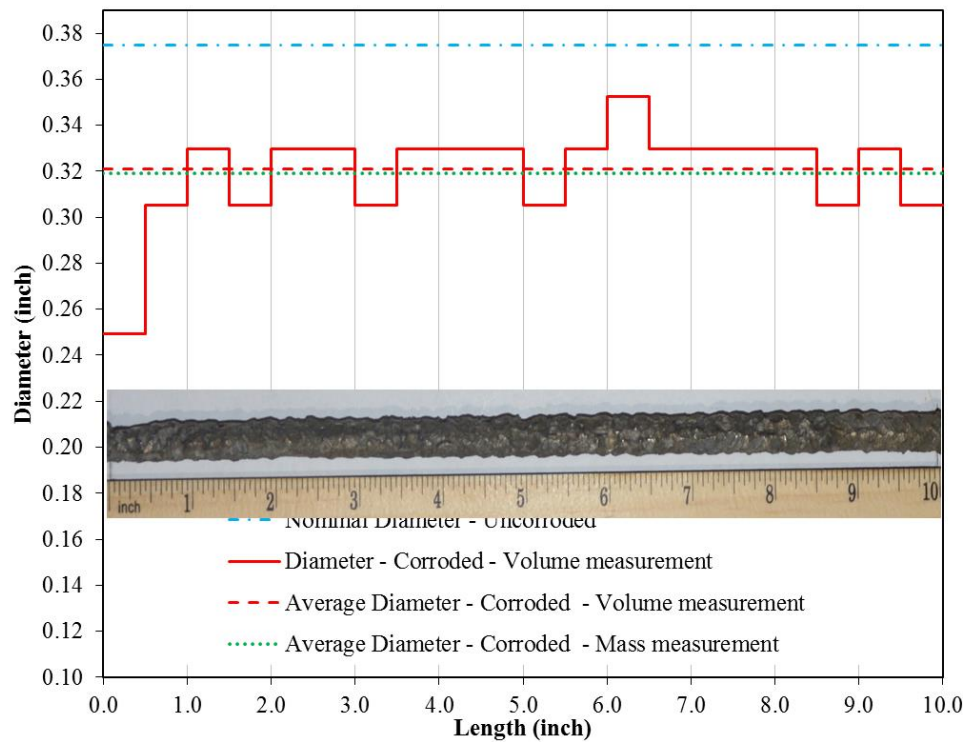
Cross section profile of SS-#3-11.9%



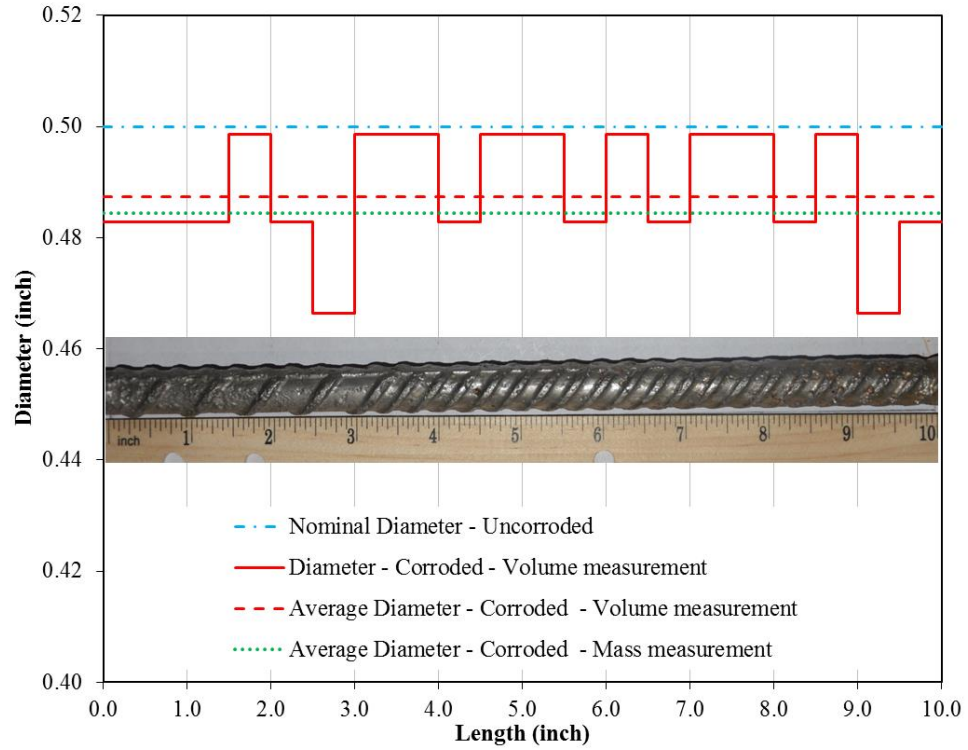
SS-#3-15.6% -Cross Section Profile



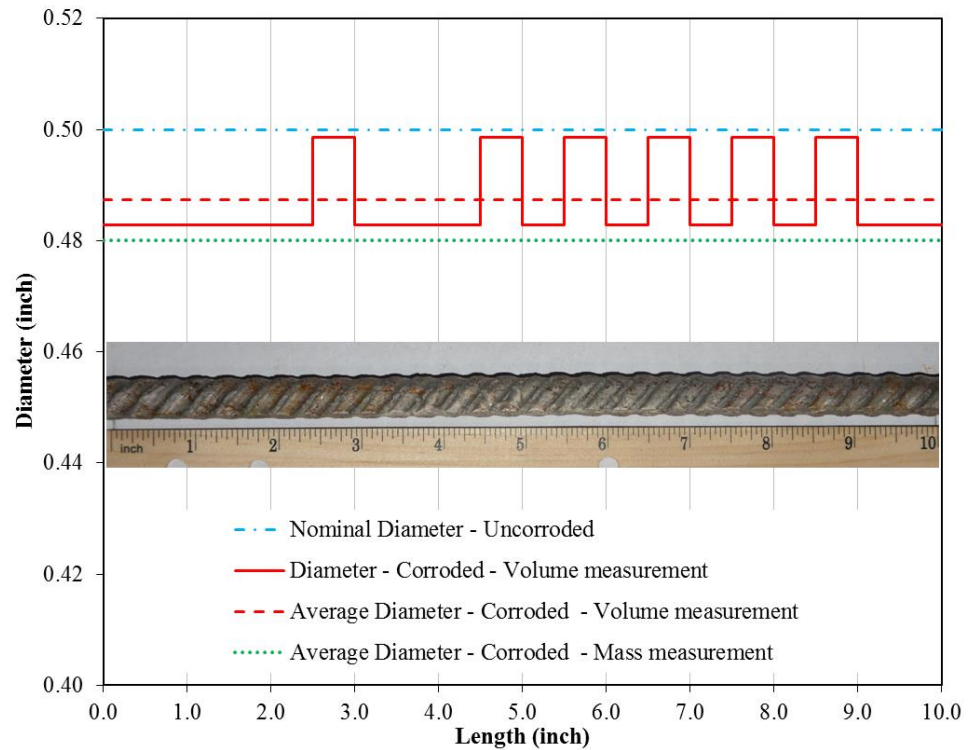
Cross section profile of SS-#3-16.0%



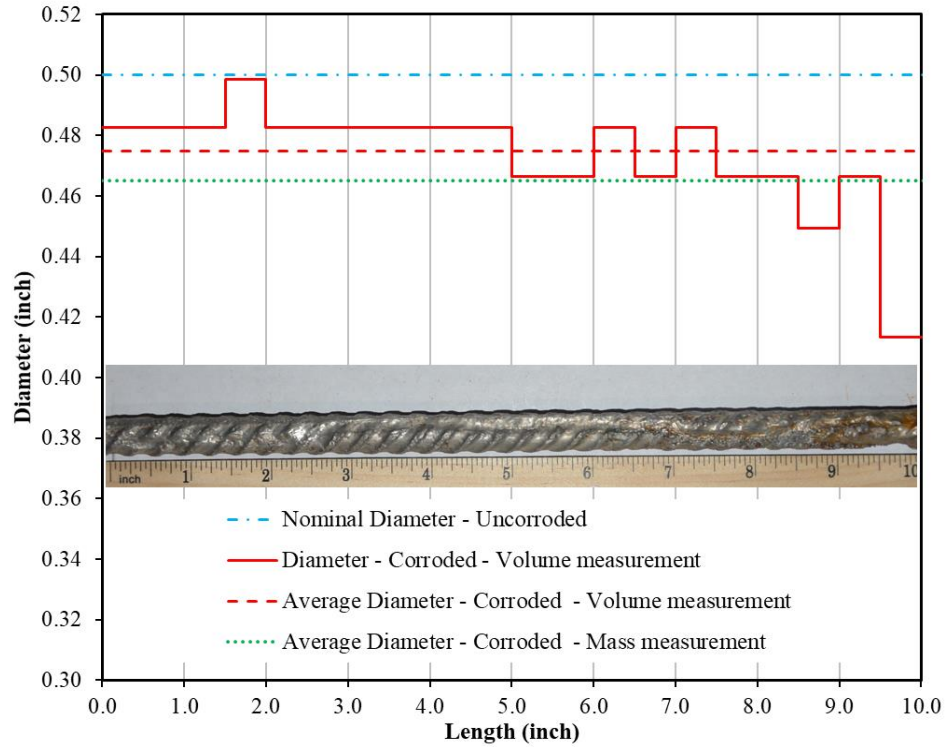
Cross section profile SS-#3-16.1%



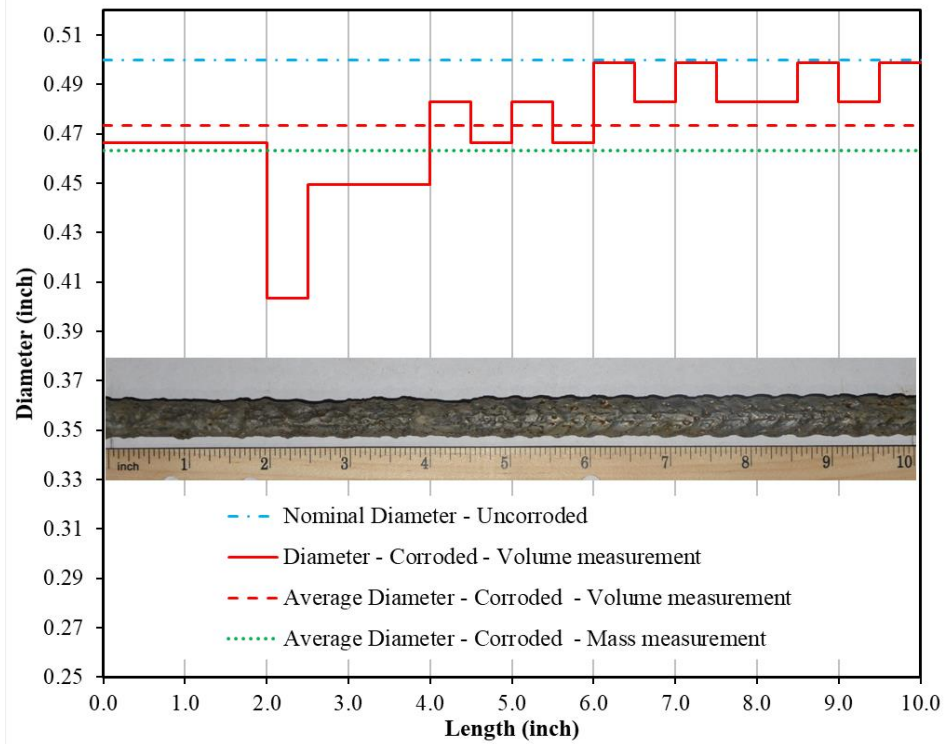
Cross section profile SS-#4-3.2%



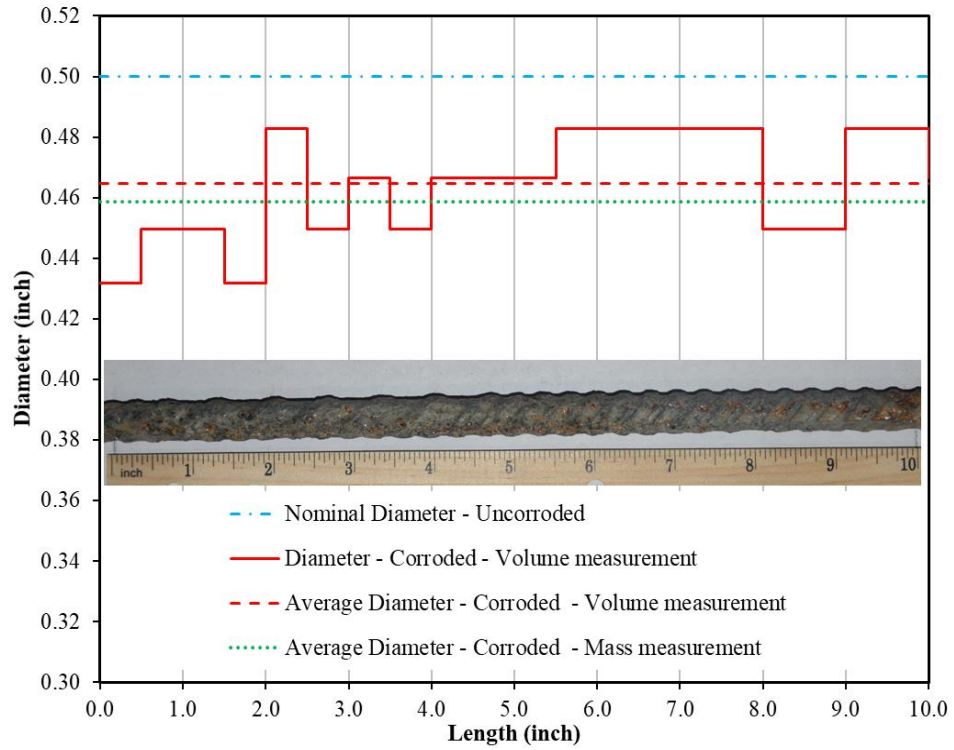
Cross section profile SS-#4-4.3%



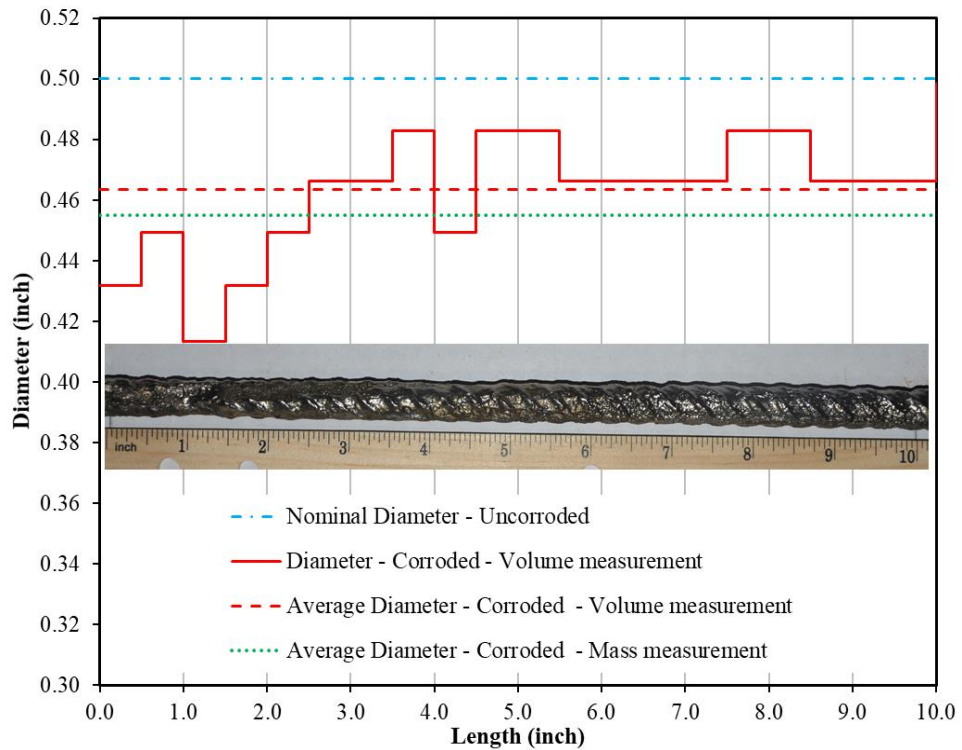
Cross section profile SS-#4-7.6%



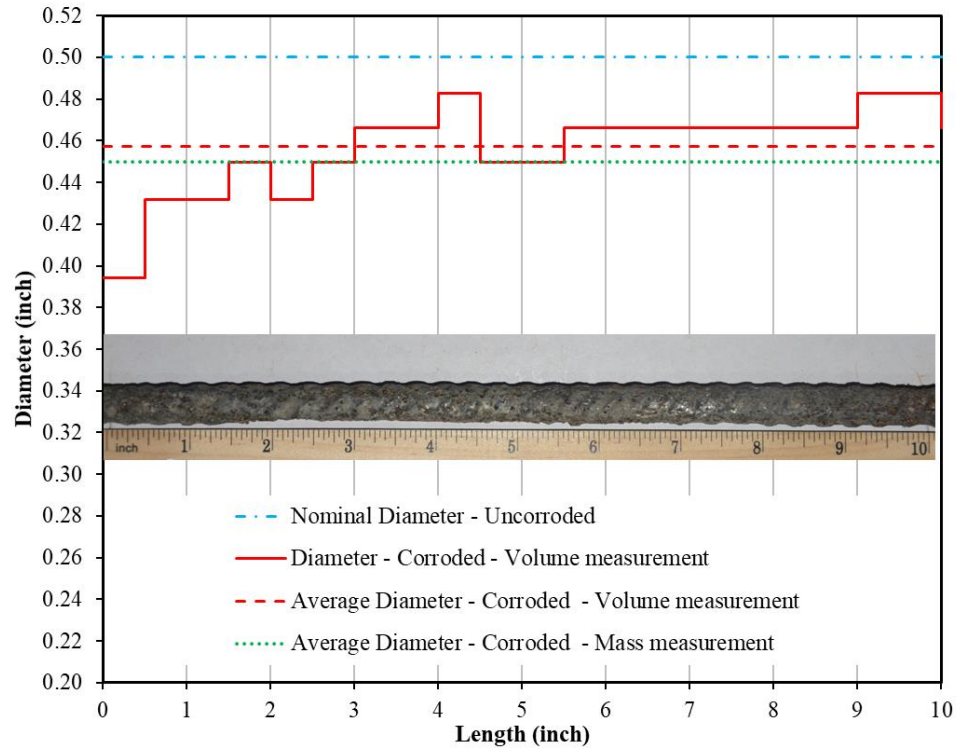
Cross section profile SS-#4-7.7%



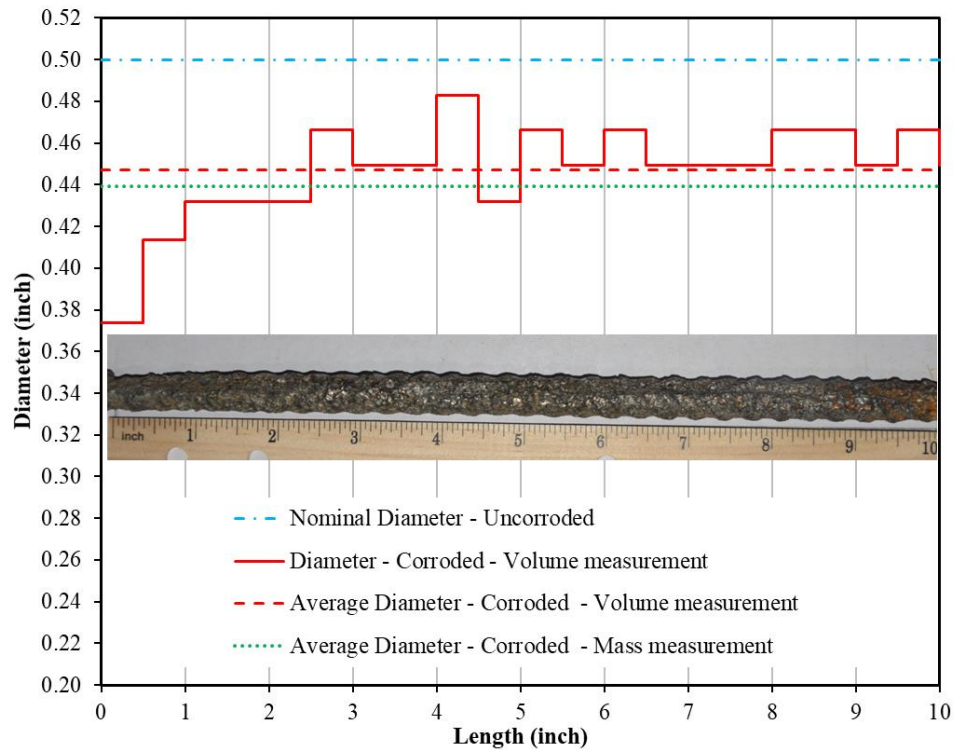
Cross section profile SS-#4-9.2%



Cross section profile SS-#4-10.1%



Cross section profile SS-#4-11.3%



Cross section profile SS-#4-13.8%

